

Stalk Forming Fouling Diatoms: A Problem for the Hydro- Electricity Industry

by

Matilde Ravizza

Submitted in fulfilment of the
requirements for the degree of

Doctor
of
Philosophy

Institute for Marine and Antarctic Studies
University of Tasmania

June 2015



Declaration of Originality

I declare that the material presented in this thesis is original, except where due acknowledgement is given, and has not been accepted for the award of any other degree or diploma

Matilde Ravizza

June 2015

Authority of Access

This thesis may be available or loan and limited copying in accordance with the *Copyright Act 1968*.

Matilde Ravizza

June 2015

Statement regarding published work contained in this thesis

The publishers of the paper comprising Chapters 3, 5 and 6 hold the copyright for that content, and access to the material should be sought from the respective journals. The remaining non published content of the thesis may be made available for loan and limited copying and communication in accordance with the *Copyright act* 1968.

Statement of Co-Authorship

The following people and institutions contributed to the publication of work undertaken as part of this thesis:

*Matilde Ravizza, School of Plant Science and Institute for Marine and Antarctic Studies, University of Tasmania= **Candidate***

*Gustaaf M. Hallegraeff, Institute for Marine and Antarctic Studies, University of Tasmania = **Author 1***

*Alan Henderson, School of Engineering, University of Tasmania = **Author 2***

*Jessica Walker, School of Engineering, University of Tasmania = **Author 3***

*Jane Sargison, School of Engineering, University of Tasmania = **Author 4***

*Dean Giosio, School of Engineering, University of Tasmania = **Author 5***

*Jennifer Shaw, School of Biological Sciences, University of Adelaide, Adelaide, South Australia = **Author 6***

*Sazlina Salleh, Center for Policy Research and International Studies, University Sains Malaysia, Penang, Malaysia = **Author 7***

*Susie Wood, Cawthron Institute, Nelson, New Zealand and Environmental Research Institute, University of Waikato, Hamilton, New Zealand = **Author 8***

*Jeanne Kuhajek, Cawthron Institute, Nelson, New Zealand = **Author 9***

*Andrew Martin, School of Biological Sciences, Victoria University of Wellington, Wellington, New Zealand = **Author 10***

Author details and their roles:

Paper 1, Environmental conditions influencing growth rate and stalk formation in the estuarine diatom *Licmophora flabellata*

Located in Chapter 3

Candidate was the primary author and with author 1 contributed with the experiment design, data interpretation and refinement of writing

Paper 2, Light and nutrients as key drivers of freshwater biofouling and surface roughness in an experimental hydrocanal pipe rig

Located in Chapter 5

Candidate was the primary author and with author 1 contributed with experimental design, data interpretation and refinement of writing. Author 2, Author 3 and Author 4 offered with engineering expertise on implications for friction and loss of flow. Author 5 contributed with experimental work at School of Engineering. Author 6 assisted with metagenomic analysis of fouling samples and Author 7 with fluorescence measurements and data analysis.

Paper 3, Ecophysiology of New Zealand *Didymosphenia geminata* nuisance diatom mats, compared to Tasmanian *Gomphonema* hydrofouling diatoms.

Located in Chapter 6

Candidate was the primary author and with author 1 contributed with the experimental design, development and refinement. Authors 8 and Author 9 assisted with local New Zealand Didymo expertise. Author 10 contributed with the fouling community health measurements and data interpretation.

We the undersigned agree with the above stated “proportion of work undertaken” for each of the above published (or submitted) peer-reviewed manuscripts contributing to this thesis:

Signed: _____

Professor Gustaaf Hallegraeff
Supervisor
Institute for Marine and
Antarctic Studies
University of Tasmania

Professor Craig Johnson
Centre for Biodiversity and Ecology
Institute for Marine and
Antarctic Studies
University of Tasmania

Date: 29 June 2015

Dedication

To my nephews

Gabriele and Giorgio Ravizza

and

To my nice, Noemi Ravizza

For they can acquire perseverance, courage and determination

To fulfil their dreams in life

Acknowledgments

This project was funded by an Australian Research Council Linkage Grant (LP100100700), between the School of Engineering, School of Plant Science and Hydro Tasmania as industry partner.

During the course of my PhD I have been fortunate in receiving invaluable assistance from many people.

I would like to express my gratitude in particular to my main supervisor, Professor Gustaaf M. Hallegraeff, for his guidance through the last four years, his enthusiasm for the project and his constant support and encouragement. I also want to thank my co-supervisors, Associate Professor Mark Hovenden for his valuable help and collaboration, and Dr Jessica Walker (nee Andrewartha) for assisting me in relation to the engineering aspect of the project.

I am extremely grateful to the technicians of the School of Engineering, Peter Seward, James Lamont and Andrew Bylett for their expertise, willingness and perseverance in fixing all sort of problems we encountered both in laboratory and in the Tarraleah field work.

I greatly thank Mrs. Helen Bond, for her precious help in lab, shared knowledge and friendship during the first two years of my PhD and Professor Andrew McMinn (IMAS) for his aid and knowledge in the use of PAM fluorometer.

To the people in New Zealand, who allowed me to study and experiment with Didymo. In particular, Dr Susie Wood and Dr Jeannie Kuhajek from Cawthron Institute, Nelson, for giving me the opportunity to work in their laboratory, for the assistance during the Buller River field work and for sharing knowledge and expertise about Didymo. To Dr Andrew Martin, Victoria University, Wellington, for his valued help and training in PAM measurements.

Many thanks go to my friends and colleagues at IMAS. To Sarah Ugalde for her immense support and assistance in lab, for her patience in fixing numerous problems making my life much easier in the last half of my PhD. To Dr Juan J.

Dorantes Aranda, Andreas Seger, Jorge Mardones Sanchez and Lee Shihong for their care, friendship and many smart suggestions and help in lab.

To my friends and colleagues in Plant Science, Lynda Prior, Stefania Ondeï, Adam McKiernan, Stuart MacDonald and Nick Fountain-Jones for their care and the great time together. In particular I wish to thank my dear friend Archana Gauli, for strongly supporting me through rough times and for the love we shared.

To my best friend in Italy, Elena Vigna for her love and for believing in me always.

I also want to thank Anissa and Karsten Goemann, for welcoming me when I first arrived in Tasmania, for their sincere friendship through these years and for looking after my beloved dog Penny any time I was away.

Finally I want to thank my family, my brother Sergio and his wife Simona for supporting me whatever I choose to do and in particular my sister, Silvia, for helping me in organizing the trip to Tasmania, for dealing with the dreadful Italian bureaucracy to ship my dogs to Australia, for looking after my precious Amapola and for her crazy ideas.

Table of contents

Chapter 1.	Hydro-electricity generation in Australia, a description of Tarraleah hydro canal system and the impact of biofouling on power generation	
1.1	Hydro-electricity generation in Australia	1
1.2	Tarraleah Hydro Canal System	2
1.3	Tarraleah Power Scheme Efficiency	3
1.4	Biofouling	5
1.5	Biofouling at the Tarraleah No. 1 Canal	5
1.6	The importance of flow for biofouling community	7
1.7	Environmental conditions in Tarraleah Hydro Canals	9
1.8	Concerns about possible <i>Didymosphenia geminata</i> introduction	11
1.9	Objectives of the thesis	11
Chapter 2.	Tarraleah Canal fouling bioassays to test light and nutrient responses on <i>Gomphonema tarraleahae</i> using PAM (Pulse Amplitude Modulated) fluorometry	
2.1	Introduction	13
2.2	PAM fluorometry	15
2.3	Application of fluorescence measurements in phytoplankton ecology	18
2.4	Aim of the investigation	20
2.5	Materials and methods	20
2.6	Results	21
2.7	Discussion	26
Chapter 3.	Role of seasonal variations of light and nutrients on Tarraleah biofouling using a pipe test rig	
3.1	Introduction	28
3.2	Pipe Test Rig	30
3.3	Materials and methods	34
3.4	Results	37
3.5	Discussion	50

Chapter 4. Environmental conditions influencing growth rate and stalk formation in the estuarine diatom <i>Licmophora flabellata</i> using new plate reader methodology	
4.1 Introduction.....	53
4.2 Materials and methods	56
4.3 Results.....	59
4.4 Discussion.....	66
4.5 Conclusions.....	68
 Chapter 5. New Zealand problems caused by the freshwater stalk-forming diatom: <i>Didymosphenia geminata</i>	
5.1 Introduction.....	69
5.2 Invasion and spread of <i>Didymosphenia geminata</i> in New Zealand.....	71
5.3 Ecology	72
5.4 Nuisance blooms	74
5.5 Control and eradication.....	76
5.6 Future investigations	78
 Chapter 6. Ecophysiology of New Zealand <i>Didymosphenia geminata</i> nuisance diatom mats, compared to Tasmanian <i>Gomphonema</i> hydrofouling diatoms using Pulse Amplitude Modulated (PAM) fluorometry	
6.1 Introduction.....	80
6.2 Aim of this investigation.....	81
6.3 Materials and methods	81
6.4 Results.....	82
6.5 Discussion	87
 Chapter 7. General conclusions, management and mitigation of biofouling.....	90
 References	96

List of Figures

- Figure 1.1 Butlers Gorge Power Station (from <http://www.hydro.com.au/>).
- Figure 1.2 Tarraleah Power Station (from <http://www.hydro.com.au/>)
- Figure 1.3 Tarraleah No. 1 Canal.
- Figure 1.4 Drained open canal section with a tractor (left) and a bobcat (right) for removal of biofouling (Andrewartha, 2010).
- Figure 1.5 (a) Tarraleah No. 1 Canal biofouling community, (b) *Tabellaria flocculosa* cells forming a characteristic chain, (c) *Gomphonema tarraleahae* cells on top of branched stalks.
- Figure 1.6 Profile of a boundary layer and illustration of freeboard. Diffusion boundary thickness varies according to current velocity. Adapted from <http://history.nasa.gov/SP-4103/app-f.htm>.
- Figure 2.1 Possible decay pathways of an excited state chlorophyll molecule. Adapted from <http://biologicalphysics.iop.org/cws/article/lectures/50852>
- Figure 2.2 Fluorescence induction curve from a PAM fluorometer, illustrating principles of quenching analysis by the saturation pulse method (from [Maxwell and Johnson, 2000](#)).
- Figure 2.3 Rapid light curve showing *Didymosphenia geminata* diatom fouling response after 1 hour dark adaptation (original data).
- Figure 2.4 Collections of fouling samples along the Tarraleah No. 1 Canal walls.
- Figure 2.5 Water analysis results from Tarraleah No.1 Canal, from September 2011 to November 2014, showing (a) silica, nitrogen (axis on left) and phosphorus trend (axis on right) and (b) the N:P ratio.
- Figure 2.6 RLC in response to light at three depths (top, medium and bottom) on the south (S) and north (N) wall of Tarraleah No. 1 Canal (T=top; M=medium; B=bottom).
- Figure 2.7 Maximum relative Electron Transport Rate values in response to nutrient addition for the south and north wall at the three depths. All $rETR_{max}$ values were reached at $PAR=1320 \mu\text{mol photons m}^{-2} \text{s}^{-1}$, except for values labelled with * ($PAR=191 \mu\text{mol photons m}^{-2} \text{s}^{-1}$).
- Figure 3.1 Artificial stream at the School of Engineering, comprising a head and an end tank and a flume.

- Figure 3.2 Pipe Test Rig set up at the Hydro Tasmania Tarraleah Power Scheme Pond No.1.
- Figure 3.3 Light test sections design in the Pipe Test Rig, set up at the Hydro Tasmania Tarraleah Power Scheme Pond No.1 (Hudson, 2013).
- Figure 3.4 HOBO Pendant light and temperature sensors and holders installed in the Pipe Rig.
- Figure 3.5 Pipe plunge employed to collect fouling samples from the pipes of the Pipe Test Rig.
- Figure 3.6 Biofouling samples scrubbed from the four pipes of the Pipe Test Rig in Tarraleah and preserved in plastic containers (Hudson, 2013).
- Figure 3.7 Water chemistry from Tarraleah No.1 Canal, from September 2011 to November 2014, showing silica, nitrogen (axis on left) and phosphorus (axis on right). Arrows indicate the timing of fouling collections from the pipes in April, May and July 2013 and November 2014.
- Figure 3.8 Light intensity and temperature data in the metal, opaque, frosted and clear PVC pipes from March 2013 to July 2013 in the Pipe Test Rig set up at the Hydro Tasmania Tarraleah Power Scheme Pond No.1.
- Figure 3.9 Microscopic characterization of fouling samples from the metal pipe of the Pipe Test Rig, collected in April, May and July 2013 and November 2014 (scale bar = 100µm).
- Figure 3.10 Microscopic characterization of fouling samples from the PVC pipe of the Pipe Test Rig, collected in April, May and July 2013 and November 2014 (scale bars = 100µm).
- Figure 3.11 Microscopic characterization of fouling samples from the frosted PVC pipe of the Pipe Test Rig, collected in April, May and July 2013 and November 2014 (scale bars = 100µm).
- Figure 3.12 Microscopic characterization of fouling samples from clear PVC pipe of the Pipe Test Rig, collected in April, May and July 2013 and November 2014 (scale bars = 100µm).
- Figure 3.13 *Gomphonema tarraleahae* in the clear pipe in November 2014.
- Figure 3.14 Biofouling wet (a) dry (b) weight from the metal, opaque PVC, frosted PVC and clear PVC test sections in April, May and July 2013 and November 2014.

- Figure 3.15 Taxonomic partitioning of eukaryote DNA sequences extracted from fouling material in the steel, PVC, frosted and transparent pipes as collected on 17 Feb 2015. Diatoms were abundant in the frosted and transparent pipes, while green plants were absent from the transparent pipe. Fouling in the metal and PVC pipes were dominated by fungal slimes. Companion prokaryote sequences (central diagram: only shown for steel pipe) were roughly similar in all pipes
- Figure 3.16 F_v/F_m average values in the four light test sections in April, May and July 2013 and November 2014. Those means with same letter within a sampling period were not significantly different ($P=0.05$).
- Figure 3.17 F_v/F_m values in the four pipes in response to P, N and Si addition in April and July 2013. Those means with same letter are not significantly different ($P=0.05$).
- Figure 3.18 F_v/F_m values in the four light test sections in response to silica, nitrogen and phosphorus in November 2014. Means with same letter within each treatment are not significantly different ($P=0.05$).
- Figure 3.19 Rapid Light Curves in response to P, N and Si addition in the metal, opaque PVC, frosted PVC and clear PVC test sections in November 2014.
- Figure 4.1 *Licmophora flabellata*.; (a) SEM. Three dimensional architecture of *Licmophora* biofouling on fish farm netting in Tasmanian waters; (b) SEM. Basal pole of cell with a row of slits through which the mucilage pads or stalks are secreted. (c) LM. Fans and branching stalks, new cells emerging from small side branches (arrow) and cells showing two discoid chloroplasts with pyrenoids (p).
- Figure 4.2 Calibration of fluorescence against microscopic cell counts of *Licmophora flabellata* cultured in 96-well plates. Average cell counts of 10 wells time course of growth.
- Figure 4.3 Figure 4.3. Response of the diatom *Licmophora flabellata* growth and stalk formation as a function of light intensity ($\mu\text{mol photons m}^{-2}\text{s}^{-1}$). (a) Time course of growth measured as in vivo fluorescence; (b) Length of exponential growth period (days) and (c) stalk length (μm).
Number of stalks of during the time course of growth (days) at different light intensities: 50 (d), 100 (e), 150 (f) and 233 (g) $\mu\text{mol photons m}^{-2}\text{s}^{-1}$.

(h) Light micrographs showing single stalk with one, two, four cells on top, in low light conditions (50, 100 and 150 $\mu\text{mol photons m}^{-2}\text{s}^{-1}$ respectively) (10x magnification) and fans of cells on top of thick, long stalks, at high light conditions (233 $\mu\text{mol photons m}^{-2}\text{s}^{-1}$) (5x magnification).

Figure 4.4 Response of the diatom *Licmophora flabellata* growth and stalk formation as a function of nutrient content. (a) Time course of growth measured as in vivo fluorescence; (b) Length of exponential growth period (days), growth rate (div/day) and (d) stalk length (μm).
Number of stalks of during the time course of growth (days) at different nutrient content: P (e), N (f) and Si (g).
(h) Light micrographs showing small fans of cells on top, in P, N and Si treatments (10x magnification).

Figure 4.5 Response of the diatom *Licmophora flabellata* growth and stalk formation as a function of temperature ($^{\circ}\text{C}$). (a) Time course of growth measured as in vivo fluorescence; (b) Length of exponential growth period (days), (c) growth rate (div/day) and (d) stalk length (μm).
Number of stalks of during the time course of growth (days) at different temperature: 12 (e), 17 (f) and 20 $^{\circ}\text{C}$ (g).
(h) Light micrographs showing stalks of different lengths at 12 (10x magnification), 17 (5x magnification) and 20 $^{\circ}\text{C}$ (10x magnification), supporting fans of cells of different shape in the three treatments

Figure 4.6 Response of the diatom *Licmophora flabellata* growth and stalk formation as a function of turbulence (Hz). (a) Time course of growth measured as in vivo fluorescence; (b) Length of exponential growth period (days), (c) growth rate (div/day) and (d) stalk length (μm).
Number of stalks of during the time course of growth (days) at different turbulence: 2.5 (e), 3.33 (f) and 4.16 Hz (g).
(h) Light micrographs showing long branched stalks supporting cells at low turbulence intensity (2.5 and 3.33 Hz) and a short single stalk in high turbulence intensity (4.16 Hz) (10x magnification).

Figure 5.1 Water quality data for pH, conductivity, temperature, total phosphorus and total nitrogen for New Zealand North and South Island compared with Tarraleah, by means of a) Non-Metric Multidimensional Scaling (NMDS) plots and b) Principal Component Analysis (PCA). (Courtesy Jon Bray, University of Canterbury).

- Figure 6.1 *Didymosphenia geminata* stalk material from Buller River, New Zealand, as it appears a) when out of water and b) covering stream bed.
- Figure 6.2 *Didymosphenia geminata* relative Electron Transport Rate after 1 and 4 hours dark adaptation (original data).
- Figure 6.3 *Gomphonema cf. manubrium* rETR after 1 and 4 hours dark adaptation (original data).
- Figure 6.4 *Gomphonema tarraleahae/Tabellaria flocculosa* rETR after 1 and 4 hrs dark adaptation (original data).
- Figure 6.5 *Licmophora flabellata* rETR after 1 and 4 hrs dark adaptation (original data).

List of Tables

Table 2.1	Estimated final concentration of the nutrients in the test samples.
Table 2.2	Influence of nutrient addition on fluorescence yield as a function of depth in Tarraleah No. 1 Canal. S= south; N= north; T= top; M= medium; B= bottom.
Table 3.1	Percentage of diatom species coverage in the frosted and clear PVC pipe of the Pipe Test Rig, in April, May and July 2013 and November 2015.
Table 4.1	Stalk categories discriminated in this study.
Table 4.2	Length of growth period, growth rate and stalk length of <i>Licmophora flabellata</i> as a function of light intensity, nutrients, temperature and turbulence.
Table 5.1	Summary of ecological requirements of <i>Didymosphenia geminata</i> , determined from literature.
Table 6.1	Final concentrations of nutrients applied in the nutrient bioassays.
Table 6.2	F_v/F_m values for <i>Didymosphenia geminata</i> , <i>Gomphonema</i> cf. <i>manubrium</i> , <i>Gomphonema tarraleahae</i> and <i>Licmophora flabellata</i> in response to silica, nitrogen, phosphorus and iron addition, after 1 and 4 h incubations.

ABSTRACT

The Tarraleah power scheme (102.2 MW) is a significant component of Tasmania's Hydro-Electric generation system operated by Hydro Tasmania, which contributes 60% of Australia's renewable energy. The efficiency of this scheme is negatively impacted by the presence of biofouling, consisting mainly of diatoms and bacterial slimes, which can grow up to 5 mm thick on the canal walls and cause up to 10% reduction in flow carrying capacity, therefore reducing power generation capability. In Tarraleah No. 1 Canal biofouling is constantly present, although the amount varies seasonally, from location to location, and dependent on canal cleaning regimes. Engineering studies have demonstrated that the effective roughness of the biofilm is much greater than its physical roughness, which has implications for the frictional drag induced by the biofilm. Observations of the canal wall during outages indicate that fouling is less prevalent on the southern wall of the canal, which is less shaded by vegetation, thus indicating that the fouling diatoms prefer low light conditions. The succession of fouling diatoms begins with *Tabellaria flocculosa* which dominates under low flow regimes ($< 2 \text{ m s}^{-1}$) and progresses to the stalk-forming *Gomphonema tarraleahae* which is the dominant species in high velocity areas.

In this study, the target species *G. tarraleahae* was compared with other stalk forming diatoms, both marine and freshwater species (*Licmophora flabellata*, *Didymosphenia geminata* and *Gomphonema cf. manubrium*), to elucidate the environmental factors promoting their stalk formation and to determine the best strategies to mitigate their impact. Both laboratory culture studies and field experiments were conducted.

Simulated laboratory trials were conducted on the marine stalk-forming diatom *Licmophora flabellata*, to define environmental factors influencing its growth and stalk formation. Growth rates in multiwell plates were estimated using *in vivo* fluorescence in a plate reader. Low to moderate light intensities (50, 100 and 150 $\mu\text{mol photons m}^{-2} \text{ s}^{-1}$) produced no or poor growth, while growth rates of 0.24 -0.42 div/day were achieved at the highest light intensities of 233 $\mu\text{mol photons m}^{-2} \text{ s}^{-1}$. High growth rates coincided with long stationary growth periods (21-36 days) and long (800-3500 μm) branching stalks. With this eutrophic estuarine diatom N, P and

Si nutrients had no effect on growth nor stalks, while high turbulence reduced stalk length but not growth.

Pulse Amplitude Modulated (PAM) fluorometry was applied to define light and nutrient responses of the diatom biofouling on both walls of Tarraleah No. 1 Canal at three different depths (top, medium and bottom). Rapid light curves (RLC) and F_v/F_m (indicators of physiological health) confirmed that biofouling was suppressed by high light (on the south wall at a depth less than 1 m) and inhibited by silica whilst nitrogen or phosphate addition had no effect.

To further confirm the critical role of light for Tarraleah hydrocanal fouling an experimental rig was designed and built on the banks beside the no.1 Canal. It comprised four pipes through which natural Tarraleah water was allowed to flow at 1.22 m s^{-1} but under varying substratum conditions (metal, opaque PVC, frosted PVC and clear PVC) and light levels (0 in the metal pipe and maximum of 6, 1937 and $2957 \mu\text{mol photons m}^{-2} \text{ s}^{-1}$ in the opaque PVC, frosted PVC and clear PVC pipes, respectively). Nutrient bioassays using PAM fluorometry on fouling samples harvested on a monthly basis during winter and spring showed significant effects of both pipe material and nutrients on photosynthetic performance. Optimal fouling dominated by *T. flocculosa* (81.4 – 96.4% of cells) occurred at medium light (in opaque and frosted PVC), and F_v/F_m responded positively to silica in April 2013 and to nitrogen and phosphate addition in July 2013. Unexpectedly, photosynthetically viable diatom fouling communities (F_v/F_m 0.36-0.59) were observed in the metal pipe even after 2 months in complete darkness.

The New Zealand stalk-forming diatom *Didymosphenia geminata* represents a potentially invasive freshwater pest, of considerable concern if it were to become established in Tasmania. Comparative PAM nutrient responses were studied for New Zealand Buller River *D. geminata*, Lake Rotoiti *G. cf. manubrium* and Tasmanian *G. tarraleahae*. Although these freshwater stalk-forming diatoms had different requirements in terms of light, flow rate and nutrients, all three species were inhibited by silica addition while *D. geminata* was also stimulated by iron. Like *G. tarraleahae*, *D. geminata* blooms preferentially occur in hydrologically stable oligotrophic waters, but are remarkably tolerant towards light and occur over a wide range of flow velocities. Comparative PAM nutrient assays on *L. flabellata*

cultures showed no prohibitive effect from silica addition with that eutrophic diatom.

The present results call for species-specific approaches towards mitigating the impact of fouling diatoms. In *L. flabellata* and *D. geminata* high light intensities stimulated stalk formation and length. While these species were adapted to stable low flow waters, *G. tarraleahae* showed preferences for high velocity flow and low light intensities. *L. flabellata* showed more tolerance towards nutrient addition and could grow under a wide range of temperatures, but *D. geminata* and *G. tarraleahae* instead were adapted to oligotrophic waters and cold temperatures. Currently mitigation methods in Tarraleah No. 1 Canal involve scrubbing of the canal walls on a regular basis, but this is expensive and benefits are short-lived with rapid fouling regrowth occurring, notably in spring. Alternative mitigation solutions including clearing vegetation along canals and the application of white paint on the canal walls have shown better promise to increase light-intensity to mitigate low-light adapted *G. tarraleahae* fouling. However, this clearly is not a universal strategy that can be applied to all fouling diatoms. Undoubtedly, the best approach for all fouling species would be to stop their attachment to the substratum, even though this remains a challenging task that requires continued research.

Chapter 1

Hydro-electricity generation in Australia, a description of Tarraleah hydro canal system and the impact of biofouling on power generation

1.1 Hydro-electricity generation in Australia

Australia has two major hydro-electric schemes: Snowy Mountains in New South Wales and Hydro Tasmania extended across Tasmania. The Hydro Tasmania contributes 60% of Australia's renewable energy through hydroelectric schemes and wind farms. The company currently operates 30 hydropower stations and a network of over 50 large dams, 230 km of open and closed conduits and has an installed capacity of 2615 MW (Hydro Tasmania, 2006). It also operates two wind farms on mainland Tasmania and two diesel power stations and a wind farm on the Bass Strait islands. Hydro Tasmania's hydropower stations have been built in six high-rainfall water catchments, which are formed from natural river systems in Tasmania's rugged landscape. The water systems and power stations are interlinked through natural and man-made water channels (<http://www.hydro.com.au/energy/our-power-stations>).

In 1914, the State Government set up the Hydro-Electric Department (changed to the Hydro-Electric Commission in 1929) to complete the first HEC power station. Hydro Tasmania was formed upon the disaggregation of the Hydro-Electric Commission on July 1, 1998. Since April 2006, Hydro Tasmania has been connected directly to the National Energy grid (NEG), through Basslink, which is the world's second longest undersea power cable. It connects Tasmania to the national electricity grid, running under Bass Strait. Basslink runs from George Town in Tasmania to Loy Yang in Victoria and its undersea section is 290 km long.

1.2 Tarraleah Hydro Canal System

Hydro Tasmania created Lake King William in 1950 with the construction of the 70 m high Clark Dam across the Derwent River, successively raised a further 6 m in 1964. The scheme includes two power stations. The 12.2 MW Butlers Gorge Power Station (Fig. 1.1), located at the foot of Clark Dam, was commissioned in 1951 and is supplied by the water stored in Lake King William. The water which powers the Tarraleah Power Station (Fig. 1.2), covers 26 km overland (via canals, siphons and pipes) from the Butlers Gorge Power Station, and ends in the Nive River. The first three generators were commissioned in 1938. Three more generators were commissioned between 1943 and 1950, bringing the capacity to 90 MW. This is the second oldest working station operated by Hydro Tasmania.



Figure 1.1 Butlers Gorge Power Station
(from <http://www.hydro.com.au/>)



Figure 1.2 Tarraleah Power Station
(from <http://www.hydro.com.au/>)

Water flows from Butlers Gorge Power Station to Tarraleah and drops 290 metres through penstocks (steel pipes) to the power station. The main canal in the system, Tarraleah No. 1 Canal (Fig. 1.3), is 19.7 km in length, with 192 000 m² of concrete surface. The Tarraleah No. 2 Canal is smaller and includes a tunnel, wood stave pipelines and open channels.



Figure 1.3 Tarraleah No. 1 Canal.

1.3 Tarraleah Power Scheme efficiency

The amount of the electricity produced by Hydro Tasmania is limited not only by rain water supply, but also by the structures and machinery employed in the generation system. Therefore maximising the efficiency of this system is paramount in attaining the highest possible electricity output. One of the main limiting factors in hydro-generation is loss of head over conduit length, chiefly due to friction-induced resistance to flow. All systems involving the relative movement between a fluid and a solid boundary can result in a loss of energy due to skin friction at the solid/fluid interface (Andrewartha et al., 2010; Barton et al., 2010).

A reduction in carrying capacity of canals and pipelines occurs due to two main factors:

1. the deterioration of the conduit surface through the loss of fines, causing an increase of surface roughness, and therefore decreased hydraulic smoothness, which is a critical factor in long conduits with high velocity, such as Tarraleah;

2. the development of biological growths, or biofouling, consisting of algal and bacterial slimes, causing an additional frictional loss and reduction in freeboard (distance between the water surface and the top of the canal walls).

These two factors are not independent as algal biomass growth is expected to be more prolific on rougher surfaces. Moreover in the Tasmanian hydro scheme these problems are enhanced due to the aging of the canal systems, which were built in the first half of the last century. The presence of biofouling in Tarraleah No. 1 canal results in increased drag, which in turn results in either a reduction in freeboard to maintain the clean canal flow rate or a decrease in flow rate to maintain an acceptable freeboard level to avoid overtopping events (Andrewartha et al., 2007; Barton et al., 2010; Perkins et al., 2010).

The overtopping is highly undesirable for two reasons:

1. loss of water that could have been used for electricity generation;
2. overtopping causes weathering and degradation of the canal foundation material, resulting in landslides.

In order to limit the loss of efficiency due to presence of biofouling, the canal has been scrubbed using rotating brushes attached to tractors and bobcats (Fig. 1.4), since 1996. This process is intended to be carried out approximately twice a year but even though it temporarily results in better water movement through the canal, the longer term effectiveness of this method is not clear.



Figure 1.4 Drained open canal section with a tractor (left) and a bobcat (right) for removal of biofouling (Andrewartha, 2010).

1.4 Biofouling

Biofouling is the undesirable accumulation of microorganisms, plants and animals on artificial submerged structures. Diatoms are the most common and successful microalgal foulers of illuminated submerged artificial surfaces (Meseguer Yebra et al., 2006; Patil and Anil, 2005). In particular, raphid diatoms are the most frequent early algal colonizer of natural and artificial substrata, where they adhere and produce copious quantities of adhesive mucilage during the construction of primary biofilm (Wetherbee et al., 1998), together with bacteria and other algae. Adhesion of raphid diatoms to surfaces is mediated by the secretion of extracellular polymeric substances (EPS) and represents an important strategy for growth and survival (Thompson et al., 2008). The EPS comprises a highly hydrated, three-dimensional structure and constitutes 50-80% of the overall biofilm organic matter. It is due to the secretion of EPS that biofilms obtain their slimy characteristic (Andrewartha et al., 2007). The thickness and morphology of biofilms are a function of the hydrodynamic operating conditions through, for example, nutrient transport and the formation of filamentous strands. It has been observed that the viscoelastic character of the biofilm combined with its filamentous nature seems to cause additional energy dissipation that can lead to higher frictional resistance (Picologlou et al., 1980). Biofouling diatoms have been found to adhere tenaciously and colonise even the most resistant of artificial surfaces and characteristically proliferate to the point where they completely dominate the substratum (Molino and Wetherbee, 2008).

1.5 Biofouling at the Tarraleah No. 1 Canal

This research focused on Tarraleah No. 1 Canal, the major water transport canal within the Tarraleah hydropower system. Fouling is constantly present in this canal, though the amount varies from location to location and according to the seasons, with more fouling visible during summer and spring than over winter and autumn months (Perkins et al., 2009). Moreover observations of the canal wall during outages indicates that fouling is more abundant on the northern canal wall which

receives more shading (Perkins et al., 2009). Biofouling in the Tarraleah hydrocanals represents an estimated 1.8-17.6 tonnes (dry weight) of fouling in the 20 km long canal (Perkins et al., 2009), causing reductions up to 10% in flow carrying capacity (Andrewartha et al., 2010). The successional path to a climax community followed by fouling community at Tarraleah No. 1 Canal differs from that of stagnant natural freshwater systems (Perkins et al., 2009). Commonly, epilithic community succession follows a precise order, with bacterial fouling established first, followed by small diatoms, then green algae, larger stalked diatoms, and finally green algae and cyanobacteria. In Tarraleah No. 1 Canal bacteria and small, low profile diatoms establish first, followed by stalked diatoms which end the succession, and are rarely associated with chlorophytes and cyanobacteria.

The succession begins with the low profile diatoms *Tabellaria flocculosa* (Fig. 1.5), which is commonly found in lower velocity areas, progressing to stalking diatoms such as *Gomphonema* spp., found in high velocity areas (Perkins et al., 2009). These species form a brown jelly-like skin at the water interface and are low-form gelatinous slimes dominated by EPS. Organic matter, dirt and leaves are trapped in the biofilm forming a dense mat structure (Andrewartha et al., 2007). The main biofilm species has been identified as the diatom *Gomphonema tarraleahae* Perkins and Hallegraeff (Perkins et al., 2010). This is a raphid diatom, with cells around 35µm long and 6µm wide, which as do a number of other fouling diatom species, secretes stalks (Fig. 1.5).

The stalk provides a permanent and persistent attachment which allows the cell to remain in areas where light and nutrients are accessible (Wetherbee et al., 1998) and guarantees a strong adhesion in high velocity flows or physical disturbance (Callow, 1993). Also it may provide a competitive advantage over other members of the biofilm by elevating the cell above the substratum, and longest stalk production was positively correlated with the high cell density (Lewis et al., 2002). The stalks observed at Tarraleah are hundreds of microns long, tens of times the size of the cell itself. Often older fouling samples consist of a great number of stalks without attached cells: it is probable that old stalk material is left behind after the algae have died or become detached (Perkins et al., 2010).

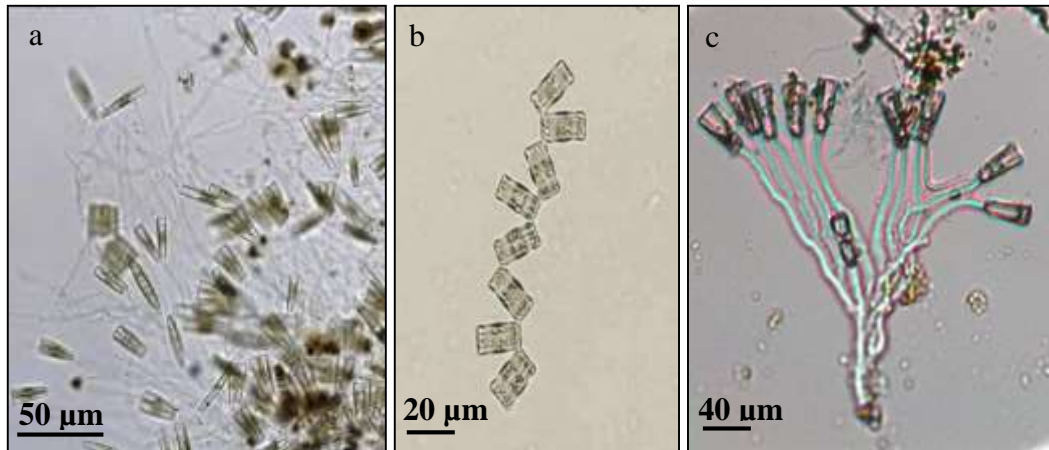


Figure 1.5 (a) Tarraleah No. 1 Canal biofouling community, (b) *Tabellaria flocculosa* cells forming a characteristic chain, (c) *Gomphonema tarraleahae* cells on top of branched stalks.

Also the cells are able to release from the stalk if environmental conditions deteriorate, and to reattach somewhere else to form new stalks (Wetherbee et al., 1998). Accordingly, cleaning methods that attempt to kill cells but leaving stalks at the wall (i.e. heat treatment) are not successful in preventing or removing fouling. By contrast, understanding stalk formation and the initial adhesion (“the first kiss”) is critical to address the Tarraleah biofouling problem.

1.6 The importance of flow for the biofouling communities

It has been demonstrated that water velocity positively affects periphyton biomass in streams (Reiter, 1986; Stevenson, 1983). With unidirectional flow over the benthos, water movement varies from high current velocities away from the substratum to extremely low velocities in the areas near the substratum (the so-called boundary layer) (Dodds, 1990). The regions in which viscous forces constrain movement of water molecules are called flow boundaries (viscous sublayers). Within it, the current decreases relative to the open-channel current velocity and friction with the substratum causes a reduction in flow velocity (Silvester and Sleight, 1985). The diffusion boundary is narrower than the flow boundary because some turbulent mixing occurs on the outer edge of the flow boundary, causing eddy diffusion to exceed molecular diffusion. Hydrodynamic factors influence flow boundary and diffusion boundary thickness in the same

manner. The thickness of the diffusion boundary can vary: it decreases as current velocity increases and as the substratum protrudes into the flow. Generally, the diffusion boundary is < 1 mm thick (Nowell and Jumars, 1984) (Fig. 1.6).

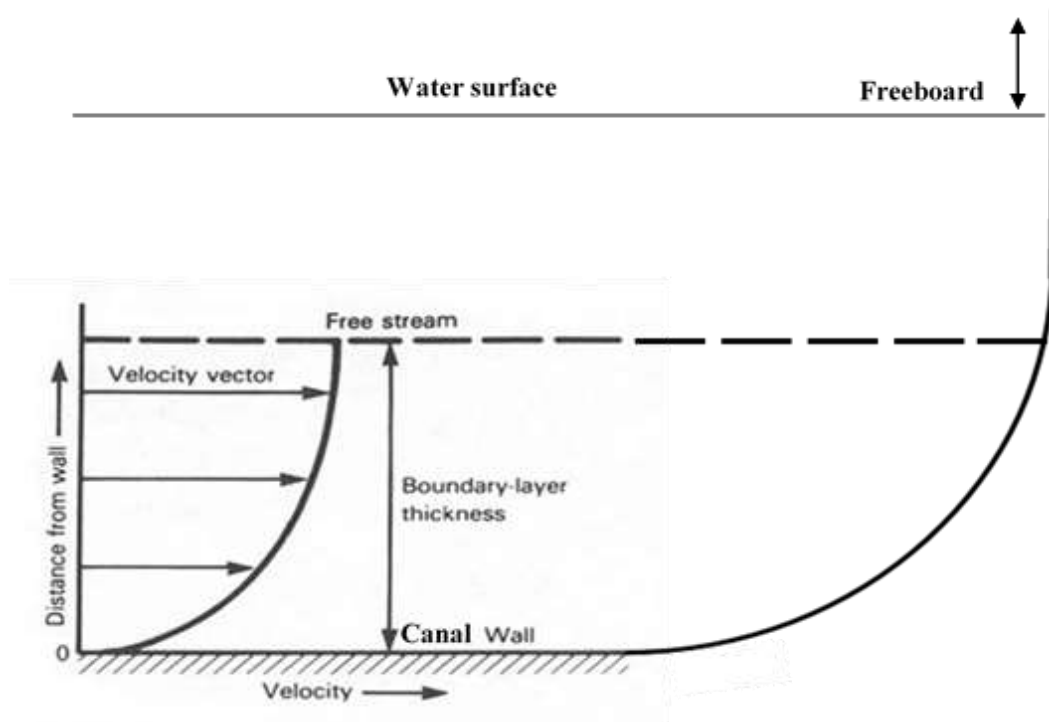


Figure 1.6 Profile of a boundary layer and illustration of freeboard. Diffusion boundary thickness varies according to current velocity. Adapted from <http://history.nasa.gov/SP-4103/app-f.htm>

There is evidence that the current velocity can stimulate photosynthesis (Pfeifer and McDiffett, 1975), nutrient uptake (Lock and John, 1979; Whitford and Schumacher, 1961), respiration and efflux of waste products (Whitford and Schumacher, 1961) of benthic algae, by reducing the thickness of the unmixed layer around the cells, thereby renewing dissolved gases and increasing nutrient supply (Stevenson and Glover, 1993). Also, it promotes the attachment and the removal rate of cells which are transported through the diffusion boundary, by reducing its thickness (Reiter, 1986; Stevenson, 1983). Nutrients are well known to be a key driver controlling phytoplankton community structure and biomass (Hutchinson, 1967). Nutrient availability and optimum nutrient ratio for fouling communities are

dependent on the flow and vary with irradiance, light and temperature (Borchardt, 1996): with increasing water velocity, a nutrient mass transfer subsidy can occur. Algal taxa respond differently to variations in flow velocity (Borchardt, 1996): the biomass of mucilaginous communities increases with increasing water velocity, while in the same conditions filamentous communities show a monotonic decrease, with shear stress dominating biomass accumulation (Biggs et al., 1998). Because water movement plays a significant role in determining biofilm conditions and community composition, it is important to set up experiments which include all these factors, to reproduce the conditions under which the Tarraleah biofouling community grows.

1.7 Environmental conditions in Tarraleah Hydro Canals

The environmental conditions in hydropower canals differ from those of a natural stream (Andrewartha et al., 2010). Tasmania has been identified as a biogeographically isolated area, with numerous endemic algal species (Vanormelingen et al., 2008; Vyverman et al., 1998). Diatoms respond directly to the physical, chemical and biological changes in their aquatic ecosystem (Stevenson and Pan, 1999), and this species-specific sensitivity of diatom physiology to many habitat conditions is manifested in the great variability in biomass and species composition of diatom assemblages in river and streams. In order to investigate the fouling community present at Tarraleah, it is essential to quantify environmental conditions. This allows matching diatom species to these conditions and understand the success of certain species. Such information could in turn help in finding a way to mitigate the algal fouling problem which affects the Tarraleah No.1 Canal.

1.7.1 Water velocity

The water flow is steady and the surface of the canals is lined with concrete. Thus, the water velocity is higher than would normally be found in a natural river with an average of 2 m s^{-1} and maximum flow rate is $24 \text{ m}^3/\text{s}$ with average of $18 \text{ m}^3 \text{ s}^{-1}$

(Perkins et al., 2009). The available nutrients are low, but constantly replaced due to the high flow velocity.

1.7.2 Water temperature

Water temperature in Tarraleah No. 1 Canal exhibits a strong seasonal variation, with a minimum of 5°C over the winter months. Water temperature then increases over spring to reach a maximum of 15°C during February and March.

1.7.3 Water chemistry

The nutrients considered most important for phytoplankton growth are silica (Si), nitrogen (N) and phosphorus (P) (Rousseau et al. 2002; Smayda, 1990). On average, in freshwater situations P is the most likely of the macronutrients to become limiting to algal growth, while in the marine systems P, Si and N are all possible candidates. Furthermore diatoms and some groups within the Chrysophyta, have an absolute requirement for significant amounts of silica (Hecky and Kilham, 1988), which is used to build their frustules and for the growth and reproduction.

The Redfield C:N:P stoichiometry of 106C:16N:1P describes the average elemental composition of phytoplankton (Redfield, 1958) and in particular the nitrogen-to-phosphorus (N:P) ratio of 16 N to 1 P is often used as a benchmark for differentiating N-limitation from P-limitation (Goldman, 1986).

In Tarraleah No. 1 Canal, water analysis was performed from September 2011 until November 2014, recording seasonally the amount of silica (0.95-4.80 mg L⁻¹), nitrogen (0.12-0.69 mg L⁻¹) and phosphorus (0.005-0.01 mg L⁻¹) (see chapter 4). The form of silica measured was defined by the analytical method as molybdate-reactive silica, whilst the total nitrogen and phosphorus were considered.

1.7.4 Light

Tarraleah has an average of 152.7 rain days, with 27.0 clear days and 147.4 cloudy days annually (Bureau of Meteorology, 2008), calculated over a period of time of 30 years (1981-2010). Subsurface light attenuation readings taken in May 2007 show that at the surface at midday light intensity varies according to the meteorological conditions: during sunny days it is $750 \text{ photons m}^{-2} \text{ s}^{-1}$ and decreases to $167 \text{ photons m}^{-2} \text{ s}^{-1}$ with overcast weather, and the light extinction coefficient would indicate that light intensity would drop to around 10% of that at the surface by 2 m depth (Perkins et al., 2009).

1.8 Concerns about possible *Didymosphenia geminata* introduction

The nuisance value and negative impacts from extensive New Zealand *Didymosphenia geminata* (Lyngbye) M. Schmidt diatom fouling, or ‘rock snot’ are of considerable concern to the Hydropower operations, were this species ever to be accidentally introduced into Tasmania. As with *G. tarraleahae*, the New Zealand *Didymosphenia* problems derive from massive production of persistent extracellular stalks, but these problems are worse because of the much larger cell size of the latter.

Chapter 2 provides an extensive review of *D. geminata*, including its ecology and control and eradication.

1.9 Objectives of the thesis

This research is aiming to identify the environmental requirements that promote growth and stalk formation in *Gomphonema tarraleahae* and to compare it with other stalk-forming diatoms such as the New Zealand freshwater species *Didymosphenia geminata* and *Gomphonema* cf. *manubrium* Fricke, and the marine species *Licmophora flabellata* (Carmichael ex Greville) C. Agardh diatoms.

1.9.1 Hypothesis to test

1. To confirm that *G. tarraleahae* is sensitive to high light and has preferences for high flow and to investigate its response to nutrient addition;
2. *D. geminata* is tolerant towards light but is sensitive to high nutrient levels;
3. To compare the response of the estuarine *L. flabellata* towards different light intensities, nutrients, temperatures and turbulence conditions.

Chapter 2

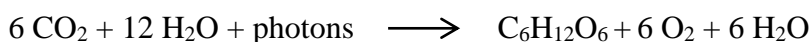
Tarraleah Canal fouling bioassays to test light and nutrient responses on *Gomphonema tarraleahae* using PAM (Pulse Amplitude Modulated) fluorometry

2.1 Introduction

To assess the response of *G. tarraleahae* to light and nutrient conditions, the *in situ* application of PAM fluorometry techniques have been explored.

2.1.1 Photosynthesis

Photosynthesis is an endothermic oxidation-reduction process by which plants, algae and photosynthetic bacteria convert light energy into chemical energy, stored in carbohydrate molecules as summarized by the equation:



This process takes place in the chloroplasts, where four major protein complexes are located in the thylakoid membrane: Photosystem I (PSI), Cytochrome b₆f complex, Photosystem II (PSII), and ATP synthase. It occurs in two stages: light dependent and light independent reactions (Calvin cycle). In the former, light is captured and converted to make the energy-storage molecules ATP and NADPH (Falkowski and Raven, 2013), and then utilised in the Calvin cycle to convert carbon dioxide into glucose (Quick and Neuhaus, 1997).

2.1.2 Chlorophyll fluorescence

When a chlorophyll *a* molecule receives a photon $h\nu$, the outer electrons of its conjugated double bonds jump from the ground state (S_0) to a higher energy level,

or first excited singlet state (S_1). The excited molecule has three main fates (Fig. 2.1), during which it will return to the lowest singlet state.

1. *Non photochemical quenching* (NPQ) – the excited state returns by direct decay to the ground state by emitting the energy as heat or fluorescence;
2. *Resonance energy transfer* (RET) – the excited state is transferred from a chlorophyll molecule to another one with an absorption spectrum at higher λ than the donor, via the exchange of a virtual photon;
3. *Photochemical quenching* (qP) – excitation is gradually passed to the photochemical reaction centres PSI and PSII where energy is used in photosynthesis.

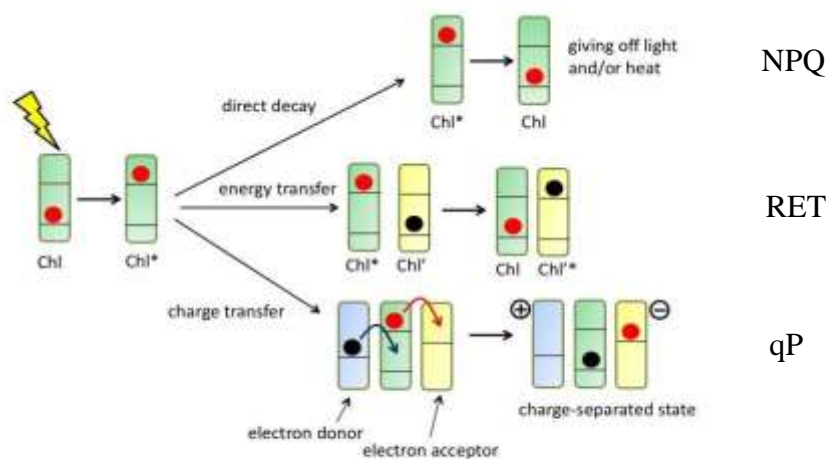


Figure 2.1 Possible decay pathways of an excited state chlorophyll molecule.

Adapted from <http://biologicalphysics.iop.org/cws/article/lectures/50852>

These processes occur in competition, so that an increase in the efficiency of one results in a decrease in the yield of the other (Maxwell and Johnson, 2000). For this reason, by measuring chlorophyll fluorescence yield important information about the efficiency of photochemical processes can be obtained.

2.1.3 Fluorescence emission

Fluorescence emission is mainly due to Chl *a* molecules located in the reaction centres and in the light-harvesting complexes in PSII (Müller et al., 2001). Kautsky et al. (1960) observed that when dark-adapted photosynthetic material is exposed to light, chlorophyll fluorescence goes through a series of responses (fluorescence induction). The kinetics of the response depends upon the intensity of excitation light, the light history of the cell and wavelength of excitation energy (Falkowski and Kiefer, 1985). In the dark adapted state of the photosynthetic apparatus, the primary electrons acceptor (Q_A) normally is fully oxidized and the reaction centres are said to be “open” (Krause and Weis, 1991). Under continuous illumination, fluorescence increases to the initial state F_o in less than 1 second. From F_o , if the actinic light is high enough to assure a rate of Q_A reduction faster than its reoxidation, the yield rises to an intermediate state F and then to a maximum F_m (Falkowski and Kiefer, 1985), representing full reduction of Q_A . The difference ($F_m - F_o$) is called variable fluorescence (F_v). In this period, the reaction centre is said to be “closed”. Fluorescence yield is around 3% when all reaction centres of PSII are “closed” and only 0.3% when they are “open” (Krause and Weis, 1991).

2.2 PAM fluorometry

One of the most commonly used fluorometers nowadays is the PAM fluorometer, introduced in the mid-80s. This is a pulse modulation technique which, in combination with the repetitive application of saturation light pulses, yields information not available by using conventional fluorescence induction curves (Schreiber et al., 1986). PAM fluorometers measure the relative quantum yield of Chl *a* fluorescence by applying pulse-modulated light, which in most PAM fluorometers is generated by a light-emitting diode (LED). LEDs can be modulated at high frequencies and have the additional advantage of being easy to handle and of low cost. Photodiodes are commonly employed as fluorescence detectors, being linear over a large range of light intensities, and maintaining low noise level even at extremely high signal levels (Schreiber, 2004).

The rationale of the saturation pulse method is easily understood taking into account the fluorescence quenching process. The peak of fluorescence emission, F_m , is followed, over a time-scale of few minutes, by the decline in fluorescence (Maxwell and Johnson, 2000). This phenomenon, called quenching of fluorescence, indicates all the processes that lower the fluorescence yield below its maximum and includes both photochemical and non-photochemical paths to dissipate excitation energy. The most common parameters used to quantify fluorescence quenching, in addition to those already mentioned (F_o and F_m), are best explained by reference to a typical fluorescence trace (Fig. 2.2).

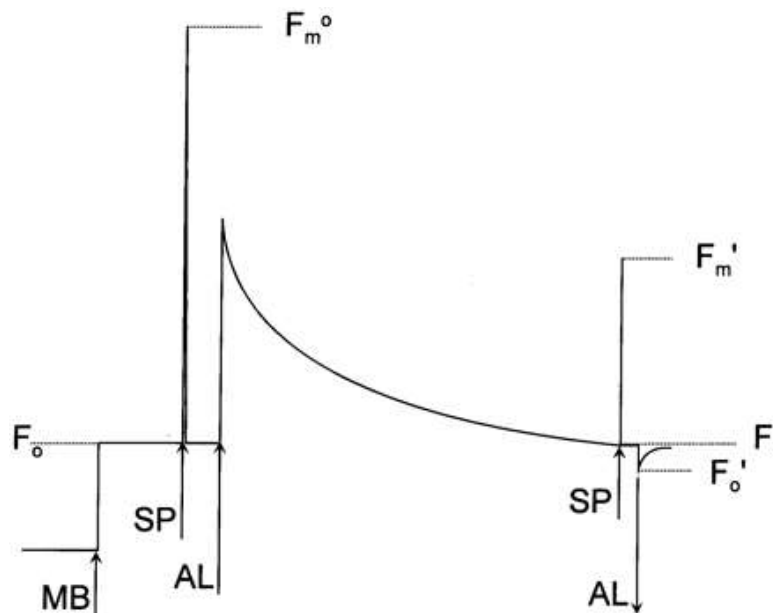


Figure 2.2 Fluorescence induction curve from a PAM fluorometer, illustrating principles of quenching analysis by the saturation pulse method (from Maxwell and Johnson, 2000).

When a measuring beam is switched on ($0.05 \mu\text{mol photons m}^{-2} \text{s}^{-1}$), F_o is measured. Application of saturating flash of light ($8,000 \mu\text{mol photons m}^{-2} \text{s}^{-1}$) allows measuring F_m in the dark-adapted state F_m^o . Then the actinic light, which drives photosynthesis ($80 \mu\text{mol photons m}^{-2} \text{s}^{-1}$), is applied. After a while, more saturating flashes of light are applied, allowing measuring maximum fluorescence in the light F_m' . The steady state value of fluorescence immediately before the saturating flash is termed F_t . By removing the actinic light, in the presence of far red light, it is

possible to measure F_o' . The quenching parameters are measures of the proportion of energy allocated to each de-excitation pathways

Rapid light curves (RLC) provide detailed information on the saturation characteristics of electron transport as well as a reliable assessment of photosynthetic activity and can be used to illustrate the acclimation of the photosynthetic apparatus to a range of light intensities (Ralph and Gademann, 2005). The electron transport rate (ETR) was found to be closely related to the photosynthetic activity when measured by oxygen evolution or CO_2 uptake (Beer et al., 1999). Relative ETR is an approximation of the rate of electrons pumped through the photosynthetic chain (Beer et al., 2001).

$$\text{Relative transport rate (rETR)} = \Phi_{PSII} \times \text{PAR}$$

A rapid light curve measures the effective quantum yield (Φ_{PSII}) as a function of irradiance (PAR) (Ralph and Gademann, 2005) (Fig. 2.3).

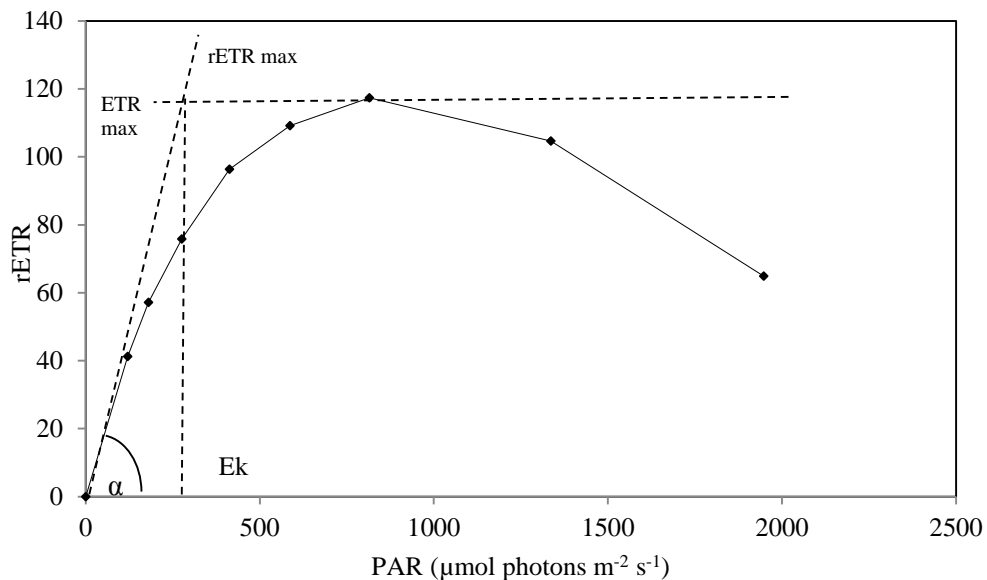


Figure 2.3 Rapid light curve showing *Didymosphenia geminata* diatom fouling response after 1 hour dark adaptation (original data).

The initial slope of the RLC (α) is a measure of the light harvesting efficiency of photosynthesis and the asymptote of the curve, the maximum rate of photosynthesis (ETR_{max}), is a measure of the capacity of the photosystems to utilize the absorbed light energy (Marshall et al., 2000). Minimum saturating irradiance (E_k) is determined by finding the intercept of α with the maximum photosynthetic rate (Sakshaug et al., 1997) and is related to quenching: photochemical quenching dominates below E_k and non-photochemical quenching dominates above E_k (Henley, 1993).

$$E_k = \text{ETR}_{\text{max}} / \alpha$$

Under moderate irradiance, the capacity of the electron transport chain limits photosynthesis and the curve reaches a plateau, where maximum photosynthetic capacity occurs (rETR_{max}) (Schreiber, 2004). With even supra-saturating irradiance the curve tends to decline, which could be related to dynamic down-regulation of PSII (White and Critchley, 1999).

2.3 Application of fluorescence measurements in phytoplankton ecology

Identification of factors limiting growth of algae is of considerable importance for understanding their ecology and guiding water policies and management practices (Shelly et al., 2007). Aquatic primary productivity, especially in surface waters, is frequently limited by availability of nutrients. The photosynthetic light harvesting and energy transduction apparatus is rich in N, Fe, and P and plays an important role in cellular metabolism, as a membrane component, and in energy transduction, as ATP (Beardall et al., 2001). Thus cellular physiology of nutrient-depleted algal cells can manifest itself in major impairment of photochemical efficiency expressed as a decline of F_v/F_m (Beardall et al., 2001; Lippemeier et al., 1999; Parkhill et al., 2001). Several studies have used Chl *a* fluorescence measurements to analyse the effect of nitrogen, phosphate and iron (Berges et al., 1996; Geider et al., 1993; Lippemeier et al., 1999; Petrou et al., 2008) on the photosynthetic capacity of phytoplankton in both natural communities and cultures (Berges et al., 1996; Geider

et al., 1993). Changes in fluorescence signals in response to silica limitation have also been observed in diatoms (Lippemeier et al., 1999). Compared to other methods such as nutrient enrichment bioassays and nutrient uptake kinetics, Chl *a* fluorescence measurements have the advantage of being rapid, sensitive and minimally invasive (Beardall et al., 2001; Parkhill et al., 2001; Wood and Oliver, 1995). It is pointed out that such chlorophyll fluorescence nutrient bioassays are not identical to Nutrient Induced Fluorescence Transients as described below.

2.3.1 Nutrient Induced Fluorescent Transient (NIFT)

NIFT is a technique which allows almost instantaneous assessment of phytoplankton nutrient status. When nutrients, such as nitrogen or phosphorus, are added to phytoplankton cultures limited by that particular nutrient, a change in fluorescence is detectable within minutes (Wood and Oliver, 1995). Conversely, if a non-limiting nutrient or control (water) is added, a fluorescence change generally does not occur (Beardall et al., 2001). The fluorescence response to nutrient addition is believed to increase as nutrient limitation become more pronounced (Holland et al., 2004), it can be either a drop or a rise in fluorescence, depending on the limiting-nutrient and which nutrient form is supplied (Beardall et al., 2001). This change in fluorescence is termed Nutrient Induced Fluorescence Transient (Wood and Oliver, 1995) and it is believed to be attributable to a reallocation of energy from photosynthesis to nutrient uptake (Holland et al., 2004). Because reduction of F_v/F_m is the relative measure of the maximal photochemical efficiency of PSII centres (Wykoff et al., 1998), a decline in F_v/F_m suggests damage to some PSII centres resulting in a reduced fraction of functional PSII reaction centres with increased nutrient starvation (Lippemeier et al., 2001).

NIFTs studies have been consistently demonstrated in laboratory cultures in relation to nitrogen and phosphate in freshwater microalgae (Holland et al., 2004; Shelly et al., 2007; Wood and Oliver, 1995) but none have reported a NIFT response in diatoms. Lippemeier et al., (1999) used PAM techniques to investigate silicate limitation in the diatom *Thalassiosira weissflogii* (Grunow) G.Fryxell & Hasle, showing the influence of silicate metabolism on the variable Chl fluorescence of

diatom cells. Wood and Oliver (1995) demonstrated NIFTs in a number of field samples (mostly in response to ammonia addition), concluding that the technique would be suitable for natural populations to test nitrogen and phosphate limitation.

2.4 Aim of the investigation

In the present study Pulse Amplitude Modulated measurements were performed on fouling samples collected along the two canal walls, to assess the response of *Gomphonema tarraleahae* to light and nutrient (silica, nitrogen and phosphorus) addition. This aimed to confirm the fact that *G. tarraleahae* grows preferably in low light conditions and define the limiting nutrients for bloom formation.

2.5 Materials and methods

Samples of fouling were collected from Tarraleah No. 1 Canal during a canal drainage on 5th November 2012, along the south (S) and north (N) wall at 0.5 (top), 1.4 (medium) and 2.1 m (bottom) below the water surface (Fig. 2.4). The samples were stored in small plastic containers filled with canal water and placed in the dark at ambient temperature for 20 min before the first fluorescence measurement was performed using a Water-Pulse Amplitude Modulated (PAM) fluorometer (Waltz, GmbH, Effeltrich, Germany). Nutrients (0.10 ml) were added to each container to attain a nutrient sufficient solution as below (Table 2.1) and the samples stored in dark conditions for 20 min before the first fluorescence measurement was taken. Samples in the cuvette were static.



Figure 2.4. Collections of fouling samples along the Tarraleah No. 1 Canal walls.

Table 2.1. Estimated final concentration of the nutrients in the test samples

Container	Nutrient
Control	nothing added
Silica	Na_2SiO_3 [36 mg L ⁻¹]
Nitrogen	NaNO_3 [77 mg L ⁻¹]
Phosphorus	K_2HPO_4 [8 mg L ⁻¹]

Rapid Light Curves (RLC) and F_v/F_m values were used as indicators of physiological health. Light curves were constructed by plotting average relative electron transport rate (rETR) against photosynthetically active radiation (PAR).

2.6 Results

2.6.1. Water analysis

Chemical water analysis showed the seasonal trend of silica, nitrogen and phosphate from September 2011 to November 2014 (Fig. 2.5a). The major variation occurred in dissolved silica content, which fluctuated with high values from autumn

to late winter (around 4.5 mg L⁻¹) and falling (around 1 mg L⁻¹) in the spring time. Nitrogen levels showed minimal variations (0.16-0.3 mg L⁻¹) during the sampling period, apart from peaks in October 2012 (0.71 mg L⁻¹) and April 2014 (0.69 mg L⁻¹). Phosphorus exhibited small variations from its basal level (0.005 mg L⁻¹) with peaks in October 2012, April and December 2013 and June 2014 (0.022, 0.015 and 0.01 mg L⁻¹) (Fig. 2.5a). N:P ratio deviated from the Redfield 16N:1P stoichiometry, fluctuating between 12 in August 2014 and 46 in April 2013 (Fig. 2.5b).

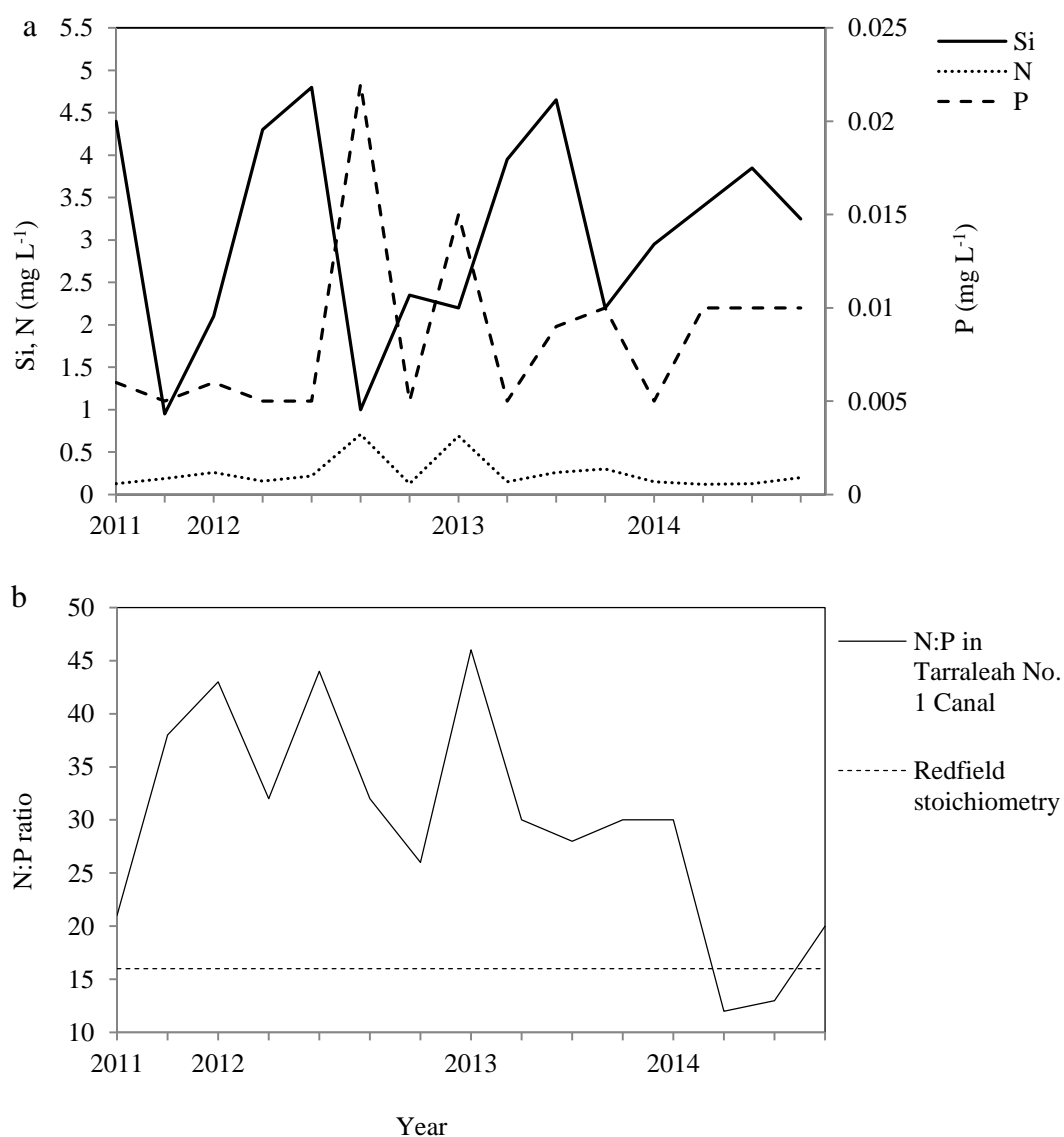


Figure 2.5 Water analysis results from Tarraleah No.1 Canal, from September 2011 to November 2014, showing (a) silica, nitrogen (axis on left) and phosphorus trend (axis on right) and (b) the N:P ratio.

2.6.2 Fluorescence measurements

On the south wall the light curve from the bottom sample had the highest $rETR_{max}$ 138.6, whilst the top and medium were more depressed ($rETR_{max}$ 58.08 and 22.32, respectively). Also, the top and bottom curves showed a progressive increase reaching the $rETR_{max}$ value at the maximum light intensity provided ($1320 \mu\text{mol photons m}^{-2} \text{ s}^{-1}$), whilst the medium sample declined at $558 \mu\text{mol photons m}^{-2} \text{ s}^{-1}$. The top, medium and bottom light curves from the north wall instead were close to each other, not reaching light saturation levels and showing $rETR_{max}$ values (122.76, 120.12 and 105.60 for top, medium and bottom, respectively) at the highest light intensity ($1320 \mu\text{mol photons m}^{-2} \text{ s}^{-1}$) (Fig. 2.6).

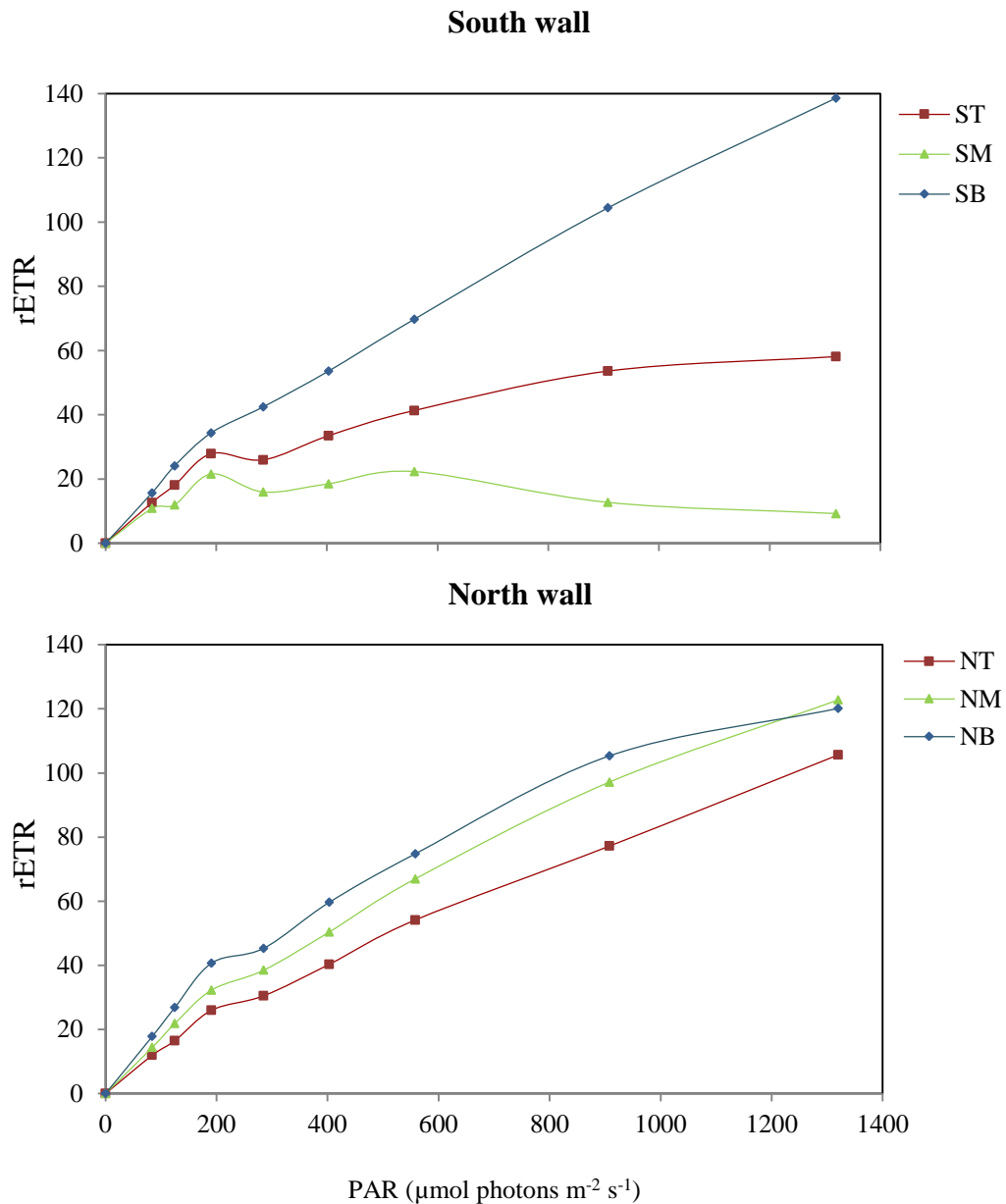


Figure 2.6 Rapid Light Curves in response to light at three depths (top, medium and bottom) on the south (S) and north (N) wall of Tarraleah No. 1 Canal (T=top; M=medium; B=bottom).

Nutrient additions revealed that silica depressed the rETR_{max} values at all three depths, both on the south and the north wall, with a decline of curves corresponding to $191 \mu\text{mol photons m}^{-2} \text{ s}^{-1}$, whilst nitrogen stimulated rETR_{max} at the two walls at both top and medium, whilst there was no effect at the bottom. Phosphorus stimulated rETR_{max} at the two walls at all three depths (Fig. 2.7).

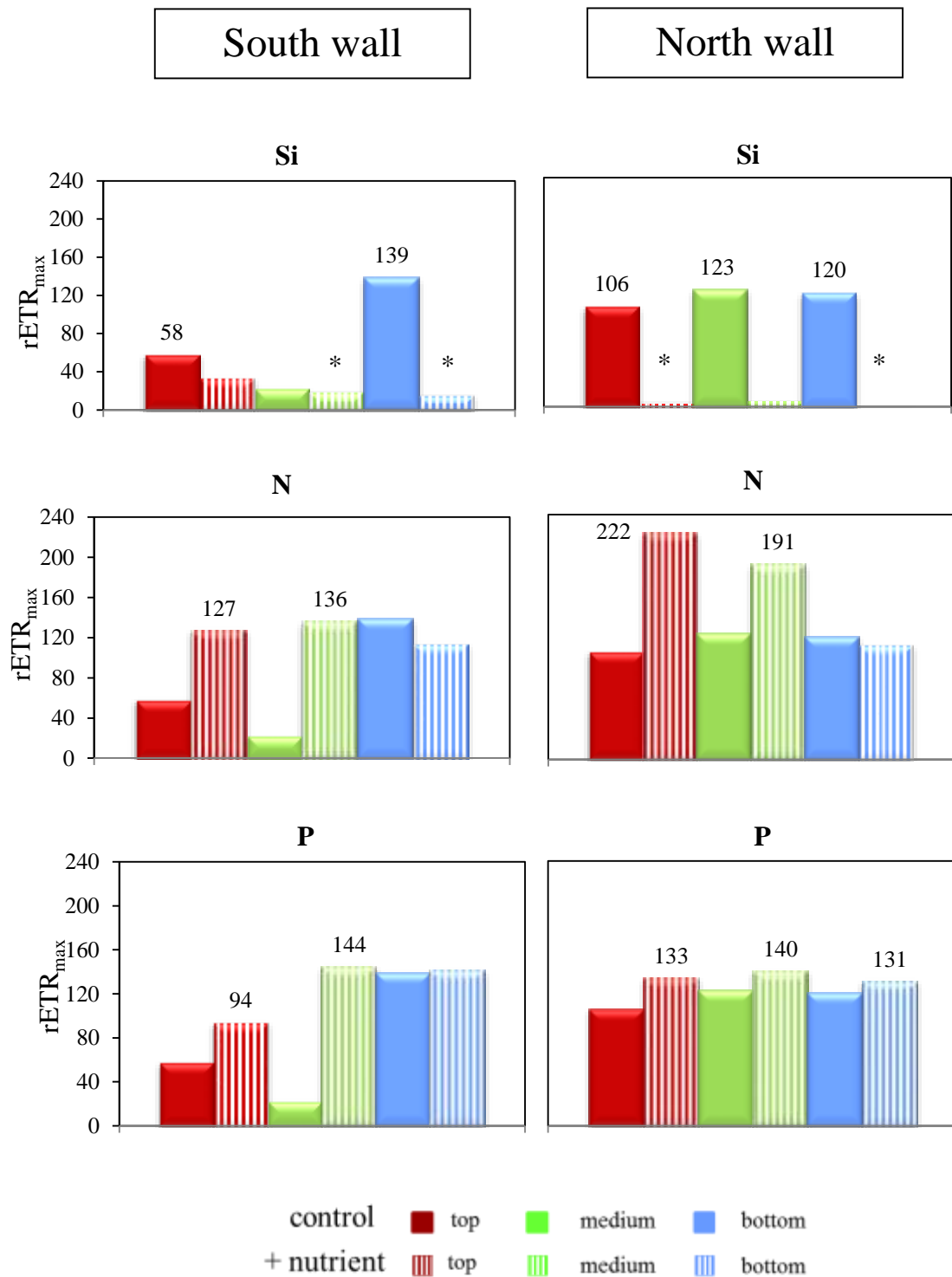


Figure 2.7 Maximum relative Electron Transport Rate values in response to nutrient addition for the south and north wall at the three depths. All rETR_{max} values were reached at PAR=1320 $\mu\text{mol photons m}^{-2} \text{s}^{-1}$, except for values labelled with * (PAR=191 $\mu\text{mol photons m}^{-2} \text{s}^{-1}$).

F_v/F_m values were generally low (0.03-0.31), with silica responsible for the lowest values both in the south (0.13 average of three depths) and north (0.07 average) wall, whilst the highest values were due to nitrogen addition both at the south (0.24 average of three depths) and north wall (0.26 average). Phosphorus slightly increased F_v/F_m above control at the two walls at all three depths (0.18 average at south wall, 0.20 average at north wall) (Table 2.2).

Table 2.2 Influence of nutrient addition on fluorescence yield as a function of depth in Tarraleah No. 1 Canal. S= south; N= north; T= top; M= medium; B= bottom.

Wall and depth	Treatment	F_v/F_m	Wall and depth	Treatment	F_v/F_m
ST	control	0.20	NT	control	0.10
SM	control	0.05	NM	control	0.20
SB	control	0.19	NB	control	0.23
ST	Si	0.12	NT	Si	0.03
SM	Si	0.10	NM	Si	0.08
SB	Si	0.15	NB	Si	0.10
ST	P	0.12	NT	P	0.13
SM	P	0.21	NM	P	0.17
SB	P	0.21	NB	P	0.31
ST	N	0.23	NT	N	0.31
SM	N	0.23	NM	N	0.24
SB	N	0.25	NB	N	0.24

4.7 Discussion

Previous studies already established that the biofouling at Tarraleah No. 1 preferred low light conditions and grew more prolific on the north wall which received less light (Perkins et al., 2010). The RLC confirmed these results, showing the highest light curve for the bottom south wall, which received less light (maximum 80 $\mu\text{mol photons m}^{-2} \text{ s}^{-1}$) compared to medium (maximum 200 $\mu\text{mol photons m}^{-2} \text{ s}^{-1}$) and top locations (maximum 700 $\mu\text{mol photons m}^{-2} \text{ s}^{-1}$). Furthermore, the light curve of the bottom sample was still increasing at 1320 $\mu\text{mol photons m}^{-2} \text{ s}^{-1}$ (maximum light provided), showing that even though the fouling at this depth was adapted to low

light, it remained healthy and its photosynthetic apparatus was able to perform at very high light intensities when provided. In contrast the light curve of the top sample was about to reach its plateau at $1320 \mu\text{mol photons m}^{-2} \text{ s}^{-1}$, whilst that of the medium depth sample reached its peak at $558 \mu\text{mol photons m}^{-2} \text{ s}^{-1}$, indicating that the fouling at these depths was not in optimal conditions and could not perform well at higher light intensities. Reinforcing these results, the light curves from the north wall were similar to the bottom curves for the south wall, with a similarly steep slope which did not show a decline, indicating that the cells remained in optimal conditions along this wall at all three depths.

The novel application in the present work of PAM nutrient bioassays showed a surprising decline of light curves in response to silica addition at both walls at all three depths. This was confirmed by the F_v/F_m results, which also showed a decrease in response to silica. The role of silica in the formation of the diatom frustule is well known (Reimann et al., 1965), and indeed the silica content in the canal water fluctuated seasonally according to diatom abundance, with high values in autumn and winter and rapidly falling with the spring diatom bloom. Therefore the fluorescence $rETR$ and F_v/F_m decrease in response to silica addition was unexpected, and the precise physiological mechanism underpinning this is unclear. Our results cannot be directly compared to the positive changes in fluorescence signals (NIFTs) by diatoms in response to silica limitation as observed by Lippemeier et al. (1999). The generally low F_v/F_m values in our work confirmed how in Tarraleah No. 1 the fouling community on November 2014 was dominated by stalk forming diatoms, typical of a mature community, and characterized by little living material (Perkins 2010). In the long term, the nutrient stress from unbalanced N:P ratios in the canal water might also affect the photosynthetic capacity of the cells and therefore be responsible for their low photosynthetic performance (Beardall et al., 2001). The supply of nitrogen and phosphorus instead triggered an increase in F_v/F_m , most likely due to limitation of these nutrients in the canal water.

Chapter 3*

Role of seasonal variations of light and nutrients on Tarraleah biofouling explored using an experimental pipe test rig

3.1 Introduction

Experiments performed on still algal cultures in flasks do not adequately simulate the conditions under which biofouling grows in the Tarraleah No. 1 Canal, which is subject to high flow rates. Furthermore, because of the distance from the laboratory, security issues and limited access, it was not readily possible to run regular field experiments at Tarraleah Canal. A limited number of biofouling experiments have been previously conducted both in the field (Biggs et al., 1998; Larned and Santos, 2000) and in artificial streams (Biggs et al., 1998; Larned and Santos, 2000; Sabater et al., 2002). Biggs et al. (1998) tested if variations in fouling biomass as a function of velocity could be explained by differences in community growth forms. For this purpose, velocity data were collected from four rivers in New Zealand (Mataura, Cust, Waiau and Hawea) and mucilaginous, short and long filamentous communities surveyed. Furthermore, using an artificial stream, the water was diverted from Kaiapoi River into an unshaded flat channel lined with coarse cobbles. Five out of six communities surveyed displayed biomass responses as a function of velocity, supporting the hypothesis that mucilaginous communities increase as a function of increasing velocity, stalked/short filamentous communities are expected to be more vulnerable to dislodgement by shear stress because of the greater form drag than the mucilaginous communities and filamentous algal

* In preparation for publication (in part) in the journal *Biofouling* as: Matilde Ravizza, Alan Henderson, Jessica Walker, Jane Sargison, Dean Giosio, Jennifer Shaw, Sazlina Salleh, Gustaaf Hallegraeff. Light and nutrients as key drivers of freshwater biofouling and surface roughness in an experimental hydrocanal pipe rig.

communities decrease with increasing velocity.

Sabater et al. (2002) investigated whether variations in current velocity influenced the effects of copper on community structure, biomass and photosynthesis of diatom-dominated communities in artificially lit perspex channels receiving continuous water flow (1.5 L min^{-1}) from a well. It was found that copper effects on photosynthesis occurred earlier at moderate than at low current velocities and this effect was permanent. Larned and Santos (2000) investigated the hydraulic conditions under which nutrient uptake was controlled by mass transfer through diffusive boundary layers or by membrane kinetics. The experiments were performed in a 150 cm long x 40 cm wide acrylic flow tank (150 L) lit by a halogen lamp at $275 \mu\text{mol m}^{-2}\text{s}^{-1}$. Nutrient uptake is mass-transfer limited under all hydraulic conditions used; there is no indication of kinetic control. Optimal velocities for growth vary with nutrient concentration and periphyton stature.

In the present study an artificial stream was first designed by Perkins (2010) and constructed at the School of Engineering. It included a head and end tank, a flume and connecting pump, as shown in Fig. 3.1.



Figure 3.1 Artificial stream at the School of Engineering, comprising a head and an end tank and a flume.

For reasons unknown, the artificial lab stream failed to produce significant biofouling. Limited fouling included *Gomphonema* attached to rocks and glass

slides but this did not survive for more than 15-20 days. Similarly, in spite of repeated attempts, it was not possible to culture *G. tarraleahae* under stationary laboratory conditions.

3.2 Pipe Test Rig

To continue performing experiments in running water, a test rig was designed and built in collaboration with the School of Engineering and installed on the 1st of March 2013 at the Hydro Tasmania Tarraleah Power Scheme Pond No.1 (Fig. 3.2).



Figure 3.2 Pipe Test Rig set up at the Hydro Tasmania Tarraleah Power Scheme Pond No.1.

The setup consisted of a submergible pump and four test sections arranged in series with varying light transmittance (metal, opaque PVC, frosted PVC and clear PVC) (Fig. 3.3), two additional clear PVC test sections with static pressure tapings and Pitot probe openings and connection/extension piping (flanges, flexible piping), five light and temperature sensors, and photogrammetry plates. Three different types of materials were used for the pipes within the rig: metal painted in Interzone 954, white PVC and UV resistant clear plastic.

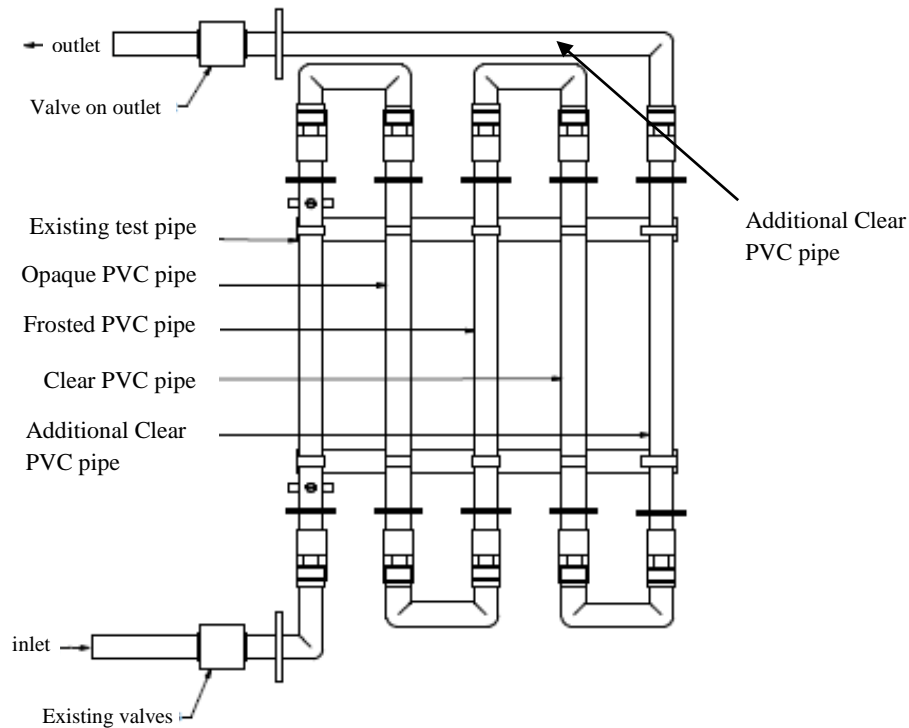


Figure 3.3 Light test sections design in the Pipe Test Rig, set up at the Hydro Tasmania Tarraleah Power Scheme Pond No.1 (Hudson, 2013).

For simplicity, in the rest of the thesis the terms metal, opaque PVC, frosted PVC and clear PVC will be used when referring to the different substrates.

Two additional pipes and photogrammetry plates were used for engineering purposes only. The water was piped to the rig and discharged back into the canal through two flexible PCV pipes. A two valve T-section controlled the flow into the pipe. This arrangement allowed the water to be re-directed out of the rig for each monthly visit, without deactivating the pump and preventing cavitation. The discharge pipe was elevated above the rig ensuring the water was constantly flowing through the test pipes and preventing air entering due to lower than atmospheric pressure in the filled sections (Hudson 2013).

3.2.1 Pump

A D150V submersible pump manufactured by Davey Water Products Pty. Ltd was used to circulate the canal water through the rig. The pump was an open faced, vortex, centrifugal impeller selected due to the ability to pump soft solids (including plant matter) and reduced susceptibility to blockage. It was run from a single phase, two-pole 220-240V motor capable of a speed of 2850 rpm and was installed on the canal wall upstream of the control gate of Tarraleah pond 1. Air pockets were observed passing through the pipes while the pump was in function, suggesting cavitation of the pump (Hudson, 2013).

3.2.2 Light test sections

The first four pipes in series were used to get temperature and light data from the sensors and to test the effect of temperature, seasonal insolation and different combinations of substrata and light treatments on the biofouling community. The pipes were set up in the on-site rig to create a light gradient so the metal pipe would have the lowest light intensity, followed in sequence by the opaque, frosted and clear PVC pipes. Each pipe was 1.5m in length. Due to a malfunction during installation, the clear PVC test pipe was replaced with clear pipe designed for pressure tapings. As a result, the assembly had static pressure tapings and two Pitot tube traverse entrances (Hudson, 2013), used for pipe friction studies.

3.2.3 Light and temperature sensors

Five HOBO sensors 8K/64K Pendants, model UA-002, were installed in the pipes. These sensors were waterproof, two-channel temperature and relative light level data loggers. Data were taken at one-hour intervals and recorded both in Fahrenheit and Celsius for temperature, and both Lumen per ft² and Lux for light intensity. Data were used in Celsius for temperature and converted to $\mu\text{mol photons m}^{-2} \text{ s}^{-1}$ by multiplying Lux by the conversion factor 0.0185 for sunlight provided by <http://www.apogeeinstruments.co.uk/conversion-ppf-to-lux> and these values are in

agreement with the light intensities measured ourselves using a light meter, for light intensity. The device was launched and read-out using an optic base station and coupler with a USB link connected to computer with respective software installed. The sensors, as well as the photogrammetry plates, were located in the flow downstream of the test sections, not to affect biofouling growth, using an aluminium bracket to hold them horizontally oriented (Fig. 3.4).



Figure 3.4 HOBO Pendant light and temperature sensors and holders installed in the Pipe Rig.

3.2.4 Flow velocity

The test rig setup was determined to have a flow at the constant speed of 1.22 m s^{-1} . This was measured by collecting the water in a known volume container and accurately recording the time with a stop watch. Throughout the duration of the study flow velocity was monitored to ensure no blockage effects occurred from the pump.

3.3 Material and methods

3.3.1 Sampling

Four samplings were conducted in April, May and July 2013 approximately every six weeks and in November 2014, 82 days since the last cleaning of the pipes. A plunger with long handle (Fig. 3.5) was used to quantitatively collect biofouling samples from each pipe.



Figure 3.5 Pipe plunge employed to collect fouling samples from the pipes of the Pipe Test Rig.

Pipes were then rinsed with a small amount of water, which was kept and used to maintain the fouling alive. Samples from each pipe were stored separately (Fig. 3.6) and used to quantify the fouling dry and wet weight.



Figure 3.6 Biofouling samples scrubbed from the four pipes of the Pipe Test Rig in Tarraleah and preserved in plastic containers (Hudson, 2013).

Four fouling samples were also collected from non-scrubbed parts of the rig (providing the same light conditions of the corresponding pipe but in which fouling was growing undisturbed) and kept in separate containers for microscopy and PAM measurements.

3.3.2 Microscopy

Fouling samples from each pipe were analysed by optical microscopy to determine species composition and percentage of coverage. For this purpose, a few drops of fouling were pipetted on to a glass slide and covered with a cover slip, then after choosing a desirable area, all the visible cells were counted at 200x magnification. Furthermore, several subsamples were analysed to determine the recurring species in the fouling and to obtain a taxonomic overview of the biofouling community.

3.3.3 Wet and dry weight

The fouling samples from each pipe were filtered separately using a 20µm metal screen so that all the fouling was retained. The wet weight was measured once the fouling was well drained. Straight after the fouling was placed in aluminium foil open containers, covered with perforated aluminium foil and left in a 42°C oven until dry. Then the remaining amount of fouling was weighted again to record the dry weight.

3.3.4 Metagenomic analysis

The fouling samples from the pipes were sent for metagenomics analysis to the University of Adelaide and carried out by Jennifer Shaw. Four DNA extractions were carried out per sample using the MoBio PowerSoil DNA Isolation Kit (MoBio Laboratories Inc., Solana Beach, CA, USA) according to the manufacturer's protocol. Extraction blank controls, where the environmental sample is substituted for DNA-free molecular-grade water, were processed in parallel to assess potential

background contamination from the laboratory environment and reagents. DNA was PCR-amplified using two primer sets: a bacteria-specific 16S rDNA primer pair (Caporaso *et al.*, 2012) and a eukaryote-specific 18S rDNA primer pair targeting the V9 hypervariable region (Amaral-Zettler *et al.*, 2009). Both primer sets contain the Illumina MiSeq (Illumina, San Diego, CA, USA) sequencing adapters (Caporaso *et al.*, 2012) and a 12bp sample-specific barcode (Earth Microbiome Project: <http://www.earthmicrobiome.org/emp-standard-protocols>) to allow eDNA sequences to be assigned back to the respective sample post-sequencing. All extracts (including extraction blanks) were PCR-amplified in triplicate reactions to reduce PCR bias (Polz and Cavanaugh, 1998). The DNA extraction, PCR master-mix preparation, and the addition of the DNA to the PCR master-mix were all carried out in separate rooms within dedicated, ultraviolet irradiated hoods to reduce the likelihood of laboratory- and cross-contamination. PCR reactions were prepared as 25 µl reactions, consisting of 14.65 µl H₂O, 1x HiFi Buffer, 1 mg/ml RSA, 2 mM MgSO₄, 0.4 mM of the forward and reverse primer, 0.25 mM dNTPs, 0.02 U/µl HiFi Taq, and 2 µl of DNA template in a 25 µl reaction volume. Cycling conditions for 18S rDNA primers were as follows: hot start at 72°C for six minutes, followed by 35 cycles of 72°C for 40 s, 55°C for 30 s, and 72°C for 40 s, with a final extension of 72°C for ten minutes. Cycling conditions for bacterial 16S primers were as above except the number of cycles were reduced to 30x. PCR products were visualized by gel electrophoresis on 2% agarose gels. Replicate PCR reactions were pooled and cleaned with Agencourt AMPure XP beads, (Beckman Coulter, Brea, CA, USA) as per the manufacturer's instructions. Samples were quantified using fluorometric quantitation (Qubit 2.0, Life Technologies, CA, USA) and pooled to equimolar concentrations. The pooled DNA library was quantified using the Illumina KAPA library quantification kit (KAPA Biosystems, Wilmington, Massachusetts, USA) and sequenced on the Illumina MiSeq using 2x 150bp chemistry and custom sequencing primers.

3.3.5 PAM fluorometry measurements

Pulse Amplitude Modulation fluorometry measurements were performed on biofouling samples collected from the four test pipes in April, May and July 2013 and November 2014. The photosynthetic parameters of the fouling samples were measured using a high resolution chl *a* fluorometer (Water-Pulse Amplitude Modulated [PAM], Walz GmbH, Effeltrich, Germany). The fluorescence reading of the PAM was set to zero prior to any measurements using distilled water. Samples from each pipe were dark-acclimated for 20 min prior to measurement. In April and July 2013 and November 2014, nutrient bioassays were also performed to check the fouling response to phosphate, nitrogen and silica. Nutrients (0.10 ml) were added to each container to attain a nutrient sufficient solution as follows: Na₂SiO₃ [36 mg L⁻¹]; NaNO₃ [77 mg L⁻¹]; K₂HPO₄ [8 mg L⁻¹] and the samples stored in dark conditions for 20 min before performing the first fluorescence measurement. In all cases, each sample was exposed to three measurements and F_v/F_m measured. The average of three measurements was then taken. Samples in the cuvette were static. In November 2014 Rapid Light Curves (RLC) were constructed by plotting rETR against PAR values. The average of three curves was considered for each treatment.

3.4 Results

3.4.1 Water analysis and sampling

The samples from the pipes were collected in April 2013 when nitrogen and phosphorus concentrations were high (0.69 and 0.015 mg L⁻¹, respectively) and whilst silica level was high but not at its peak (2.20 mg L⁻¹) (Fig. 3.7). In July instead nitrogen and phosphorus concentration fell (0.15 and 0.005 mg L⁻¹, respectively), whilst silica increased (3.95 mg L⁻¹). In November 2014, the situation changed again, with nitrogen and phosphorus at intermediate concentrations (0.2 and 0.01 mg L⁻¹), whilst silica level was reduced (3.25 mg L⁻¹).

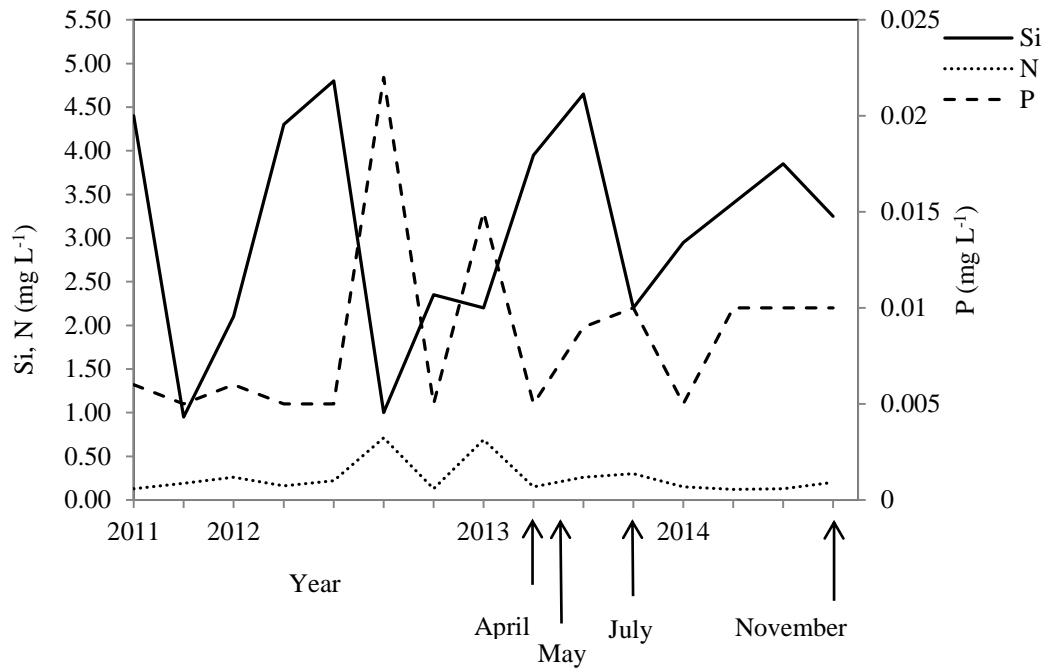


Figure 3.7 Water chemistry from Tarraleah No.1 Canal, from September 2011 to November 2014, showing silica, nitrogen (axis on left) and phosphorus (axis on right). Arrows indicate the timing of fouling collections from the pipes in April, May and July 2013 and November 2014.

3.4.2 Light and temperature

Plots from the HOBO sensors confirmed that the metal pipe had the lowest light intensity ($0 \mu\text{mol photons m}^{-2} \text{s}^{-1}$), followed by the opaque PVC (max $6 \mu\text{mol photons m}^{-2} \text{s}^{-1}$), frosted PVC (max $1937 \mu\text{mol photons m}^{-2} \text{s}^{-1}$) and clear PVC (max $2957 \mu\text{mol photons m}^{-2} \text{s}^{-1}$). The temperature in the four pipes showed comparable seasonal trends throughout the period (Fig. 3.8).

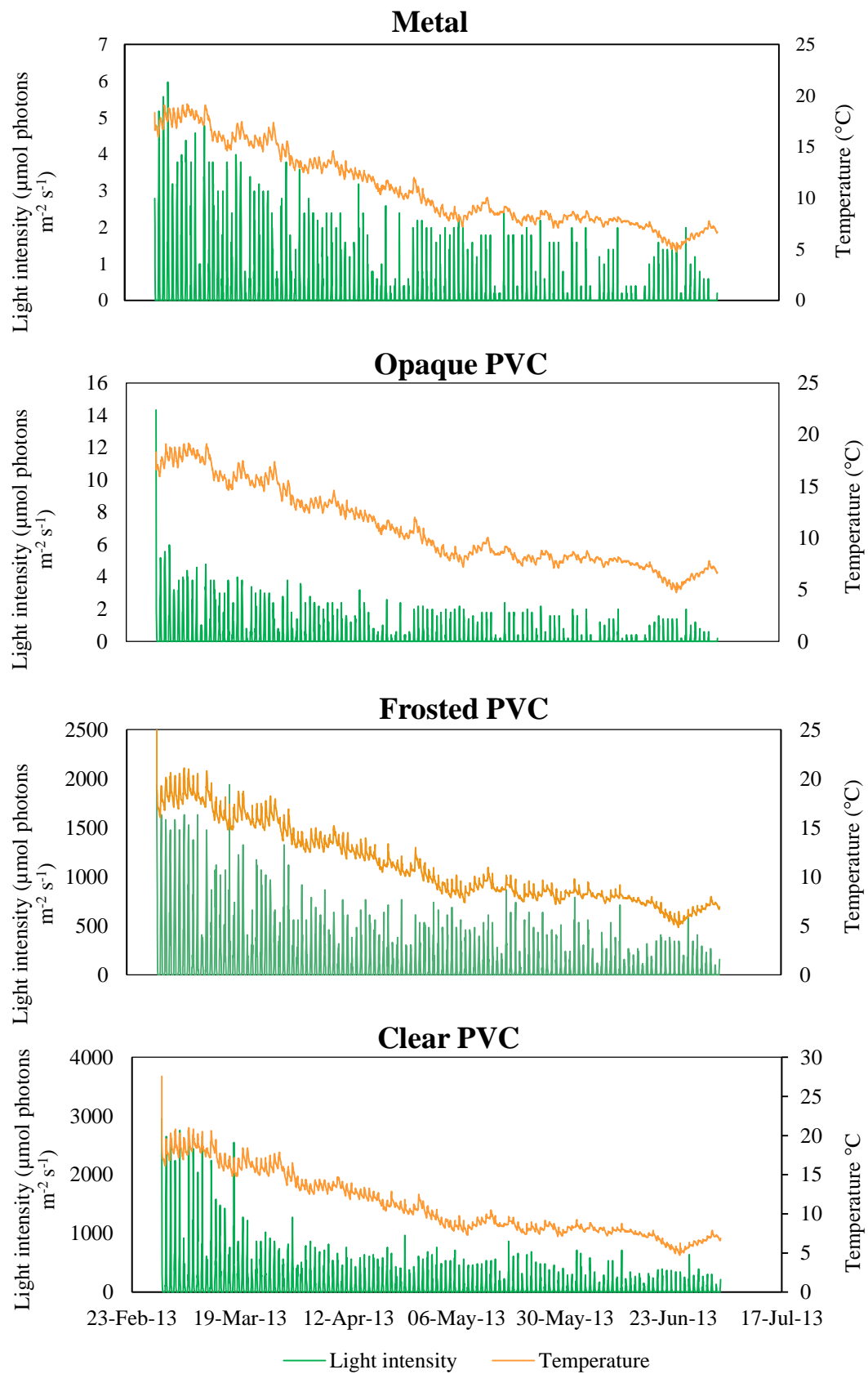


Figure 3.8 Light intensity and temperature data in the metal, opaque, frosted and clear PVC pipes from March 2013 to July 2013 in the Pipe Test Rig set up at the Hydro Tasmania Tarraleah Power Scheme Pond No.1.

3.4.3 Species composition and percentage of coverage

The fouling in the metal and opaque PVC pipes was covered in iron-encrusted organic matter, as a result of which it was not possible to estimate percentage of coverage of individual species (Fig. 3.9 and 3.10).

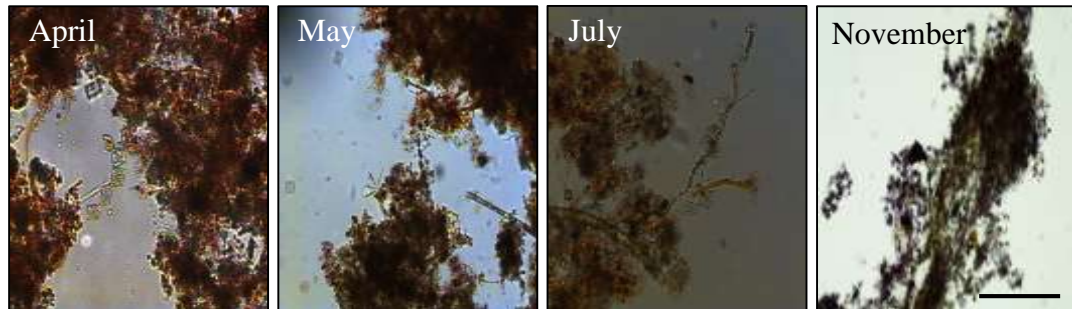


Figure 3.9 Microscopic characterization of fouling samples from the metal pipe of the Pipe Test Rig, collected in April, May and July 2013 and November 2014 (scale bar = 100µm).

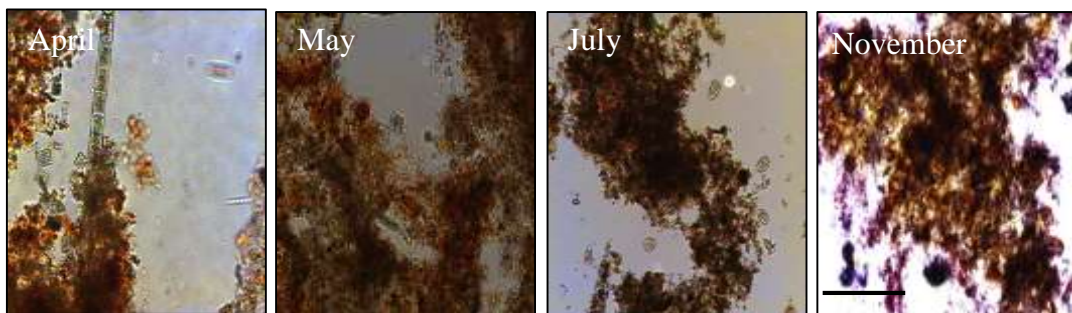


Figure 3.10 Microscopic characterization of fouling samples from the PVC pipe of the Pipe Test Rig, collected in April, May and July 2013 and November 2014 (scale bars = 100µm).

For the fouling in the frosted and clear PVC pipe, it was possible to give a numerical percentage of coverage for *T. flocculosa* and *G. tarraleahae*. The rest of species were included in a single category called “other cells”. *T. flocculosa* dominated the community throughout the period considered, with percentages above 90% in the winter and 70% in the spring, whilst *G. tarraleahae* increased in coverage from below 3 in winter to above 10% in spring (Table 3.1, Fig. 3.11 and 3.12).

Table 3.1 Percentage of diatom species coverage in the frosted and clear PVC pipe of the Pipe Test Rig, in April, May and July 2013 and November 2015.

		16 April 2013	14 May 2013	3 July 2013	11 November 2014
Frosted PVC	<i>Tabellaria flocculosa</i>	94	96	94	79
	<i>Gomphonema tarraleahae</i>	3	2	3	12
	Other species	3	2	3	9
Clear PVC	<i>Tabellaria flocculosa</i>	95	96	95	71
	<i>Gomphonema tarraleahae</i>	3	2	2	11
	Other species	2	2	3	18

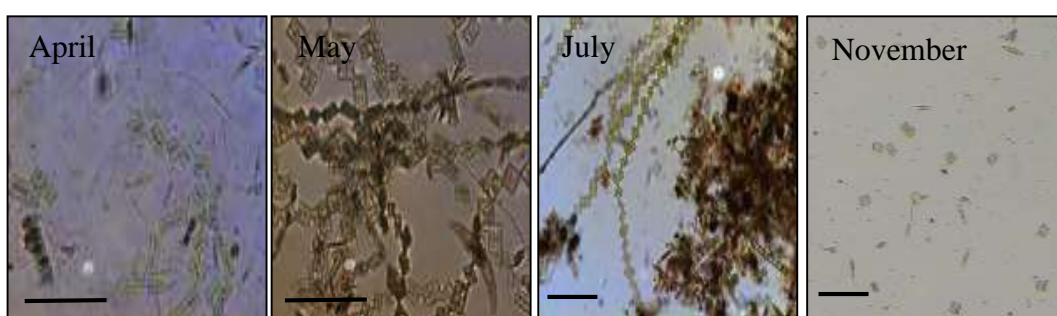


Figure 3.11 Microscopic characterization of fouling samples from the frosted PVC pipe of the Pipe Test Rig, collected in April, May and July 2013 and November 2014 (scale bars = 100µm).



Figure 3.12 Microscopic characterization of fouling samples from clear PVC pipe of the Pipe Test Rig, collected in April, May and July 2013 and November 2014 (scale bars = 100µm).

The species composition comprised mainly pennate diatoms (*Craticula* cf *cuspidata*, *Cymbella* sp., *Diadmesmis* sp., *Fragilaria crotonensis*, *Gomphonema tarraleahae*, *Nitzschia* sp., *Pinnularia* sp., *Synedra* sp., *Tabellaria flocculosa*), sparse centric diatoms (*Aulacoseira granulata*), a moderate number of green algae (*Cylindrocystis*, *Genicularia elegans*, *Golenkinia radiata*, *Pediastrum boryanum*,

Spirogyra sp.) and one dinoflagellate species (*Peridinium* sp.). *G. tarraleahae* was found in patches, producing long stalks with cells on top (Fig. 3.13). At this early fouling stage, *G. tarraleahae* was not dominating the fouling community in terms of number of cells but where present its stalks were forming a noticeable mat.



Figure 3.13 *Gomphonema tarraleahae* in the clear pipe in November 2014.

3.4.4 Fouling wet and dry weight

The amount of fouling collected varied with the different pipes and according to the season. During autumn-winter months (April, May and July 2013) the opaque PVC pipe showed a very small amount (11.83, 8.06 and 16.03 g wet weight, respectively) of fouling at each collection, approximately one third of what was present in the other pipes. For the opaque, frosted and clear PVC pipes the quantity of fouling slightly decreased from April to May and then drastically increased until July, while for the metal pipe it was constant until May and then decreased (Fig. 3.14). Also, for the metal, frosted and clear PVC pipes the dry weight was between 10 and 15 times less than the wet weight. For the opaque PVC pipe the dry weight was instead between 20 and 36 less than the wet weight. In addition, the metal and opaque PVC pipes fouling samples had a different iron-encrusted texture compared to those from the frosted and clear PVC pipes. The former appeared as brown particles homogeneously distributed in the water and with brown colour, while the latter were slimy, patchy and greenish. In the spring (November 2014) the amount of fouling was lower in the metal, frosted and clear PVC pipes, compared to the

autumn-winter months. In the opaque PVC pipe, however, the amount of fouling did not vary from previous months, maintaining also the same proportions between dry and wet weight. The ratios between wet and dry weight increased instead to 23 and 25 in the clear and metal pipes respectively and to 43 in the frosted PVC pipe (Fig. 3.14).

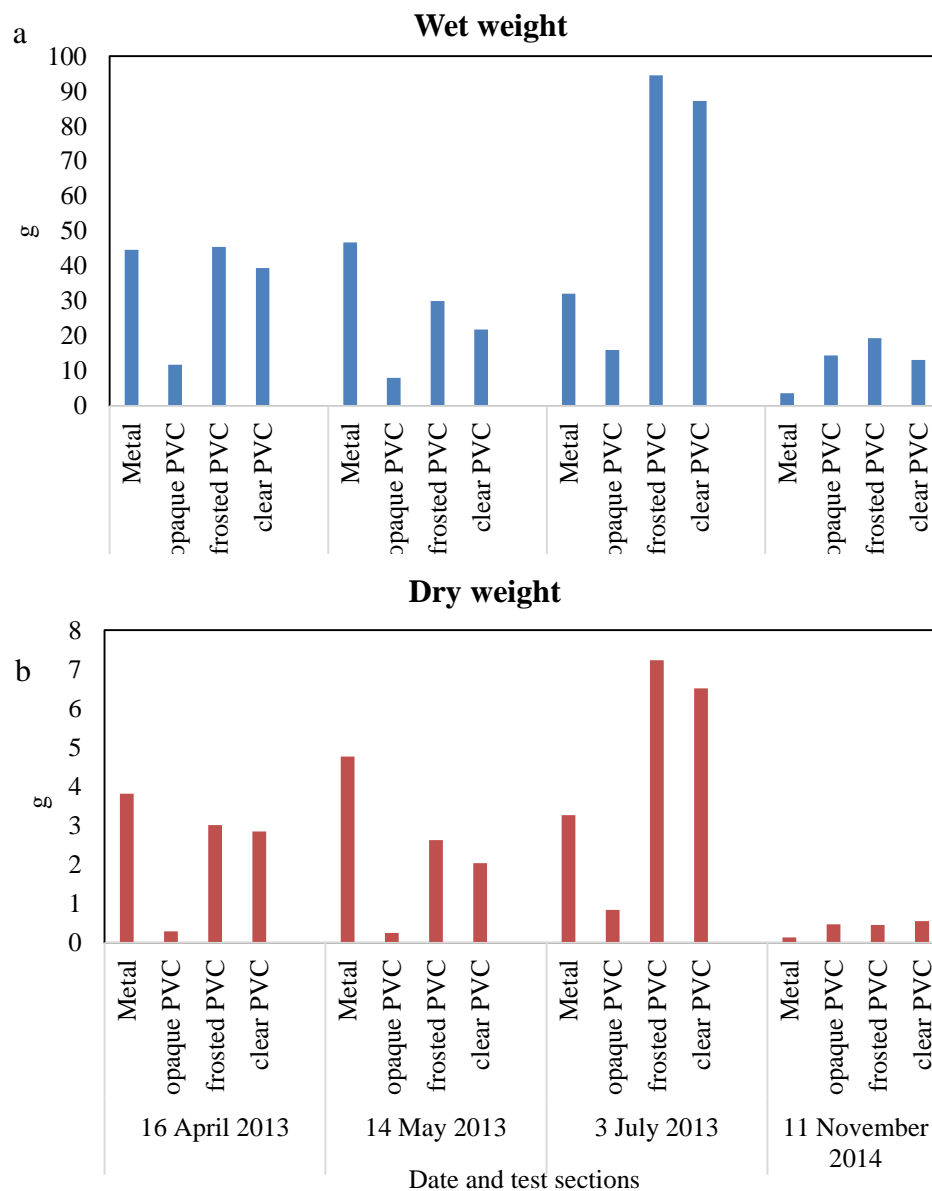


Figure 3.14 Biofouling wet (a) dry (b) weight from the metal, opaque PVC, frosted PVC and clear PVC test sections in April, May and July 2013 and November 2014.

3.4.5 Metagenomic analysis

Eukaryote diatom sequences (including *Tabellaria* and *Gomphonema*) were evident in both PVC frosted (13% of total eukaryotes) and PVC clear (22%) pipes but negligible (1-2%) in the metal and opaque PVC pipes. Green plants (mostly vascular plants) showed the opposite pattern and were prominent in the metal and opaque PVC (32%), less abundant in the PVC frosted pipe (20%) but negligible in the high light PVC clear pipe (0.25%). Fungi (including *Leotiomyces* and *Lemonniera*) were slightly more abundant in the metal pipe (33%) but equally present (20-25%) in all other pipes. Bacterial diversity was roughly similar in all pipes, except for the higher abundance in the dark metal pipe of *Planctomyces* including Gemmata (21% vs 12-15% of total prokaryotes in other pipes) and Rhizobiales including Methylocystaceae (15% vs 7-9% in other pipes). Shannon diversity indices for higher in the metal pipe for both eukaryote (3.5 in steel, versus 2.8-3.2 in other pipes) and notably prokaryote sequences (5.3 in steel, versus 4.5-5.0 in other pipes) (Fig. 3.15).

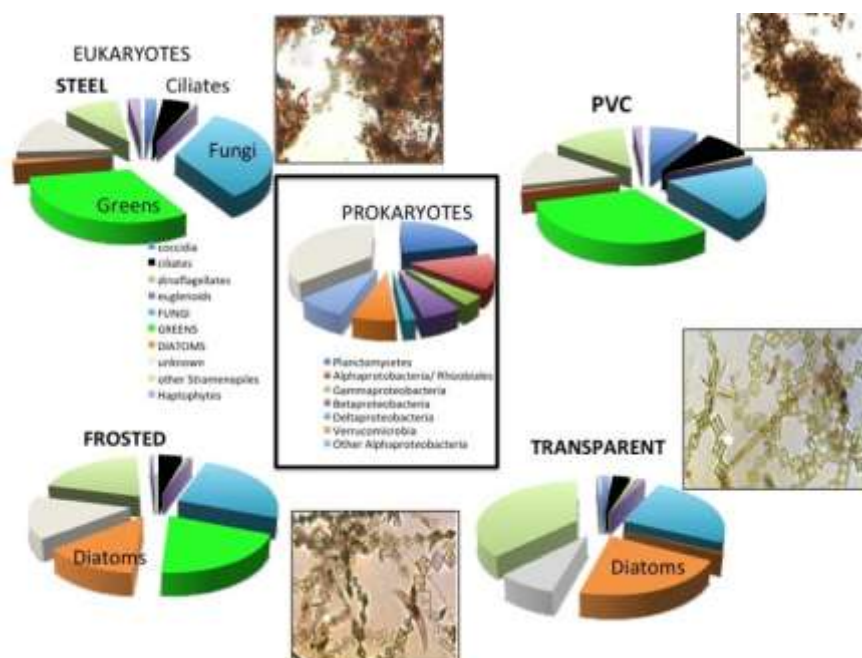


Figure 3.15 Taxonomic partitioning of eukaryote DNA sequences extracted from fouling material in the steel, PVC, frosted and transparent pipes as collected on 17 Feb 2015. Diatoms were abundant in the frosted and transparent pipes, while green plants were absent from the transparent pipe. Fouling in the metal and PVC pipes were dominated by fungal slimes. Companion prokaryote sequences (central diagram: only shown for steel pipe) were roughly similar in all pipes.

3.4.5 PAM data

F_v/F_m values increased from April to July for the samples from the metal, frosted and clear PVC pipes, reaching high values for phytoplankton (0.62, 0.69 and 0.65 respectively), while they slightly decreased from May to July in the opaque PVC pipe, though remaining high (0.59) (Fig. 3.15). In April F_v/F_m was highest in opaque PVC and lowest in metal pipes and was intermediate in the frosted and clear PVC pipes ($F_{3,20}=3.71$, $P<0.03$; Fig. 3.15). The situation changed, however, in May at which time the F_v/F_m levels were highest in the opaque and clear PVC pipes and lower in the frosted PVC and metal pipes ($F_{3,8}=8.53$, $P<0.007$; Fig. 3.15). In July the situation was different again with F_v/F_m being highest in the frosted PVC and lowest in the opaque PVC with the metal and clear PVC pipes being intermediate ($F_{3,20}=4.46$, $P<0.02$; Fig. 3.15). In November F_v/F_m values were generally lower, with the highest value for the frosted pipe (0.51; $F_{3,36}=3.43$, $P<0.27$) and the lowest for the clear pipe (0.43), whilst for the opaque PVC and metal pipes they were intermediate (Fig. 3.16).

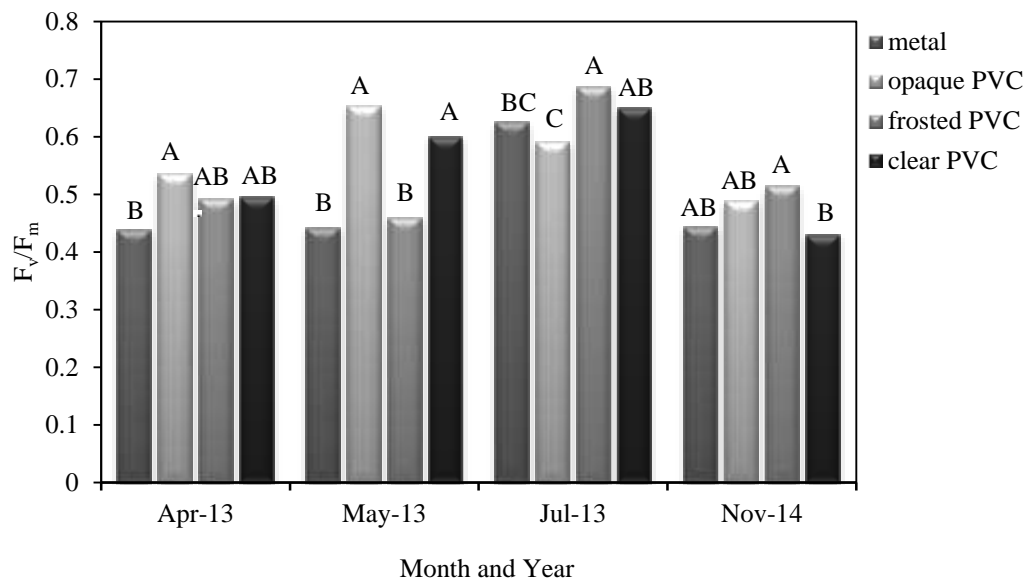


Figure 3.16 F_v/F_m average values in the four light test sections in April, May and July 2013 and November 2014. Those means with same letter within a sampling period were not significantly different ($P=0.05$).

Nutrient bioassays showed that F_v/F_m increased in all treatments from April to July. In April F_v/F_m was lowest for the control (0.45) and highest for silica (0.54), whilst in July the fouling responded with highest values of F_v/F_m to N addition (0.66) and lowest to silica (0.60), even though the difference was small and the F_v/F_m values were above 0.6 in all treatments. The increase in F_v/F_m from April to July was particularly sharp for the control, P and N and (29, 24 and 29%, respectively) and less pronounced for silica (10%) (Fig. 3.16). Analysis of variance indicated that in winter there were significant effects of both the pipe material and nutrient treatments on photosynthetic efficiency of the biofouling film but that these effects varied substantially with sample date. Thus, there was a significant Date x Pipe material interaction ($F_{6,48}=6.53$, $P<0.0001$) as well as significant Date x Nutrient interaction ($F_{3,48}=5.32$, $P<0.003$). Significantly, there was neither Nutrient x Pipe material nor Date x Pipe material x Nutrient interaction, indicating that the effect of nutrients was independent of the pipe material and that the effect of the pipe material on F_v/F_m was consistent across all the nutrient treatments (Fig. 3.17).

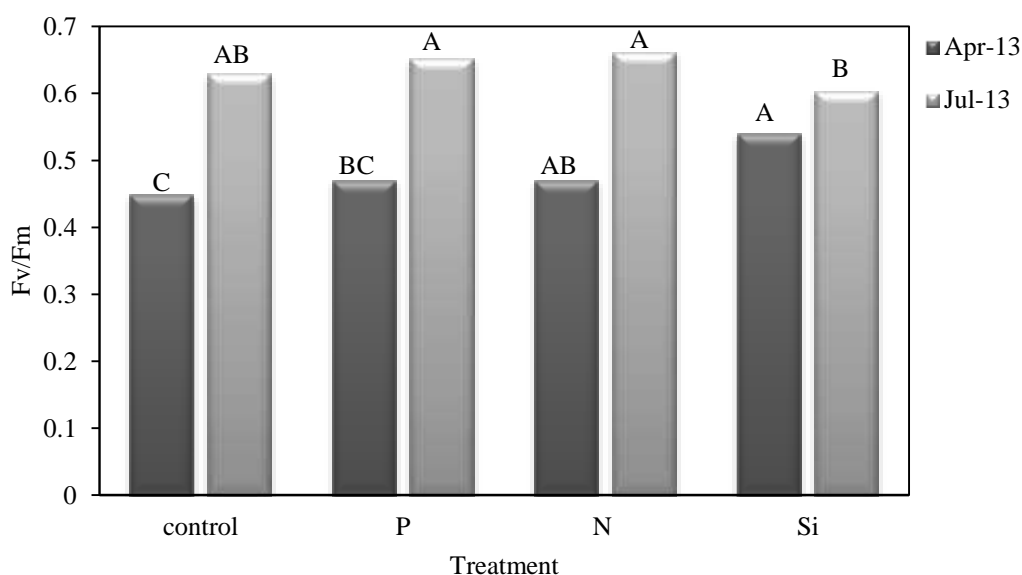


Figure 3.17 F_v/F_m values in the four pipes in response to P, N and Si addition in April and July 2013. Those means with same letter are not significantly different ($P=0.05$).

Analysis of variance showed that in spring there was instead a significant influence of pipe material on the nutrient treatment. For this reason, the spring data were treated separately from other values. In the metal pipe all treatments increased F_v/F_m above control ($F_{3.6}=18.37$, $P<0.002$), whilst in the opaque PVC pipe phosphorus was the only equivalent to the control value (0.56), and there were strong effects of both nitrogen and in particular silica (0.44 and 0.32, respectively; $F_{3.6}=49.74$, $P<0.0001$) in depressing fluorescence. Silica was responsible for lowering fluorescence also in the frosted PVC pipes (0.46), whilst phosphorus and nitrogen did not have any effect. In the clear pipe instead nutrients addition had no effect on F_v/F_m ($F_{3.6}=0.75$, $P<0.57$) (Fig. 3.18).

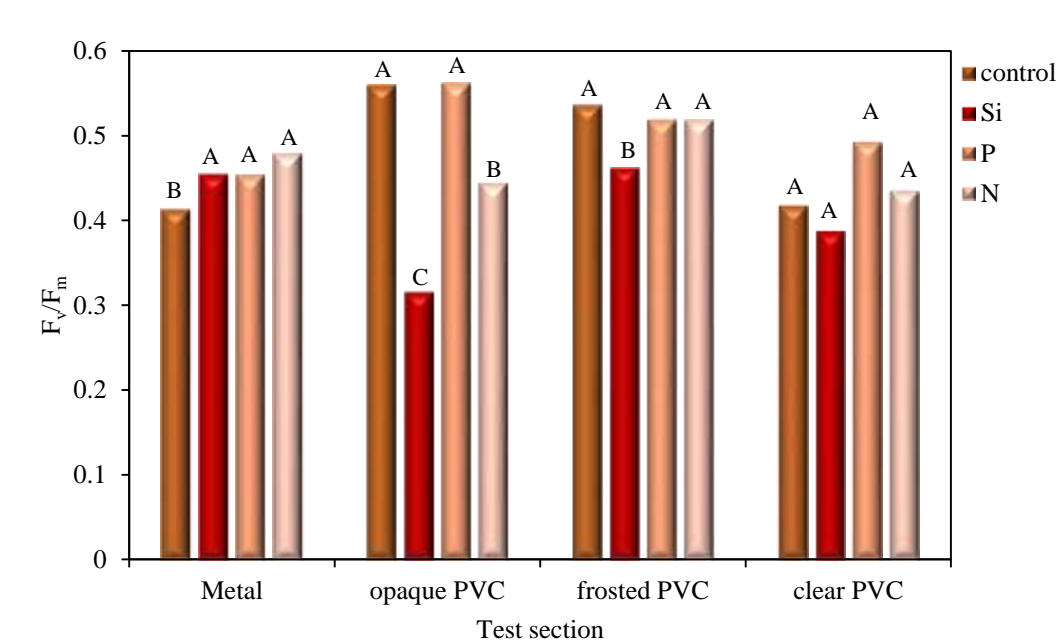


Figure 3.18 F_v/F_m values in the four light test sections in response to silica, nitrogen and phosphorus in November 2014. Means with same letter within each treatment are not significantly different ($P=0.05$).

In November 2014 the RLC showed different responses of the fouling to nutrient addition, according to the pipes. In the metal pipe the fouling was positively responding to phosphorus (68.50 $rETR_{max}$) and nitrogen (77.16 $rETR_{max}$) addition, whilst the response to silica was similar to the control (46.01 and 42.81, respectively

rETR_{max}). Fouling in the opaque PVC pipe was instead inhibited by silica (9.73 rETR_{max}) and nitrogen (34.25 rETR_{max}) and did not respond to phosphorus (71.16 rETR_{max}, excluding an outlayer, similar to the control). In the frosted and clear PVC pipes all the curves from the different treatments showed the same trend. Phosphorus and nitrogen curves in the frosted PVC pipe exhibited a steep slope and high rETR_{max} (125.90 and 117.69 respectively) at 782 $\mu\text{mol photons m}^{-2} \text{ s}^{-1}$, similarly to those in the clear PVC pipe (112.21 and 89.93 rETR_{max}). Silica and control exhibited instead a lower rETR, corresponding to 57.60 and 36.80 respectively for the frosted PVC at 480 $\mu\text{mol photons m}^{-2} \text{ s}^{-1}$, and to 37.92 and 53.69 respectively for the clear PVC at 480 and 782 $\mu\text{mol photons m}^{-2} \text{ s}^{-1}$, respectively (Fig. 3.19).

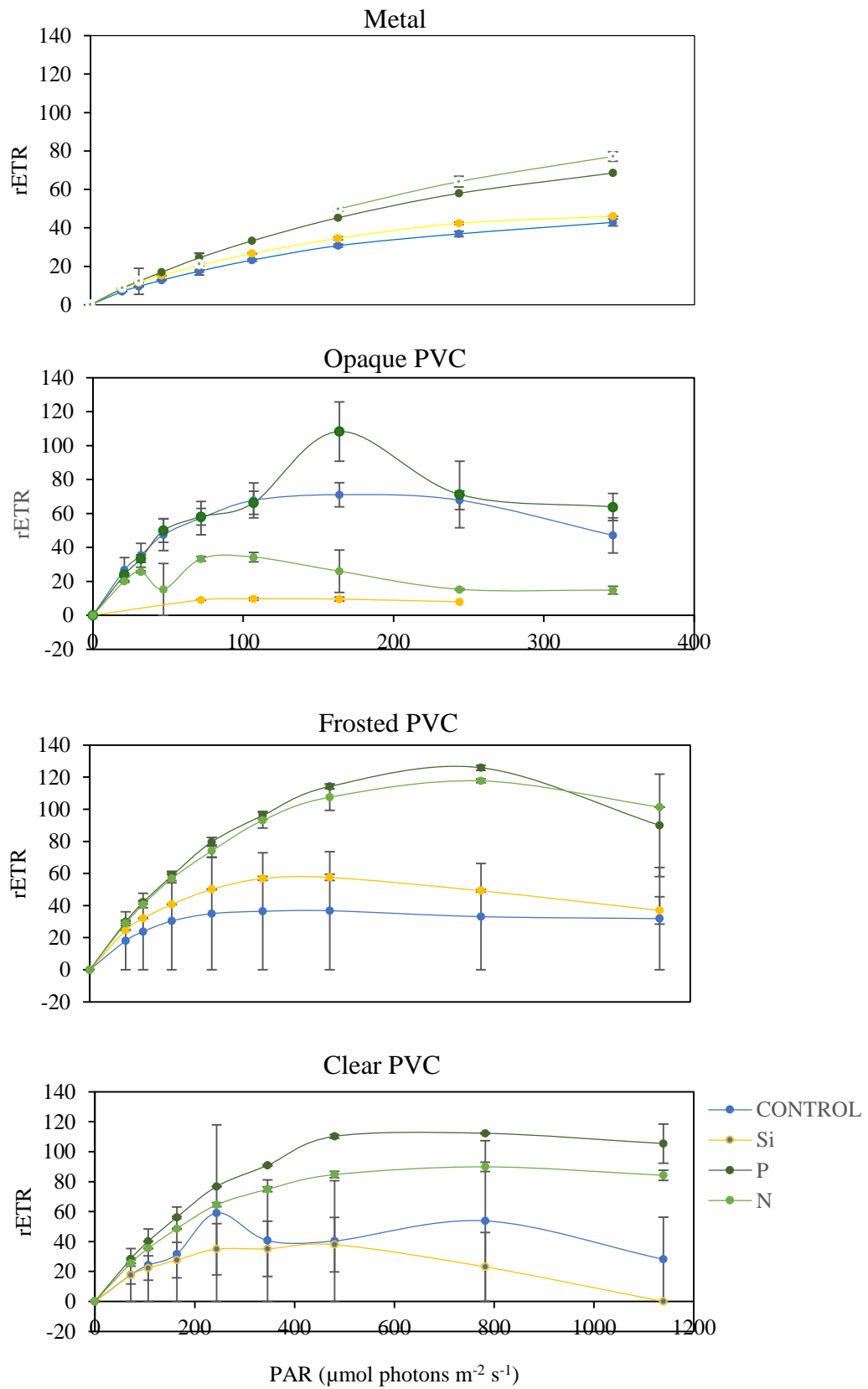


Fig. 3.19 Rapid Light Curves in response to P, N and Si addition in the metal, opaque PVC, frosted PVC and clear PVC test sections in November 2014.

3.5 Discussion

During the autumn-winter period, the early stages of the biofouling community in the frosted and clear PVC pipes of the test rig were represented mainly by benthic diatoms among which *T. flocculosa* prevailed (> 90% of total cells), whilst *G. tarraleahae* was present in small concentrations (< 3%). A similar community occurred in the spring time but with a lower percentage of *T. flocculosa* (79 and 71% in the frosted and clear PVC pipes respectively) and a higher fraction of *G. tarraleahae* (12%). This might be explained by the fact that in November 2014 the fouling had the opportunity to grow in the pipes for a longer period (82 days) before being collected and the community started to evolve towards a more mature stage, which includes *G. tarraleahae* (Perkins et al., 2010). In the autumn-winter period the amount of fouling was similar in the metal, frosted and clear PVC, whilst it was much lower in the opaque PVC pipe probably due to the smoother surface within the pipe, which discouraged the fouling species from attaching. Also, the consistent difference between wet and dry weight in the opaque PVC pipe samples indicated that a significant amount of water (above 95%) was stored in the fouling mat. In spring 2014 the amount of fouling in the metal, frosted and clear PVC pipes was lower than that recorded in the autumn-winter months. Fouling was expected to become more prolific in spring time, driven by increased temperature, light and nutrients favourable for diatoms to bloom. The low amount of fouling could be due to an outage event that occurred three months earlier, during which the canal was drained and the concrete walls brushed. Consequently, the lack of inoculum on the canal walls may also have contributed to slow down the regrowth of fouling inside the test rig. More difficult to understand is why the fouling biomass in the opaque PVC pipe remained similar to the autumn-winter period.

The amount of fouling in the Tarraleah canal varied between 197.5 and 1366.7 g m⁻², depending on the site, with a corresponding dry weight between 9.7 and 91 g m⁻² (Perkins, 2010). In the rig pipes the fouling wet weight was between 52 and 13 times less than in the canal and this was probably due to the fact that the harvesting of fouling in the pipes occurred after a shorter period of time (< 60 days). Hence, the fouling mat was not as thick as in the canal where it grew undisturbed for more

than 6 months before sample collection. In addition, the surfaces of the pipe materials used were smoother than the rough concrete canal walls.

The high F_v/F_m values (> 0.40) in the pipes revealed that the fouling was in physiologically healthy conditions even in the metal pipe, where the cells spent two months in total darkness.

The Rapid Light Curves in November 2014 showed the influence of the different light intensities on the fouling ability to photosynthesize. In the metal pipe the fouling was adapted to darkness. Thus when light was provided it took time to acclimatize and started to photosynthesize slowly (reduced initial slope for all curves) followed by a progressive increase of all light curves, indicating that the photosynthetic apparatus was operating effectively. Various studies have found that diatoms can resume their activity when re-exposed to light after long periods in the dark (Itakura et al., 1997; Smayda and Mitchell-Innes, 1974) and Veuger and van Oevelen (2011) observed natural communities of benthic diatoms surviving a full year in darkness retaining their pigments and therefore possibly also their photosynthetic capacity. All light curves started with the same slope, indicating that the fouling was responding primarily to light. Only at light intensities greater than around $150 \mu\text{mol photons m}^{-2} \text{ s}^{-1}$ did the light curves diverge, with the fouling responding positively only to phosphorus and in particular to nitrogen. Kamp et al. (2011) found that the maximum time of surviving dark/anoxic conditions was significantly positively correlated with the maximum intracellular NO_3^- concentration in various diatom species. This could be a possible explanation for the positive response of the dark-adapted fouling to nitrogen addition. To produce ecologically realistic results we only provide low light intensity during the measurement, so as not to shock the photosystems. The light curves ended before reaching a plateau and their decline is not shown, which means that the fouling became photoinhibited at light intensities $> 400 \mu\text{mol photons m}^{-2} \text{ s}^{-1}$ (the maximum provided). In the opaque PVC pipe the fouling was exposed to low light ($2 \mu\text{mol photons m}^{-2} \text{ s}^{-1}$), thus low light intensity was provided for the PAM measurement. However, the fouling responded with a steeper initial slope for the control, phosphorus and nitrogen curves, indicating a rapid start of the photosynthetic process followed by a decline of the curve around $100 \mu\text{mol photons m}^{-2} \text{ s}^{-1}$ for

nitrogen and $160 \mu\text{mol photons m}^{-2} \text{ s}^{-1}$ for the control and phosphorus. Silica instead depressed the light curve which exhibited a small α and declined around $100 \mu\text{mol photons m}^{-2} \text{ s}^{-1}$. This suggests that the fouling in the opaque PVC pipe was low light adapted and did not tolerate light intensities above $160 \mu\text{mol photons m}^{-2} \text{ s}^{-1}$. In the frosted and clear PVC pipes the fouling instead grew when exposed to high light conditions and became photoinhibited $> 800 \mu\text{mol photons m}^{-2} \text{ s}^{-1}$. Only silica depressed the curve in the clear pipe, confirming that the addition of this nutrient was, for yet unexplained reasons, not well tolerated by these oligotrophic diatoms.

In conclusion, the present work on biofouling in the Tarraleah experimental rig system has conclusively demonstrated how variations in light intensities and substratum, but at identical flow, nutrient and temperature conditions, can trigger the development of differing biofouling communities with varying proportions of bacterial and diatom slimes. In turn these fouling communities exhibited differing photosynthetic properties, differing nutrient responses and which had differing implications for friction and reduction of flow.

Chapter 4*

Environmental conditions influencing growth rate and stalk formation in the estuarine diatom *Licmophora flabellata* using new plate reader methodology

4.1 Introduction

In well-lit marine environments, any natural or artificial substrata can become quickly covered by a biofilm, of which benthic diatoms are an early dominant component (Patil and Anil, 2005; Sweat and Johnson, 2013). The attachment of diatoms on surfaces renders them important fouling organisms which, along with bacteria, constitute major problems on artificial structures, resulting in vast economic losses (Mitbavkar and Anil, 2007; Salta et al., 2013). Biofouling on ships hulls results in increased roughness, increased frictional resistance and corresponding higher fuel consumption. Additional costs include hull cleaning, paint removal and replacement and associated environmental compliance measures (Callow and Callow, 2002; Schultz et al., 2011)

Licmophora C.Agardh diatom species are a common constituent of marine, littoral, micro-epiphytic communities (Taylor et al., 1976). They are generally found colonising filamentous red, brown and green macroalgae, submerged in rock pools throughout the littoral zone. In southern Australia waters *Licmophora* is a common fouling component on salmonid farm netting (Fig. 4.1a).

In two different studies, on the Texas and British coasts respectively, *Licmophora* was found primarily during warmer months, when light intensities were at their

* Published in *Diatom Research* as: Matilde Ravizza and Gustaaf M. Hallegraeff. Environmental conditions influencing growth rate and stalk formation in the estuarine diatom *Licmophora flabellata* vol. 30, 197-208 (2015).

<http://dx.doi.org/10.1080/0269249X.2015.1020071>

maximum (Honeywill, 1998; Medlin et al., 1985) but some species can occur year round (Honeywill, 1998).

Attachment in *Licmophora* is invariably associated with the secretion of extracellular polymeric substances (EPS) (Characklis and Cooksey, 1983; Daniel et al., 1987; Hoagland et al., 1993) which are secreted from a row of slits in the basal pole of the cells (Fig. 4.1b) and may either remain as a simple layer interposed as a pad between the diatom and its substratum or, through continuous secretion, develop into a stalk (Daniel et al., 1987). The attachment of the stalks must be strong to survive intertidal forces of wave action and the pounding against rocks and macroalgae, but under suboptimal conditions the cells can easily become easily dislodged (Honeywill, 1998). The initial basal pad in contact with the substratum chiefly comprises carboxylated polysaccharide whilst the erect stalk is composed of both carboxylated and sulphated polysaccharides (Daniel et al., 1987).

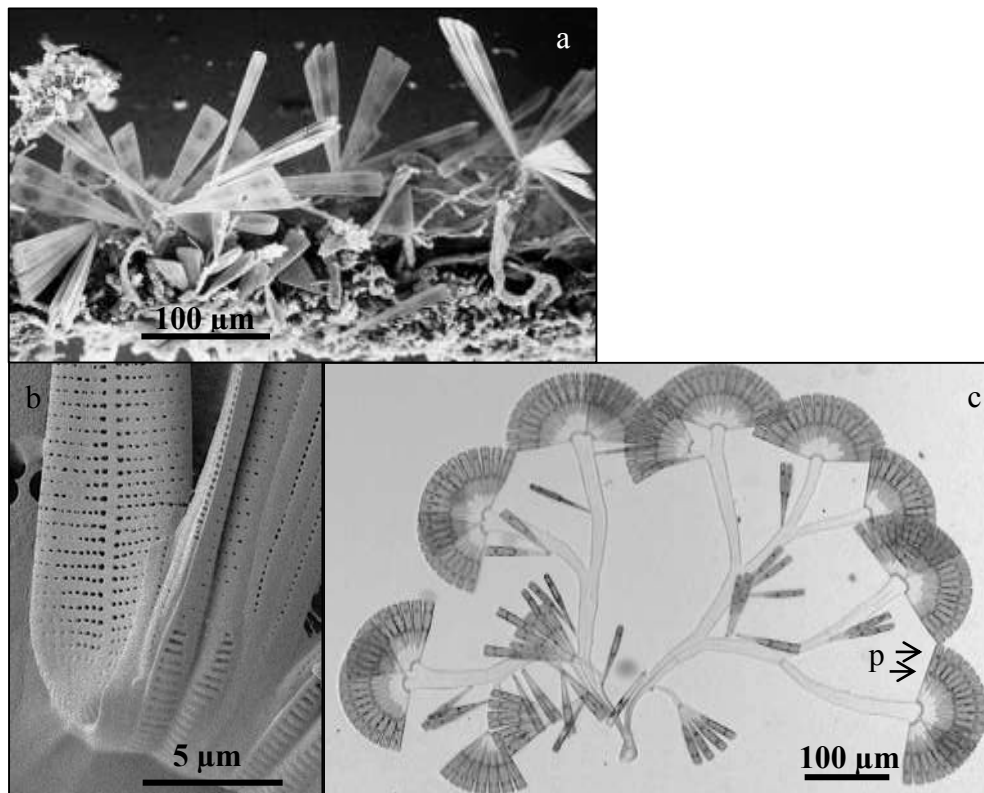


Figure 3.1 *Licmophora flabellata*.; (a) SEM. Three dimensional architecture of *Licmophora* biofouling on fish farm netting in Tasmanian waters; (b) SEM. Basal pole of cell with a row of slits through which the mucilage pads or stalks are secreted. (c) LM. Fans and branching stalks, new cells emerging from small side branches (arrow) and cells showing two discoid chloroplasts with pyrenoids (p).

Sulphated polysaccharides are associated with cell wall strengthening coupled with increased flexibility, protection and cation exchange (Percival, 1979). The stalks bear longitudinal striations which correspond to the fused secretions of the individual cells (Daniel et al., 1987) (Fig. 4.1C).

Stalk morphology is species specific and can be either a pad (*Licmophora juergensii* Agardh), a dichotomously branching stalk with a single cell at each apex (*Licmophora communis* (Heiberg) Grunow) or a compound stalk with many cells at the apex (*Licmophora flabellata*). The stalk of any one species can vary from short to extremely long, i.e. from 100 µm to 30 mm in *Licmophora paradoxa* (Lyngbye) Agardh, however the general nature of the attachment is consistent within a species (Honeywill, 1998). The stalks of many *Licmophora* species have an inner and outer layer; simpler stalks have a wrinkled outer layer, presumably for flexibility (Daniel et al., 1987).

While EPS production has been extensively investigated in several marine benthic and planktonic diatoms (see review by Hoagland et al. 1993), very few studies (Johnson et al., 1995; Kilroy and Bothwell, 2011; Lewis et al., 2002) have been conducted to define conditions promoting stalk formation in fouling diatoms. To the best of our knowledge, the only species studied include *Achnanthes subconstricta* (as *A. longipes* C.Agardh) (Lewis et al., 2002), *Didymosphenia geminata* (Kilroy and Bothwell 2011) and *Gomphonema gracile* Ehrenberg (Perkins 2010). We were fortunate to have access to a stalk forming culture of *L. flabellata*, which we did seek to study as a model organism for stalk formation in *G. tarraleahae* and *D. geminata*.

In the present study, *in vivo* chlorophyll fluorescence and microscopy were performed on unialgal cultures in multiwell plates to estimate the growth rates and stalk formation of *L. flabellata* under different conditions of light, nutrients, temperature and turbulence.

4.2 Materials and methods

Licmophora flabellata LFMI M101 was collected from Maria Island, Tasmania, Australia, on the 5th April 2010 and isolated by Helen Bond and Suellen Cook by micropipette. The diatom was routinely cultivated in sterile culture medium K⁺ (Andersen, 2005; Keller et al., 1987) in 96-well culture plates with black walls and optical bottom (Nunc, Thermo Fisher Scientific), and the growth rate and stalk properties monitored under different light, nutrient, temperature and turbulence conditions, simulating coastal Tasmanian habitats from which this species originated. A uniformly dense culture inoculum was achieved using a sonicator (Thomas Optical and Scientific Co. Pty. Ltd.), with the aim to gently release the cells from stalks. The first row of wells was filled with 300µl of K⁺ medium, whilst in the rest of the wells 50µl of inoculum was added to 250µl of K⁺ medium.

The growth rate was monitored using a plate reader (FLUOstar OPTIMA, Bmg Labtech) to measure *in vivo* chlorophyll fluorescence (IVF), with an excitation/emission of 450/680 nm. To validate the microplate algal assay, IVF was compared with cell counting using an optical microscope (Axiovert 24 Zeiss), performed in 10 wells containing an equal number of cells at initial inoculation: five wells with 20 cells and five wells with 35 cells each. In this experiment, cells were growing in basal K⁺ nutrients, temperature was kept constant at 17°C and light was 233 µmol photons m⁻² s⁻¹, which under our culture conditions produced the best growth, stalk length and stalk branching (Fig. 4.3). Fluorescence measurements and cell counts were taken every two days, at the same time of day. In all the experiments, an initial cell count was performed in each well right after inoculation. Cell counts correlated well with the microplate fluorescence assays [$y = 0.0133x^{7.8706}$ R² = 0.9339; Fig. 4.2]. In most cases fluorescence and the number of cells gradually increased until they both reached a peak around the same day, before decreasing.

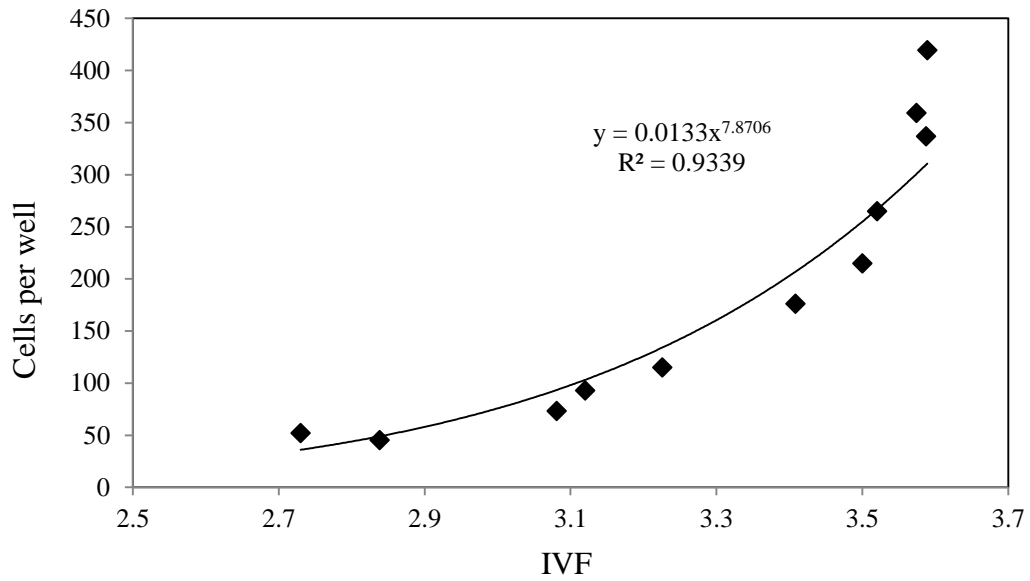


Figure 4.2 Calibration of fluorescence against microscopic cell counts of *Licmophora flabellata* cultured in 96-well plates. Average cell counts of 10 wells time course of growth.

Growth rate was calculated from fluorescence values transformed on a logarithmic scale, obtained by averaging fluorescence values for each well (and cell numbers for the first experiment) plotted against time, using the formula:

$$k' = [\ln(N_t/N_0)] / (t_1 - t_0)$$

in which: k' = growth rate; N_t = final fluorescence value (or number of cells); N_0 = initial fluorescence value (or number of cells); t_1 = final time; t_0 = initial time (Levasseur et al., 1993).

In the present study, growth rate is expressed as divisions per day calculated as:

$$\text{Div.day}^{-1} = k' / \ln 2$$

All experiments were terminated when the microalgae reached stationary phase. Stalks count and length measurements were performed on four wells, using an Axiovert 24 Zeiss optical microscope and Pentax K-30 digital camera. Eleven stalk categories were created as classified in Table 4.1.

The number of stalks was counted with the optical microscope twice a week and their length measured at the end of each experiment using the program ImageJ from digital pictures. Stalk counts were performed for a few more days beyond the end

of fluorescence measurements, as stalks kept growing even after fluorescence values started to decrease.

Table 4.1 Stalk categories discriminated in this study

0	1	2	3	4	5	6	7	8	9	10 or more
										

4.2.1 Light

Four different light conditions in basal K⁺ nutrients (Keller et al., 1987) were tested in four different experiments. Light intensity was determined using a PAR sensor (Biospherical Instruments, model QSL) measuring QSI (Quantum Scalar Irradiance). The microplates were illuminated from above at an incident irradiance of 50, 100, 150 and 233 $\mu\text{mol photons m}^{-2} \text{s}^{-1}$, produced by 3\three cool white fluorescent tubes over a 12 h light : 12 h dark photoperiod. When not growing in full light the microplates were covered with a diffuse mesh to progressively reduce the amount of incident irradiance. In all the experiments, temperature was kept constant at 17°C.

4.2.2 Nutrients

Nutrients were tested in three different experiments. A solution of K⁺ medium and different amounts of nutrients were used instead of K⁺ medium and Maria Island filtered seawater only: 10 mg L⁻¹ NO₃-N, 5 mg L⁻¹ PO₄-P and 5 mg L⁻¹ SiO₃-Si (subsequently referred to as N, P and Si), for three different microplates respectively. In all experiments the microplates were illuminated at an incident irradiance of 233 $\mu\text{mol photons m}^{-2} \text{s}^{-1}$ and temperature was kept constant at 17°C.

4.2.3 Temperature

Temperature was tested in three different experiments. Each microplate was put in

a temperature controlled room at 12, 17 and 20°C. In all experiments the microplates were illuminated at an incident irradiance of 233 $\mu\text{mol photons m}^{-2} \text{s}^{-1}$

4.2.4 Turbulence

Turbulence was tested in three different experiments, using an orbital shaker (New Brunswick Scientific) operating at different speeds, 150, 200 and 250 rpm corresponding to 2.5, 3.33, 4.16 Hz respectively, for three different microplates, in which each well was filled with 300 μL of liquid. For full definition of the turbulence characteristics of such orbital shaker design see Guadayol et al., (2009). In all experiments, the microplates were illuminated at 233 $\mu\text{mol photons m}^{-2} \text{s}^{-1}$ and temperature kept constant at 17°C.

4.3 Results

4.3.1 Microscopy

Licmophora flabellata in optimal conditions, represented by high light and low turbulence, formed extensive colonies with numerous cells creating fans at the top of long, thick, branching stalks (Fig. 4.1 a and b). Single cells or smaller fans were also visible on the sides of stalks (Fig. 4.1a). Cells had two round chloroplasts, one near the top and one in the middle of the cell, arranged in a bead-like pattern across the golden-brown fans of cells (Fig. 4.1a). Valves measured 90-150 μm length and 25-55 μm width.

4.3.2 Effects of light on growth rate and stalk length

Cultures under optimal temperature (17°C) and nutrient conditions (basal K^+ medium) at low light intensity (50, 100 and 150 $\mu\text{mol photons m}^{-2} \text{s}^{-1}$) generated short-lived growth, which lasted 3, 5 and 7 days respectively, with no measurable growth rate. In contrast, the experiment at the highest light intensity (233 $\mu\text{mol photons m}^{-2} \text{s}^{-1}$) produced continuous slow growth up to 21 days with a growth rate

of 0.55 divisions per day (Fig. 4.3a and b and Table 4.2). A corresponding increase in the length and number of the stalks (Fig. 4.3c, d, e, f and g), was observed with increasing light intensity. In the first three experiments at low light intensity (50, 100 and 150 $\mu\text{mol photons m}^{-2} \text{s}^{-1}$), stalk length exhibited limited variation: 90, 170 and 195 μm on average, respectively, with few or only single cells on top of mainly single stalks. In contrast, at higher light intensity (233 $\mu\text{mol photons m}^{-2} \text{s}^{-1}$) stalk length increased significantly up to 3476 μm on average, with highly branched and thick stalks supporting wide fans of cells (Fig. 4.3h).

4.3.3 *Effects of nutrients (Si, N and P) on growth rate and stalk length*

The lengths of the exponential growth periods in these experiments were 26, 32 and 36 days when P, N and Si were added, respectively (Fig. 4.4a and b.). Growth rates at the best temperature (17°C) and light (233 $\mu\text{mol photons m}^{-2} \text{s}^{-1}$) varied slightly upon addition of different nutrients to the basal K^+ medium and were comparable at 0.50, 0.39 and 0.35 divisions per day in the presence of P, N and Si respectively (Fig. 4.4c). Minimal variation in the length was noted in the three treatments, being 803, 857 and 883 μm on average for N, P and Si addition, respectively (Figs 4.4d, e, f, g, h and Table 4.2).

4.3.4 *Effects of temperature on growth rate and stalk length*

The lengths of the exponential growth periods are similar at at 17 and 20°C (21 and 20 days, respectively) and increased at at 12°C (33 days) (Fig. 4.5a and b). Growth rate at the best light (233 $\mu\text{mol photons m}^{-2} \text{s}^{-1}$) and nutrient conditions (basal K^+ medium) increased with temperature, being 0.39, 0.55 and 0.61 divisions per day at 12, 17 and 20°C, respectively (Fig. 4.5c). The length of the stalks was comparable at 12 and 20°C (823 and 654 μm respectively), but increased considerably at 17°C (3476 μm) (Fig. 4.5d). The stalk number was highly variable at the three temperatures: a wide range of stalk lengths was recorded throughout the experiment at 17°C, whilst at 12 and 20°C the stalks became branched more gradually with time (Figs 4.5e, f, g, h and Table 4.2).

4.3.5 *Effects of turbulence on growth rate and stalk length*

The length of the exponential growth period was 28 days for the first two treatments at low turbulence (2.5 and 3.33 Hz respectively) and 22 days at high turbulence (4.16 Hz) (Fig. 4.6a and b). Growth rate at optimum light ($233 \mu\text{mol photons m}^{-2} \text{s}^{-1}$) and nutrient conditions (basal K^+ medium) was similar for the three treatments, being 0.46, 0.45 and 0.49 divisions per day at 2.5, 3.33 and 4.16 Hz, respectively (Fig. 4.6c). In the experiments at low turbulence, stalk length exhibited limited variation, between 757 and 848 μm respectively (Fig. 4.6d) and the number of stalks increased progressively, achieving moderately branched stalks (Figs 4.6e, f and h). In contrast, at highest turbulence (4.16 Hz) the average of stalk length was only 161 μm (Fig. 4.6g and h and Table 4.2) and fans of cells were supported mainly by single stalks.

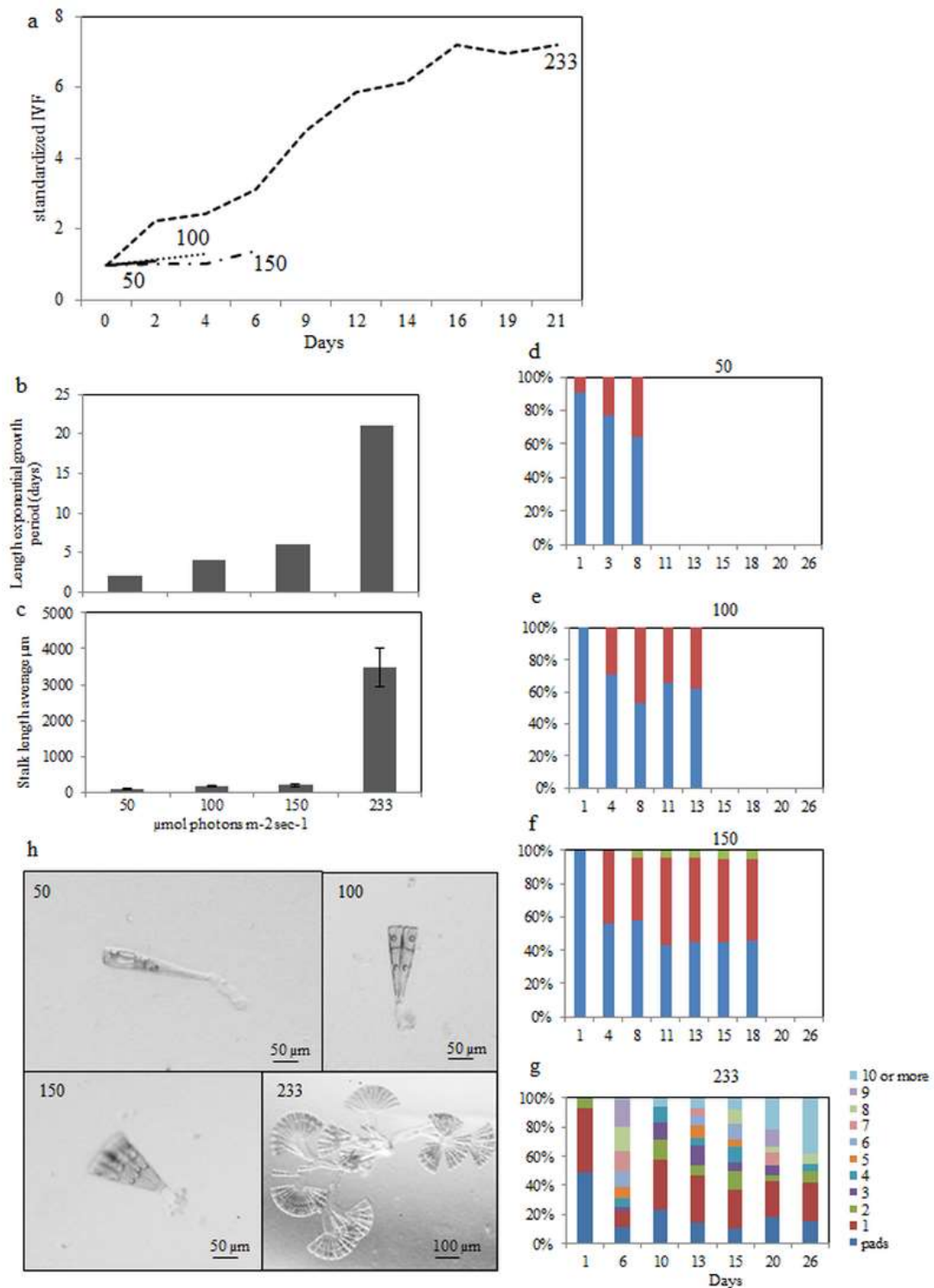


Figure 4.3. Response of the diatom *Licmophora flabellata* growth and stalk formation as a function of light intensity ($\mu\text{mol photons m}^{-2}\text{s}^{-1}$). (a) Time course of growth measured as *in vivo* fluorescence; (b) Length of exponential growth period (days) and (c) stalk length (μm). Number of stalks of during the time course of growth (days) at different light intensities: 50 (d), 100 (e), 150 (f) and 233 (g) $\mu\text{mol photons m}^{-2}\text{s}^{-1}$. (h) Light micrographs showing single stalk with one, two, four cells on top, in low light conditions (50, 100 and 150 $\mu\text{mol photons m}^{-2}\text{s}^{-1}$ respectively) (10x magnification) and fans of cells on top of thick, long stalks, at high light conditions (233 $\mu\text{mol photons m}^{-2}\text{s}^{-1}$) (5x magnification).

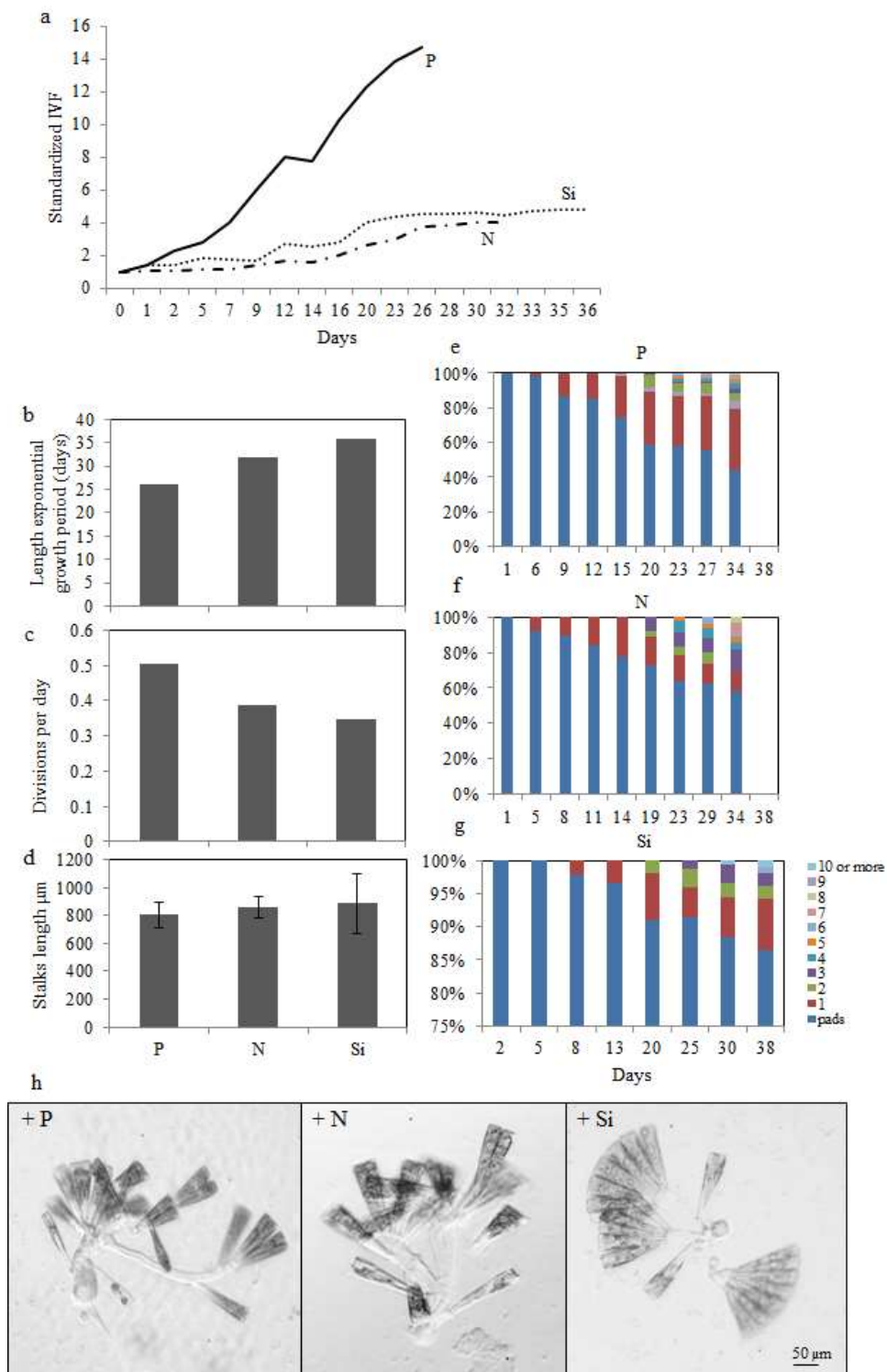


Figure 4.4. Response of the diatom *Licmophora flabellata* growth and stalk formation as a function of nutrient content. (a) Time course of growth measured as *in vivo* fluorescence; (b) Length of exponential growth period (days), growth rate (div/day) and (d) stalk length (μm).

Number of stalks of during the time course of growth (days) at different nutrient content: P (e), N (f) and Si (g).

(h) Light micrographs showing small fans of cells on top, in P, N and Si treatments (10x magnification).

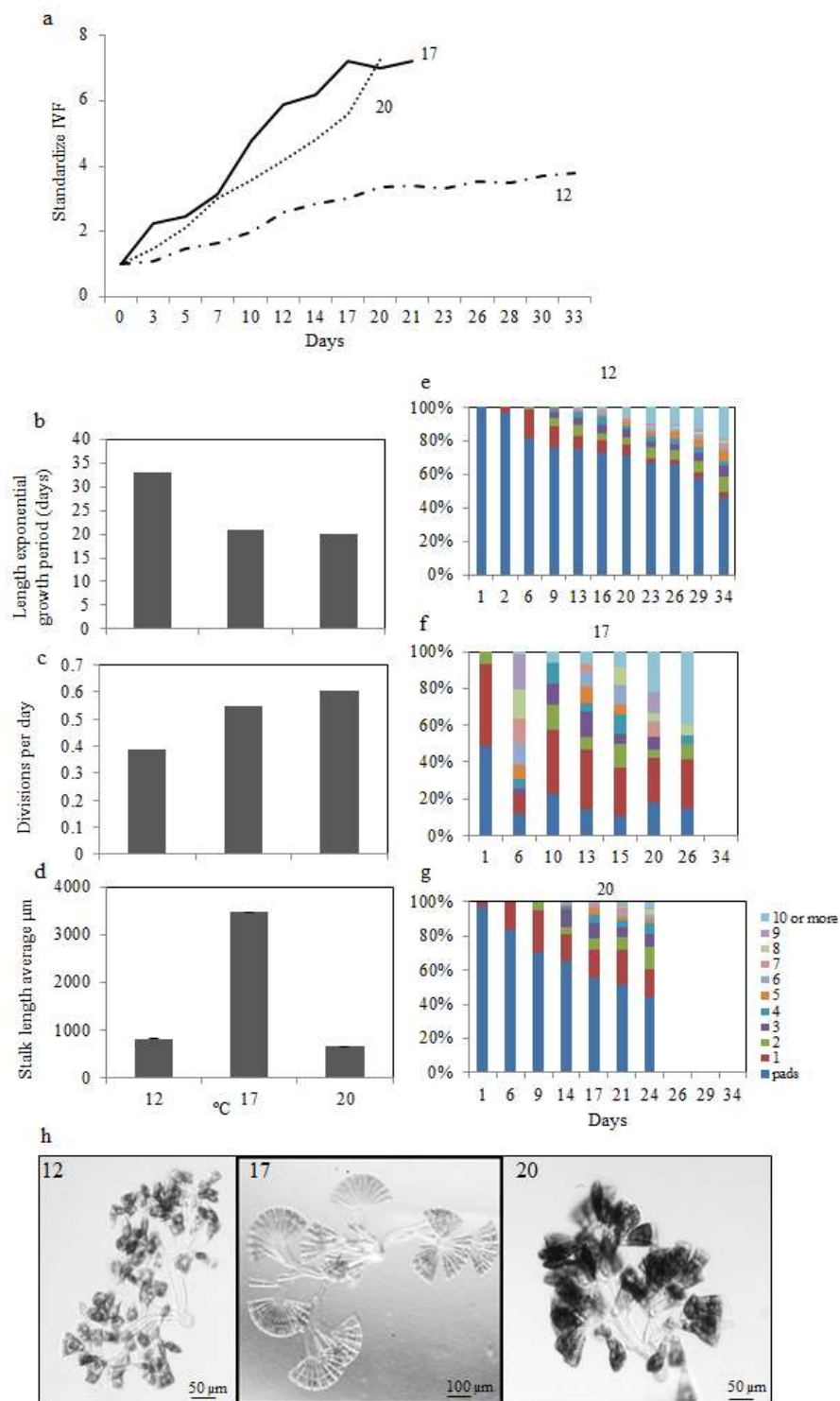


Figure 4.5 Response of the diatom *Licmophora flabellata* growth and stalk formation as a function of temperature ($^{\circ}\text{C}$). (a) Time course of growth measured as *in vivo* fluorescence; (b) Length of exponential growth period (days), (c) growth rate (div/day) and (d) stalk length (μm). Number of stalks of during the time course of growth (days) at different temperature: 12 (e), 17 (f) and 20°C (g). (h) Light micrographs showing stalks of different lengths at 12 (10x magnification), 17 (5x magnification) and 20°C (10x magnification), supporting fans of cells of different shape in the three treatments

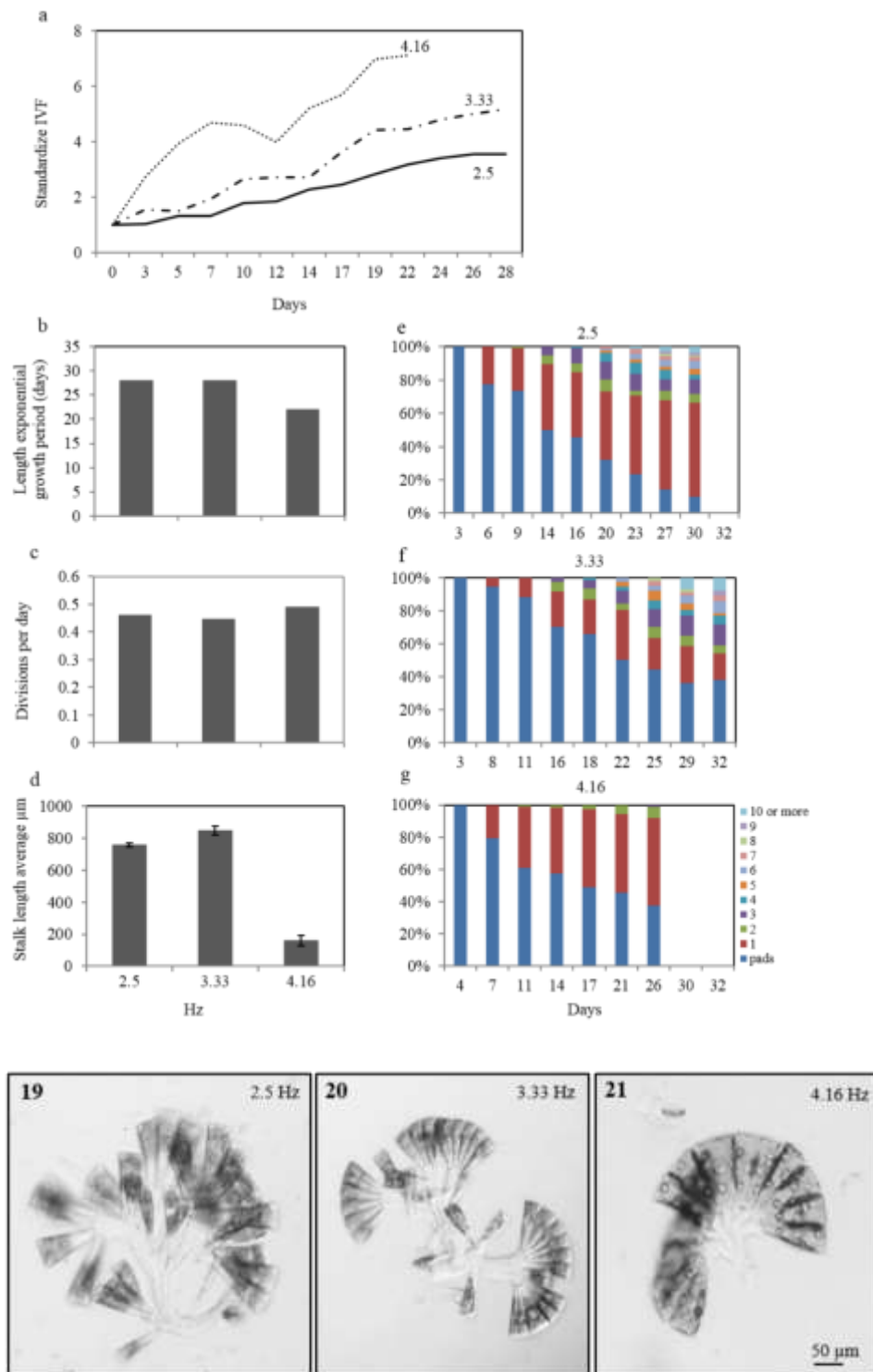


Figure 4.6 Response of the diatom *Licmophora flabellata* growth and stalk formation as a function of turbulence (Hz). (a) Time course of growth measured as *in vivo* fluorescence; (b) Length of exponential growth period (days), (c) growth rate (div/day) and (d) stalk length (μm); Number of stalks of during the time course of growth (days) at different turbulence: 2.5 (e), 3.33 (f) and 4.16 Hz (g); (h) Light micrographs showing long branched stalks supporting cells at low turbulence intensity (2.5 and 3.33 Hz) and a short single stalk in high turbulence intensity (4.16 Hz) (10x magnification).

Table 4.2. Length of growth period, growth rate and stalk length of *Licmophora flabellata* as a function of light intensity, nutrients, temperature and turbulence.

		Length of growth period (days)	Divisions per day	Stalk length average (μm)	Number of stalks % per each category (when represented)									
Light intensity ($\mu\text{mol photons m}^{-2} \text{ sec}^{-1}$)					Pads 1 2 3 4 5 6 7 8 9 10									
	50	2	.*	90 ± 15	60	40								
	100	4	.*	170 ± 28	58	42								
	150	6	.*	195 ± 32	40	50	10							
17°C, medium K ⁺		233	21	0.55	3476 ± 528	15	23	8	8			8		38
PO ₄ -P (mg l ⁻¹)		5	26	0.50	803 ± 90	44	34	5	4	3	4	3	1	1
NO ₃ -N (mg l ⁻¹)		10	32	0.39	857 ± 79	57	10		14	3	3	3	7	3
SiO ₃ -Si (mg l ⁻¹)		5	36	0.35	883 ± 211	85	7	2	2		2			2
$233 \mu\text{mol photons m}^{-2} \text{ sec}^{-1}, 17^\circ\text{C}$														
Temperature °C	12	33	0.39	823 ± 119	46	3	9	6	3	6	3	3	3	18
	17	21	0.55	3476 ± 528	15	23	8	8				8		38
	20	20	0.61	654 ± 58	44	18	14	6	6	3	3		3	3
$233 \mu\text{mol photons m}^{-2} \text{ sec}^{-1}, \text{medium K}^+$														
Turbulence Hz	2.50	28	0.46	757 ± 64	10	55	5	10	3	4	4	3	1	4
	3.33	28	0.45	848 ± 91	36	17	6	14	6	3	6	3		6
	4.16	22	0.49	161 ± 12	37	54	7	2						

*Short growth followed by death

* Outlying clump removed from data

3.4 Discussion

In comparison to other marine and freshwater stalk forming diatoms, such as *Achnanthes subconstricta*, *Didymosphenia geminata* and *Gomphonema gracile*, *L. flabellata* exhibited a different growth and stalk formation response to environmental conditions. In their study on nutrient-replete *Achnanthes subconstricta* (as *A. longipes*) Lewis et al. (2002) observed that while growth rate increased with increasing light and temperature (maximum at $60 \mu\text{mol photons m}^{-2} \text{ s}^{-1}$ and 26°C respectively), cell density had an overriding stimulatory effect on stalk production. At high cell density, temperature influenced stalk production (but not stalk length), and this effect increased with increasing optimum temperature (optimum at 20°C). Stalk production was interpreted as serving as a means to elevate the cells above the substratum to avoid competition for light and nutrients in the dense biofilm. Surprisingly light intensity had little or no effect with *A. subconstricta* on either the number of cells producing stalks or stalk length.

In outdoor flume experiments with *D. geminata*, from the Waitaki River, New Zealand, Kilroy and Bothwell (2011), elucidated the relationship between stalk length, cell division rate and light intensity under ambient and nutrient enriched conditions. *Didymosphenia geminata* stalk length was stimulated by light intensity but stalk production was truncated by cell division. The influence of light on stalk length was more pronounced when cell division was more nutrient limited. Rapid cell division rates (frequency of dividing cells 30-40%) leads to shorter stalk lengths and therefore stalk length was shorter in nutrient enrichment. These authors concluded that *D. geminata* stalk length was primarily driven by photosynthesis.

In *D. geminata* culture experiments Kuhajec & Wood (2014) found that *D. geminata* cells survived, attached and underwent cell division in waters with a wide range of chemistries, including water where *D. geminata* was absent. No correlation was found between cell survival, attachment, or division and any of the individual elements, compounds, or nutrient ratios tested, suggesting that water chemistry was unlikely to be the sole variable responsible for *D. geminata* distribution in New Zealand.

In *G. gracile* from Tasmanian freshwater streams, stalk formation was primarily a response to environmental stress from high temperatures, with only a marginal effect of light. *Gomphonema gracile* cell growth was reduced by temperatures above 10°C whilst stalk production was increased, suggesting that more resources were channeled towards EPS production when conditions for growth were not favourable (Perkins et al., 2010).

In contrast, in the present work *L. flabellata* was a high-light adapted fouling diatom, exhibiting highest growth rates at 233 $\mu\text{mol photons m}^{-2} \text{s}^{-1}$. The higher light tested stimulated growth rates, stalk formation and stalk length. Even though UVB radiation can reduce growth rates in several diatom species (Hannan et al., 1980; Thomson et al., 1980), some species appear to be tolerant to full sunlight conditions even over an extended period (Jokiel and York, 1984). Bothwell et al., (1993) demonstrated that benthic diatom communities exposed to UV for prolonged periods had greater mean cell sizes than those not exposed to UV, as large-sized cells seemed to offer more protection to the centrally located nucleus, limiting damage to the DNA. Moreover, UV resistant species were found to colonize areas

nearer the surface, whilst sensitive species preferred deeper waters (Jokiel and York, 1994). Due to its cell size and habitat preferences, *L. flabellata* may fulfil the requirements to be considered a high light/UV-tolerant species, even though more experiments at higher light intensities than used in this study should be performed to confirm this.

Enrichment of N, P and Si did not significantly influence growth nor stalk formation and length. Temperature variations also did not seem to affect *L. flabellata* growth rates nor stalk formation, even though the greatest stalk lengths were reported at 17°C. An increase in turbulence (from 2.5 to 4.16 Hz) reduced stalk length but not growth rates, suggesting that stalk formation and branching are more likely to happen in relatively calm waters. This confirms comparable results on diatom composition on ship hulls, which show that stalked species dominate in areas where laminar flows prevail whilst prostrate genera predominate in turbulent flow areas (Woods et al., 1986). Similarly, Zargiel and Swain (2014) only observed *A. longipes* under static immersion, never under dynamic conditions: long stalks might be advantageous under static conditions, however under turbulent conditions and strong shear forces the stalk may position the cell outside the boundary layer, where removal is easier.

3.5 Conclusion

The present results are relevant to species-specific approaches towards mitigating the impact of fouling diatoms, in that conditions that trigger the longest stalks tend to have the greatest impact on human society. While removing shore-line vegetation to increase light-intensity has proven to be a successful strategy to mitigate low-light adapted *Gomphonema tarraleahae* fouling in open air Tasmanian hydrocanals (Perkins et al., 2009), this clearly is not a universal strategy that can be applied to all fouling diatoms. *Licmophora flabellata* stalk formation was consistently stimulated by higher light intensities.

Chapter 5

New Zealand problems with the freshwater stalk-forming diatom: *Didymosphenia geminata*

5.1 Introduction

Historically, there has been worldwide movement of species through natural and anthropogenic means (Mack et al., 2003). In recent decades the rate of species dispersal and the risk associated with biotic invaders has increased with human population growth, rapid movement of people and alteration of the environment (Pimentel et al., 2005) as well as with international trade (Coutts and Taylor, 2004). Nevertheless, most species deliberately or inadvertently introduced to a new region almost certainly fail to establish, and of those that survive, many do not become invasive pests (Williamson, 1996).

Invasion can be conceptualized as a staged process (Colautti and MacIsaac, 2004; Lockwood et al., 2005; Richardson et al., 2000). The number of stages and their definitions vary among authors, however, all start with transport and introduction of individuals, or propagules, into a new range and finish with spread and potentially negative impacts on other species (Catford et al., 2009). The notion of impact is based on human perception and can be subjective (Williamson, 1993), and economic and ecological impacts are not always synonymous (Pyšek and Richardson, 2006).

Since most invasions begin with the arrival of a small number of individuals (Simberloff, 1986), the costs of eliminating these is usually minor in comparison to eventual cost and effort of later control after populations have grown and established (Mack et al., 2000). Biotic invasions cause two main categories of economic impact. First is the loss in potential economic output and second is the direct cost of fighting invasion (Mack et al., 2000). Tallying the cost of non-native plant invasions is a hard task. However Pimentel et al. (2000) estimated that in the

United States as a whole, a total of \$100 million is invested annually in non-indigenous species aquatic weed control, while non-native plants are responsible for \$27 billion in damage and control of crop weeds and \$6 billion more in weeds in pastures. Mack et al. (2000) predicted that a cost-benefit analysis of many deliberately introduced invaders would demonstrate forcefully that their cost to society overwhelms any realized or perceived benefits.

The consequences of biotic invasions are often so profound that they must be curbed and new invasions prevented (Mack et al., 2000). However, prevention is often only possible early in the process, before a species arrives in a new range or at the point of entry (Lodge et al., 2006). Risk assessment is recommended as the first step to identify measures to minimize the risk at each stage of the invasion process (Byers et al., 2002). Risk analysis for biological organisms requires information on the invading species, vulnerability of habitats to invasion, modelled information on current and potential distributions, and the costs associated with containing (or failing to contain) harmful species (Stohlgren and Schnase, 2006).

Once a non-indigenous-species is introduced eradication is sometimes feasible but only under some circumstances and with potentially unpredictable results (Myers et al., 2000). Eradication is defined as the elimination of every individual of a species from a geographic area that is sufficiently isolated to prevent reinvasion (Newsom, 1978). Although some longstanding, widespread invasions have been eradicated (Simberloff, 2003a), likelihood of success is obviously improved and cost minimized if an invasion is detected early (Myers et al., 2000; Simberloff, 2003b). Unexpected outcomes will become more probable both as the variety of interacting invaders contained in an ecosystem increases, and as exotics in late stages of invasion largely or wholly eliminate native species and replace their functional roles (Zavaleta et al., 2001). Large-scale eradication projects have greater potential for non-target impacts and, consequently, tend to be more costly and controversial (Myers et al., 2000). The success of eradication is affected mainly by three factors: the biology of the target species, sufficient resources allocated to the process for enough time and the support both from government agencies and the public (Mack et al., 2000; Simberloff, 2003b).

In many more instances, species are managed at low levels even though they are not eradicated. Many introduced species have been controlled for long periods at low densities (Simberloff, 2009). Maintenance options are typically seen as mechanical, chemical, and biological control (Mack et al., 2000).

5.2 Invasion and spread of *Didymosphenia geminata* in New Zealand

The concept of invasive algae has historically focused on marine environments because free-living microalgae have rarely been reported as invaders in freshwaters (e.g. Blanco and Ector, 2009; Kilroy and Unwin, 2011). The stalked benthic diatom *Didymosphenia geminata* represents one of the few examples of a potentially invasive freshwater microalga (Flöder and Kilroy, 2009; Kilroy and Unwin, 2011). Historically described as a cosmopolitan but rare, lotic diatom (Kirkwood et al., 2007), *D. geminata* is now considered a nuisance, bloom forming and invasive species (Flöder and Kilroy, 2009).

In the Northern Hemisphere *D. geminata* has exhibited unusual blooms since 1990, e.g. in Icelandic rivers (Jonsson et al., 2000), Carpathians rivers in Poland (Kawecka and Sanecki, 2003) and Vancouver Island in British Columbia (Bothwell et al., 2009), but the events were not described as invasions because *D. geminata* was either known to be already present in the affected regions, or there was no information to confidently assess previous presence or absence. In New Zealand, *D. geminata* was first recorded in 2004 in the lower Waiau River (Kilroy, 2004; Kilroy et al., 2008) and the absence of prior reliable records suggests that this event represents a new incursion of a non-indigenous species into the Southern Hemisphere (Kilroy, 2004; Kilroy and Unwin, 2011). By winter 2008 *D. geminata* colloquially known as “didymo”, had been identified in 26 major catchments on New Zealand’s South Island (Flöder and Kilroy, 2009) and the species is now considered the first non-toxic diatom to cause strong negative effects on aquatic environments (Blanco and Ector, 2009). Because New Zealand is highly reliant on freshwater resources for power generation, agriculture, recreational activities and

tourism, the potential environmental and economic impacts of *D. geminata* are considered substantial (Campbell, 2008).

Global dispersion of *D. geminata* is thought to be via natural dispersal (wading birds) and human-mediated, e.g. by boating, kayaking, fishing, and the current known distribution in the South Island is restricted to areas where these recreational fisheries activities are popular. The occurrence of *D. geminata* as an invasive species poses an enormous challenge for invasive species management and the response to the incursion of *D. geminata* in New Zealand was difficult because of the lack of information about its potential distribution and ecological effects as well as sparse information on its environmental tolerances (Kilroy et al., 2008). According to some authors (Bothwell et al., 2006; Kilroy et al., 2005), increasing occurrence of invasive *D. geminata* may be attributed to a genetic variant that has broader tolerance than the original species. This, together with its microscopic size and the importance of humans as a vector, suggest that *D. geminata* invasion and spread may have more in common with global diseases than higher organism invaders (Flöder and Kilroy, 2009; Kirkwood et al., 2007). A *D. geminata* invasion and spread model should therefore integrate aspects of ecological invasion dynamics with aspects of pandemic models (Kirkwood et al., 2007).

5.3 Ecology

D. geminata is a large, distinctive diatom that attaches to rocks and other substrata by thick, branching polysaccharide stalks (Kilroy et al., 2009). The ability to secrete large quantities of highly organized extracellular polymer arrays differentiates *D. geminata* from other related benthic diatoms (Gretz, 2008). The stalks may be assumed to be especially important for the success of the genus (Whitton et al., 2009), as they form a greater proportion of the total biomass of a colony, reducing competition for the surface area (Hoagland et al., 1982), nutrients and light (Hoagland et al., 1993).

Historically *D. geminata* distribution has been claimed to be circumboreal in cold oligotrophic waters of forest rivers and streams of North America and Europe

(Hustedt and Pascher, 1930; Patrick and Reimer, 1975; Schmidt, 1899). In literature the presence of *D. geminata* has been associated with xenosaprobic waters at low conductivity, flow, temperature and pH (Kirkwood et al., 2007; Krammer and Lange-Bertalot, 1986; Patrick and Reimer, 1975). However, there is evidence that the ecological profile of this species has expanded in the recent decades to a broader physical and chemical range (Blanco and Ector, 2009; Falasco and Bona, 2013; Kawecka and Sanecki, 2003) (Table 5.1).

Table 5.1 Summary of ecological requirements of *D. geminata*, determined from literature

Parameter	Value/range	References
Temperature	9.5-17.1°C 11.5-14.6°C (during blooms).	Kawecka and Sanecki, 2003; Miller et al., 2009
Flow regime characteristics	Regulated flow regimes, stable channels such as downstream lakes and reservoirs	Blanco and Ector, 2009; Falasco and Bona, 2013; Kawecka and Sanecki, 2003; Kilroy et al., 2005
Flow velocity (m s ⁻¹)	0.26-0.48	James et al., 2014
Light intensity	High exposure to sunlight (not shaded streams)	James et al., 2014; Kawecka and Sanecki, 2003; Whitton et al., 2009
Turbidity NTU	0.6-1.6	James et al., 2014
TTS (mg L ⁻¹)	0.5-30	Falasco and Bona, 2013
Substratum geology	Metamorphic bedrock	Rost et al., 2011
pH	6.5-8.9	Falasco and Bona, 2013
Conductivity (µs cm ⁻¹)	56-552	Falasco and Bona, 2013
Phosphate, Tot P (mg L ⁻¹)	0.0009-0.026	James et al., 2014
Nitrogen, N-NH ₃ (mg L ⁻¹)	0.138-0.275	James et al., 2014
Silica, Si (mg L ⁻¹)	3.45-4.22	James et al., 2014
Iron, Fe (mg L ⁻¹)	0.07-0.21	James et al., 2014
Calcium, Ca ⁺⁺ (mg L ⁻¹)	0.25-65.10	Falasco and Bona, 2013

Although *D. geminata* nuisance blooms preferably occur in oligotrophic waters with low flow regime, low and stable discharge and shallow streambed (Falasco and Bona, 2013; Kirkwood et al., 2007; Spaulding and Elwell, 2007), mass developments can also be found in rivers where total phosphorus and nitrate are in high concentrations (Kawecka and Sanecki, 2003; Spaulding and Elwell, 2007) and with a wide range of flow velocities (Kilroy et al., 2005). Several authors report *D. geminata* outbreaks from watercourse systems with hydroelectric flow diversions or reservoir impoundments (Falasco and Bona, 2013; Kawecka and Sanecki, 2003;

Kirkwood et al., 2007; Miller et al., 2009). The hydrological stability (mid-level discharge, from oligo- to mesotrophic cool waters) created by flow regulators such as dams, could provide ideal conditions for *D. geminata* and be linked with massive outbreaks downstream: water quality and physical conditions below dams can be considered potential factors controlling the growth and distribution of *D. geminata* (Kirkwood et al., 2007).

5.4 Nuisance blooms

Although *D. geminata* occurs in both running and standing waters (Kilroy and Bothwell, 2011; Spaulding and Elwell, 2007), nuisance blooms are typically known only in streams and rivers (Kilroy and Bothwell, 2011; Root and O'Reilly, 2012). Nuisance blooms are defined as extensive spatial and temporal benthic mats, consisting of masses of cells and stalks that extend for greater than 1 km and persist for several months of the year. There is evidence that the legacy of the *D. geminata* stalks influences stream community composition, preventing the growth of macroalgae (Spaulding et al., 2005), decreasing the abundance of some benthic macroinvertebrate species and the increase in chironomids (Brown, 2008) and potentially have deleterious effects on fishes that consume benthic prey (Larned et al., 2006). Stalk material can persist on substrata well after the death cells that produce it (Kirkwood et al., 2007). Similarly to *Gomphonema tarraleahae* the stalks may attach to rocks, plants, or any other submerged substratum and when the diatom divides (i.e. vegetative reproduction) the stalk also divides, eventually forming a dense mass of branching stalks: it is not the diatom cell itself that is responsible for the negative impacts of *D. geminata* but the massive production of extracellular stalks, as they make up most of the biovolume of algal mats (Kirkwood et al., 2007).

D. geminata's nuisance blooms also have economic impacts. In the Western United States *D. geminata* is responsible for clogging a system of canals which transport water for hydropower generation, agriculture and human consumption (Spaulding and Elwell, 2007). In some canals the management includes regular removals by scraping *D. geminata* growth from the concrete surfaces of the canals. In New

Zealand, floating mats of *D. geminata* cause irrigation screens and power generation dam screens to clog (Kilroy, 2004) and irrigation water pumped from infected rivers causes blockage of nozzles on farm irrigators, which have to be cleared by hand (Lagerstedt, 2007).

As such the *D. geminata* problem has similarities to *G. tarraleahae* biofouling problems (Perkins et al., 2009). However, *D. geminata* is more environmentally damaging because of its large size (cell typically up to 110 µm long) compared to the size of *G. tarraleahae* (up to 45 µm long) and the high volume of stalk material produced compared to that from other stalk-producing diatom taxa (e.g. species of *Cymbella* and *Gomphoneis*).

The stalk length in *D. geminata*, on average 250µm (Kilroy and Bothwell, 2011), is controlled by light intensity and stalk production is truncated by cell division. This suggests that stalk length is driven by photosynthesis with the influence of light most pronounced when cell division is more nutrient (N+P) limited (Kilroy and Bothwell, 2011). Shorter time intervals between divisions would lead to shorter stalk length, other environmental conditions being equal, and under slower, nutrient-limited cell division and higher light levels, greater time periods for photosynthetic production consistently resulted in longer stalks.

Furthermore, blooms of *D. geminata*, in contrast with many other algal blooms, are associated with nutrient-poor waters (Spaulding and Elwell, 2007). In particular, they often occur in waters where the ratio N:P is high for much of the year but the key factor is the ratio of organic to inorganic phosphate (Whitton et al., 2009): *D. geminata* thrives where organic P is predominant and the overall P concentration is low enough for organic P to be an important P source. The 1989-1990 subset of Water Quality Monitoring Network data for freshwater streams from the New Zealand North Island and South Island were plotted against available Tarraleah data for pH, conductivity, temperature, total phosphorus and total nitrogen by means of Principal Component Analysis (PCA) and Non-Metric Multidimensional Scaling (NMDS) plots (Fig. 5.1 a and b, courtesy Dr Jon Bray, University of Canterbury). Tasmanian levels of P were comparable with conditions in New Zealand that support *D. geminata*, but never matched New Zealand bloom conditions for N (≤ 4 ppb).

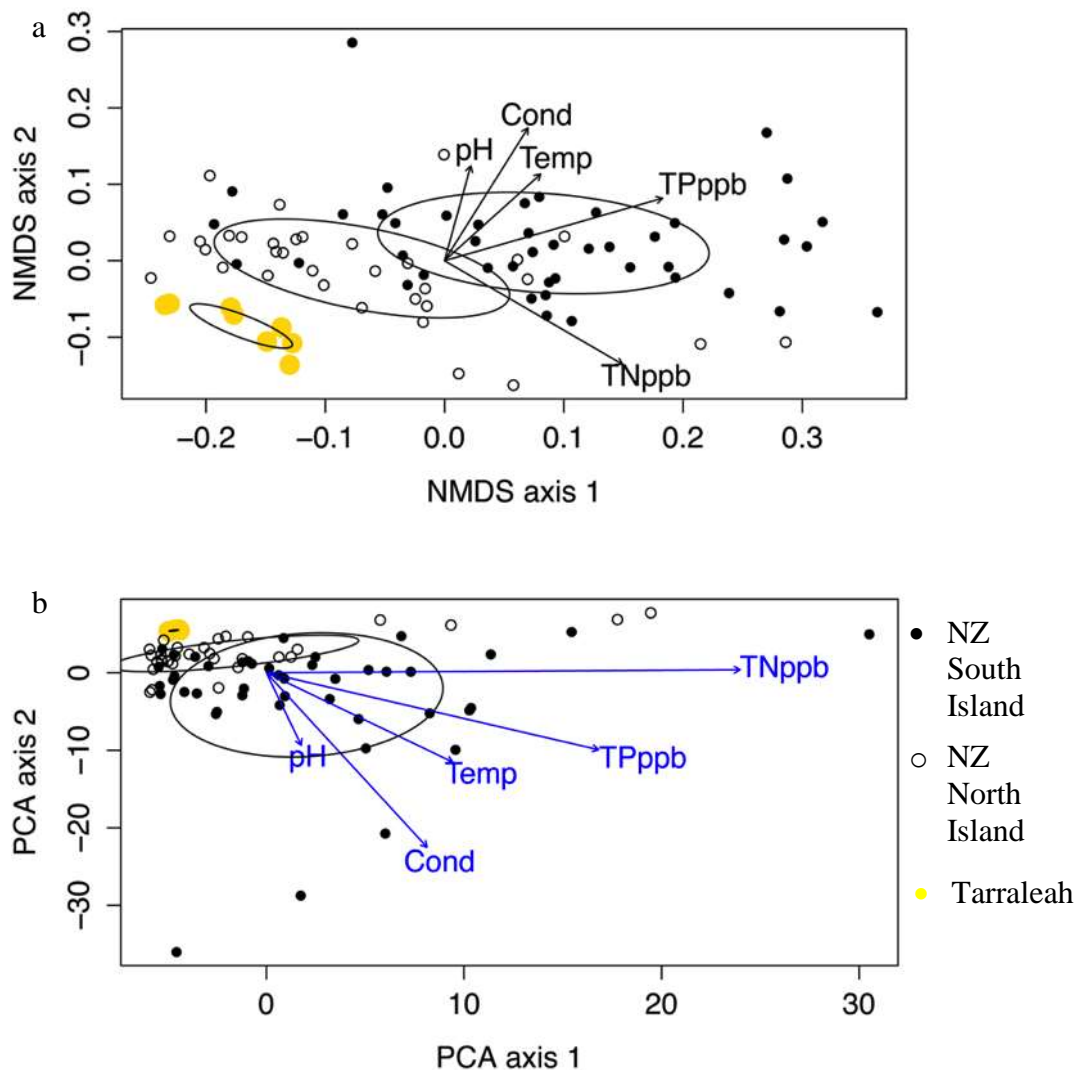


Figure 5.1 Water quality data for pH, conductivity, temperature, total phosphorus and total nitrogen for New Zealand North and South Island compared with Tarraleah, by means of a) Non-Metric Multidimensional Scaling (NMDS) plots and b) Principal Component Analysis (PCA). (Courtesy Dr Jon Bray, University of Canterbury).

5.5 Control and eradication

Studies involving the use of different biocides were undertaken to establish their impact on *D. geminata* and non-target organisms, in channels (Jellyman et al., 2011), the laboratory (Jellyman et al., 2011; Root and O'Reilly, 2012) and natural waterways (Clearwater et al., 2011). According to Clearwater et al., (2011), 1-h

pulse dose of 20 mg L⁻¹ of chelated copper formulation (Gemex™) significantly affected a well-established didymo infestation in a river, with minimal long-term effect on non-target species (algae, invertebrates and fish) after a single Gemex application, although significant localized fish mortalities occurred on the treatment day. Lower concentrations of Gemex (1, 2 and 4 mg L⁻¹) were tested in artificial stream trials by Jellyman et al., (2011), resulting in the highest didymo cell mortality at the highest Gemex concentration. Cell vitality decreased to 2.8± 1.6% then ranged from 10 to 38% at the concentration of 4 mg L⁻¹. Channel trials of Gemex also resulted in 100% fish survival at the tested concentrations. Because of its persistence in the environment and potential build-up after multiple applications, Gemex could not be considered a long-term treatment for enduring *D. geminata* control (Jellyman et al., 2011). However, its use is recommended in the short term, to treat didymo infestations at early stages, as an eradication tool to prevent *D. geminata* dispersal (Clearwater et al., 2011; Jellyman et al., 2011).

Laboratory experiments were conducted by Root and O'Reilly (2012), testing popular decontamination treatments:

- 10% salt water,
- 2% Clorox® bleach,
- 1% Virkon® Aqua,
- 5% Green Works® dish detergent,
- 5% Dawn® dish detergent,
- 10% Green Works® chlorine-free bleach.

None of these products were 100% effective at killing didymo cells. However, mortality due to decontaminants was significantly reduced for cells attached to the stalk material compared to free-floating cells, suggesting that the stalk plays an important role in cell viability. Moreover, based on tap water-treated *D. geminata* samples, there was a significant increase in mortality (for both attached and unattached cells) over the course of the summer season, emphasizing the importance of early season decontamination and the fact that decontamination products tested at the end of a didymo bloom may appear more effective than they would be at the early stages. Because the Green Works® dish detergent was found

to be the least toxic for the environment and for humans of the options tested, Root and O'Reilly (2012) suggested that it could be the best option to control didymo infestations.

5.6 Future investigations

Over the past decade, the discussion about *D. geminata* impacts has focused on the characterization of the species as native versus invasive. According to Finlay et al., (2002) random dispersal drives the large-scale distribution of diatom species and the argument in favour of endemic diatom species is untenable, because it is not possible to disprove their existence elsewhere in the biosphere. The fact that thick mats of *D. geminata* stalk material are present in both native and non-native locations (Elwell et al., 2014), makes it difficult to determine if *D. geminata* can be considered “introduced” (e.g. Kirkwood et al., 2007; Spaulding et al., 2010). On the other hand, a different school of thought supports the concept that microorganisms, diatoms included, exhibit biogeographic differences and challenges the hypothesis that “everything is everywhere” (Becking, 1934) by bringing up examples of anthropogenic introductions (Spaulding et al., 2010; Vanormelingen et al., 2008). Thus, determination of the non-native status of diatoms, as a group whose basic biology, taxonomy, biogeography, and genomes are not well known, would be possible only through the application of long term observational data and paleolimnological reconstruction (Lavery et al., 2014; Spaulding et al., 2010). Furthermore, because of the lack of data, speculation exists on why there has been a change in distribution of didymo and whether it is linked to climate change (Bothwell and Spaulding, 2008). Considering the environmental preferences of *D. geminata*, it has been suggested that the consequences of climatic change may shift river conditions, in some regions, to those favourable to this species (Ellwood and Whitton, 2007; Schweiger et al., 2011). Therefore, species like *D. geminata* could be considered sentinels of shifting climate regimes (Schweiger et al., 2011) and future investigations of anthropogenic climatic change as a potential trigger of recent *D. geminata* blooms could represent a promising research path to develop strategies to mitigate their impact (Lavery et al., 2014).

The ecophysiology of *D. geminata* compared to *G. tarraleahae* was investigated in detail in this study and is presented Chapter 6.

Chapter 6*

Ecophysiology of New Zealand *Didymosphenia geminata* nuisance diatom mats, compared to Tasmanian *Gomphonema* hydrofouling diatoms using Pulse Amplitude Modulated (PAM) fluorometry

6.1 Introduction

The stalk-forming benthic diatom *Didymosphenia geminata* occurs in both running and standing waters (Spaulding and Elwell, 2007; Kilroy and Bothwell, 2011), but nuisance blooms typically only occur in streams and rivers (Kilroy and Bothwell, 2011; Root and O'Reilly, 2012) producing masses of cells and stalks that extend for greater than 1 km and persist for several months of the year. To the observer these mats appear as fiberglass insulation, tissue paper, “rock snot”, brown shag carpet or sheep skin covering the streambed (Spaulding and Elwell, 2007; Fig. 6.1).

Stalk material can persist on substrata well after the death of the cells that produce it and comprise most of the biomass of algal mats, and are responsible for the negative impact of *D. geminata* (Kirkwood et al., 2007). Blooms of *D. geminata*, in contrast to many other algal blooms, are associated with low-nutrient waters (Spaulding and Elwell, 2007). These aspects of *D. geminata* are comparable to the nuisance diatom *Gomphonema tarraleahae* in Tasmanian hydrocanals (Perkins et al., 2009).

* Accepted for publication as: Matilde Ravizza, Jeannie Kuhajek, Andrew Martin, Susie Wood and Gustaaf Hallegraeff, Ecophysiology of New Zealand *Didymosphenia geminata* nuisance diatom mats, compared to Tasmanian *Gomphonema* hydrofouling diatoms. In MacKenzie, L. et al. *Proceedings of the 16th International Conference for Harmful Algae (ICHA)* (2015).



Figure 6.1 *Didymosphenia geminata* stalk material from Buller River, New Zealand, as it appears a) when out of water and b) covering stream bed.

6.2 Aim of this investigation

In the present study a nutrient bioassay was applied to allow instantaneous assessment of phytoplankton nutrient status of Buller River (NZ) *Didymosphenia geminata*, Lake Rotoiti (NZ) *Gomphonema* cf. *manubrium*, and Tasmanian *Gomphonema tarraleahae*/ *Tabellaria flocculosa*. Comparative laboratory tests were performed on *Licmophora flabellata*, which being an estuarine species was expected to be more tolerant to nutrient addition.

6.3 Materials and methods

Field samples of *D. geminata* and *G. cf. manubrium* were collected on 31 October 2013 from the Buller River (41°47'11.5"S 172°48'44.5"E) and Lake Rotoiti (41°48'24.2"S 172°50'37.9"E), Tasman, in NZ and of *G. tarraleahae*/*T. flocculosa* on 11 December 2013 from Tarraleah hydro canals (42°18'29.4"S 146°25'24.4"E) by gently scraping of rocks, pylons and canal walls, a few centimetres below the water surface. *Licmophora flabellata* LFM1 M101 was collected from Maria Island, Tasmania, Australia, on the 5th April 2010 and isolated by Helen Bond and Suellen Cook by micropipette. The diatom was routinely cultivated in sterile culture medium K⁺ (Andersen, 2005; Keller et al., 1987). For each species five plastic

containers were prepared with 45 ml of river, lake and canal water and medium K^+ . Nutrients (0.25 ml) were added to each container as follows (Table 6.1):

Table. 6.1. Final concentrations of nutrients applied in the nutrient bioassays

Container	Nutrient
Control	nothing added
Silica	Na_2SiO_3 [36 mg L ⁻¹]
Nitrogen	$NaNO_3$ [77 mg L ⁻¹]
Phosphorus	K_2HPO_4 [8 mg L ⁻¹]
Iron	$C_{10}H_{12}N_2NaFeO_8$ [0.00152 mg L ⁻¹]

Addition of nutrient was conducted at the ambient light (for *D. geminata*, *Gomphonema cf. manubrium* and *G. tarraleahae*/ *T. flocculosa*) and at 233 $\mu\text{mol photons m}^{-2} \text{ s}^{-1}$ for *L. flabellata*) and left for 20 min, then stored in dark conditions for 20 more min before the first fluorescence measurement was taken. The content of each container was then divided in three equal fractions, in order to obtain triplicate treatments. A section of mat or 1000 μl of inoculum for *L. flabellata* was added to each container. Containers were then placed in the dark at ambient temperature for 1 h before the first fluorescence measurement was performed using a Water-Pulse Amplitude Modulated (PAM) fluorometer (Waltz, GmbH, Effeltrich, Germany; gain setting 5 – 25). Samples were then returned to the dark for 3.5 h, followed by a second fluorescence measurement. Maximum quantum yield F_v/F_m (representing physiological health and influenced by nutrient stress) and rapid light curves (RLC) were assessed, as indicators of physiological health.

6.4 Results

D. geminata rETR and F_v/F_m values decreased after 1 and 4 h dark adaptation, in response to silica addition when compared to controls and rETR was reduced by 50 and 60%, respectively. Nitrogen supply after 1 h dark adaptation induced rETR to

increase above the control (129 and 118, respectively), whilst after 4 h rETR was only above the control in response to iron addition (Fig. 6.2). The highest F_v/F_m value after 1 and 4 h dark adaptation (0.59-0.55) was achieved after phosphorus addition and in general all F_v/F_m values decreased after 4 h of dark adaptation (Table 6.2)

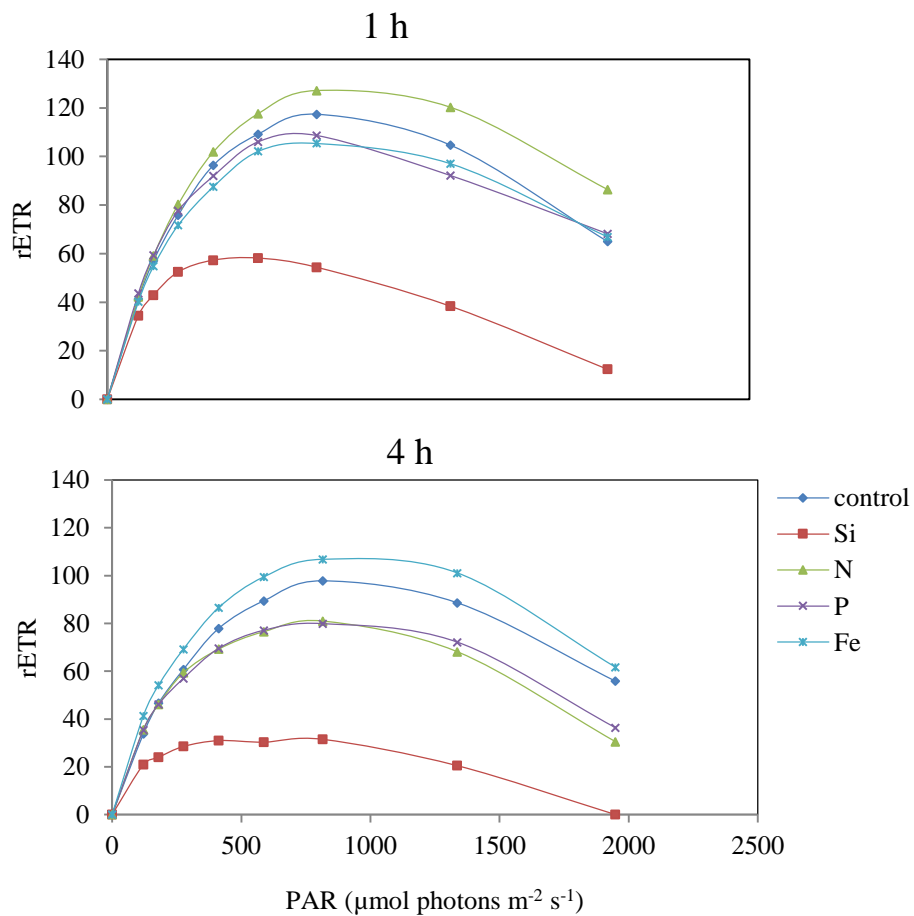


Figure 6.2 *Didymosphenia geminata* relative Electron Transport Rate after 1 and 4 hours dark adaptation (original data).

G. cf. manubrium showed a similar response to *D. geminata*, with rETR depressed in response to silica addition, in comparison to the control, both after 1 (72 and 89 respectively) and 4 hours (69 and 93 respectively) dark adaptation. Iron addition caused rETR to increase above the control and other treatments, especially after 4 hours dark adaptation (Fig.6.3). F_v/F_m was above control in all treatments, both after 1 and 4 hours dark adaptation (Table 6.2).

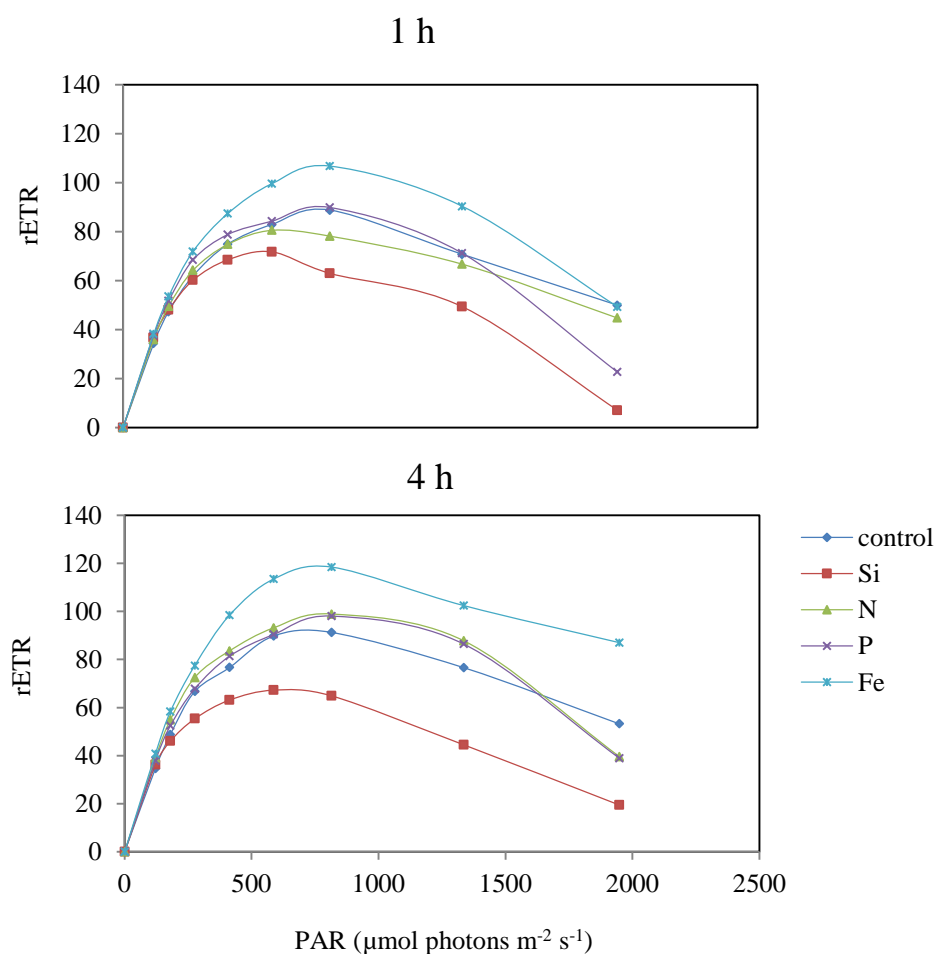


Figure 6.3 *Gomphonema cf. manubrium* relative Electron Transport Rate after 1 and 4 hours dark adaptation (original data).

With *G. tarraleahae*/*T. flocculosa* silica supply induced rETR to decrease both after 1 and 4 h dark adaptation of 40 and 25% respectively compared to the control. The other rETR values were similar to the control after 1 h and only iron addition depressed values by 10% after 4 h dark adaptation (Fig. 6.4). All F_v/F_m values were high (>0.7) after 1 h dark adaptation. After 4 h, phosphorus treatment showed the lowest F_v/F_m but still considered high for phytoplankton (> 0.6) (Table 6.2).

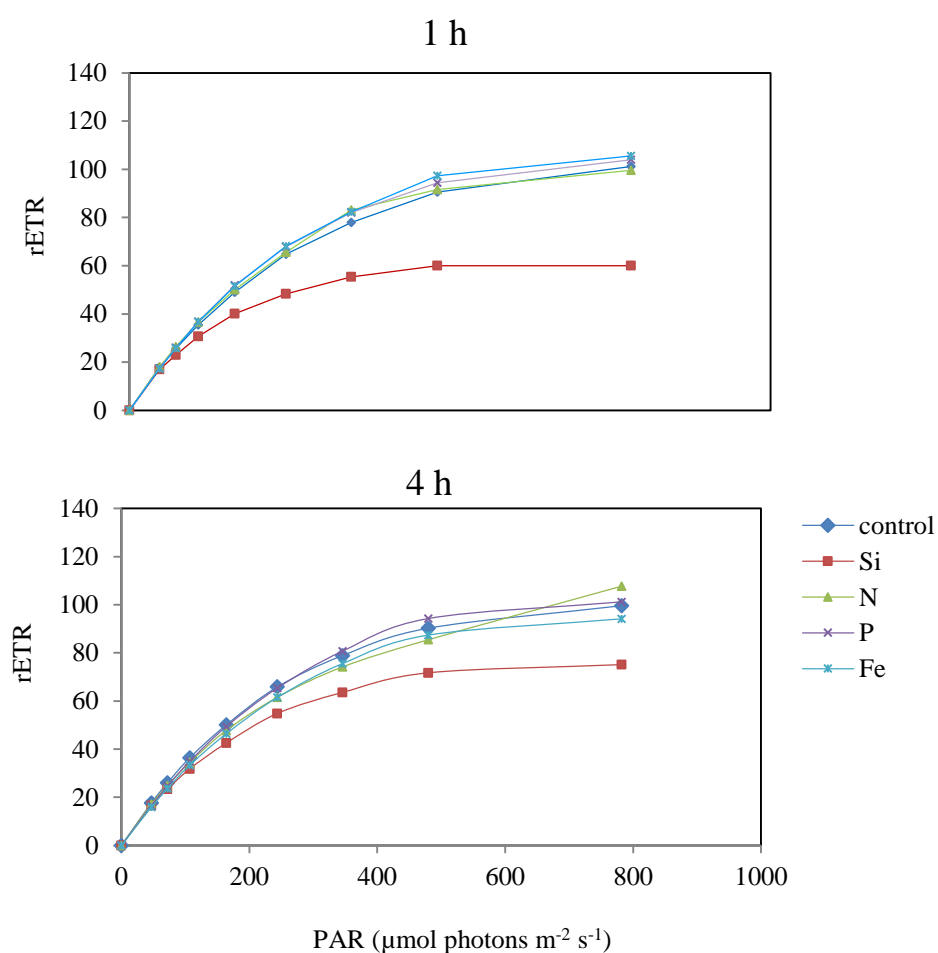


Figure 6.4 *Gonphonema tarraleahae*/*Tabellaria flocculosa* relative Electron Transport Rate after 1 and 4 hrs dark adaptation (original data).

L. flabellata did not show a significant response to nutrient addition, with all rETR values similar to the control. Phosphorus addition induced the maximum rETR value, both after 1 and 4 h dark adaptation (93 and 89, respectively) (Fig. 6.5). F_v/F_m values were high (≥ 0.7), both after 1 and 4 h dark adaptation and phosphorus addition generated for the highest value (0.78) (Table 6.2).

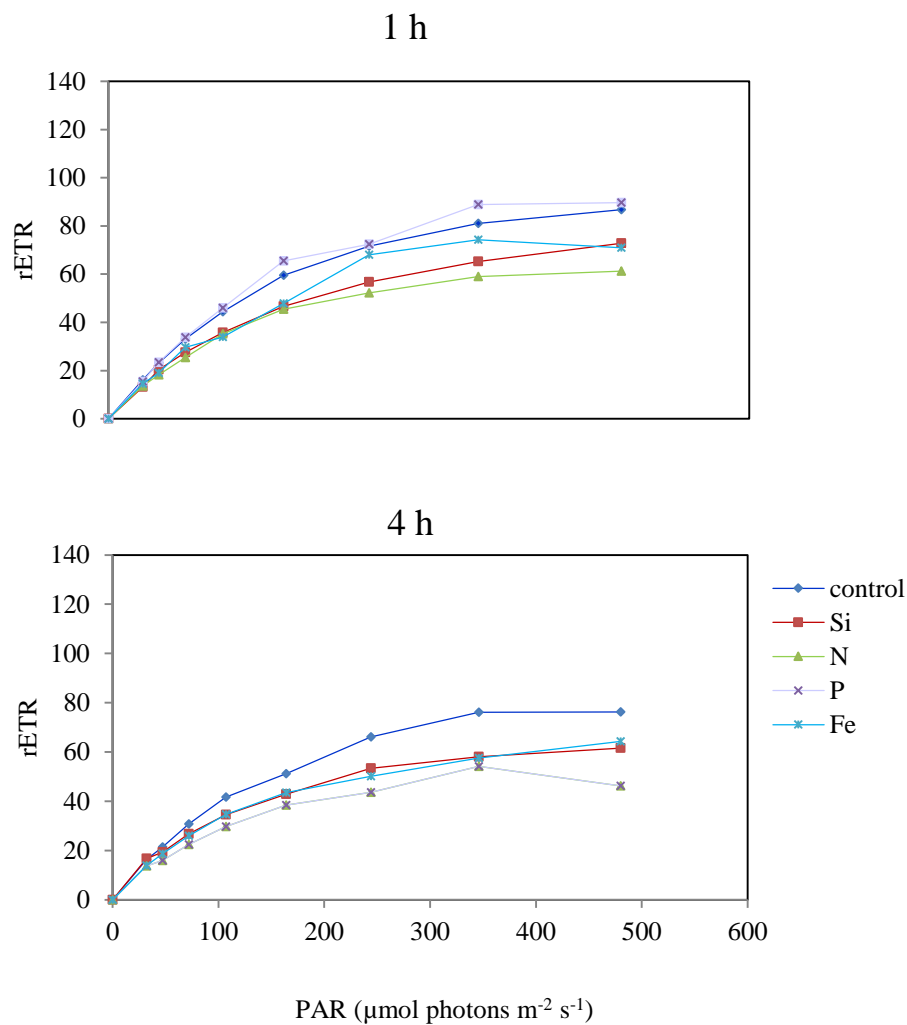


Figure 6.5 *Licmophora flabellata* relative Electron Transport Rate after 1 and 4 hrs dark adaptation (original data).

Table 6.2. F_v/F_m values for *Didymosphenia geminata*, *Gomphonema cf. manubrium*, *Gomphonema tarraleahae/Tabellaria flocculosa* and *Licmophora flabellata* in response to silica, nitrogen, phosphorus and iron addition, after 1 and 4 h incubations.

Species	Dark adaptation	Control	Si	N	P	Fe
<i>D. geminata</i>	1 hr	0.57 ± 0.01	0.43 ± 0.03	0.56 ± 0.02	0.59 ± 0.04	0.56 ± 0.02
	4 hrs	0.53 ± 0.01	0.35 ± 0.04	0.53 ± 0.01	0.55 ± 0.01	0.54 ± 0.03
<i>G. cf. manubrium</i>	1 hr	0.44 ± 0.04	0.50 ± 0	0.52 ± 0.01	0.50 ± 0	0.50 ± 0.01
	4 hrs	0.44 ± 0.04	0.50 ± 0.01	0.51 ± 0.01	0.50 ± 0	0.50 ± 0.01
<i>G. tarraleahae/T. flocculosa</i>	1 hr	0.70 ± 0.09	0.78 ± 0.03	0.76 ± 0.02	0.73 ± 0.02	0.72 ± 0.01
	4 hrs	0.74 ± 0.02	0.74 ± 0.01	0.72 ± 0.02	0.62 ± 0.08	0.66 ± 0.04
<i>L. flabellata</i>	1 hr	0.68 ± 0.08	0.68 ± 0.04	0.68 ± 0.08	0.78 ± 0.02	0.73 ± 0.02
	4 hrs	0.68 ± 0.06	0.74 ± 0.02	0.63 ± 0.07	0.78 ± 0.07	0.66 ± 0.03

6.5 Discussion

The New Zealand diatom species *D. geminata* and *G. cf. manubrium* and the Tasmanian *G. tarraleahae/T. flocculosa* exhibited similar responses to silica addition, which in all cases surprisingly depressed their fluorescence rETR responses and in *D. geminata* also depressed F_v/F_m . The role of silica in the formation of the diatom frustule is well known, and therefore the fluorescence F_v/F_m and rETR decrease in response to silica addition was unexpected. Lippemeier et al (1999; 2001) reported a decrease in F_v/F_m due to silicate starvation in cultures of *Thalassiosira weissflogii*. Decreased protein synthesis occurs in silicon-starved cells, leading to reduced repair of damaged PSII centres causing in turn a reduction in F_v/F_m . A possible explanation for our results relates to the application of unrealistically high silica concentrations (36 mg L^{-1}) to these diatom species, which are all adapted to oligotrophic waters ($0.95\text{--}4.8 \text{ mg L}^{-1}$ silica content for Tarraleah No.1 canal; $1.82\text{--}2.28 \text{ mg L}^{-1}$ for Buller River, average between two sites from Oct

2013 to March 2014). This is also suggested by the results of the nutrient bioassay with *L. flabellata*, which instead was not inhibited by silica and slightly stimulated by phosphorus addition.

Iron addition triggered an increase in fluorescence in *D. geminata* and *G. cf. manubrium*, but not for Tasmanian *G. tarraleahae*/*T. flocculosa*. Considering that the photosynthetic light harvesting and energy transduction apparatus are driven by proteins which bind iron atoms to mediate electron transfer, a positive fluorescence response to iron addition could be explained by a lack of this critical micronutrient ($75\text{--}118\ \mu\text{g L}^{-1}$ in Tarraleah; $0\text{--}2719.97\ \mu\text{g L}^{-1}$ for Buller River, average between two sites from Oct 2013 to March 2014). According to Sundareshwar et al. (2011), mucopolysaccharide stalks in *D. geminata* play a role in nutrient adsorption because soluble iron can be absorbed from the stalks in the oxidized surface layer where, due to strong affinity, it binds phosphorus which is not bioavailable. Through an abiotic process phosphorus then becomes available in the inner layer of the mat, at a concentration at least an order of magnitude greater than present in surface water. Iron reactivity and concentration have thus been implied as key factors for *D. geminata* distribution. These processes may create a positive feedback between stalk biomass, which forms under low phosphorus, and cell division rates, which occur in phosphorus-replete conditions. This concept matches that suggested by Cullis et al. (2012) claiming that the key to the *D. geminata* paradox (high biomass, low nutrients) is the temporal separation between mat growth and cell division, driven by nutrient content of the water: under high light levels, in low nutrient conditions stalk production is high and cell division low, whilst when nutrient content increases cell division become predominant (Kilroy and Bothwell, 2011). In contrast, Bothwell et al. (2012) suggested that *D. geminata* blooms can only occur in waters with low phosphorus and iron content and that iron is not responsible for promoting or sustaining the blooms in phosphorus-depleted waters. Whilst the role of phosphorus and iron in *D. geminata* blooms is still debated, our results show a short term positive response of *D. geminata* to iron and this requires further investigation at more sites and with varying concentration of iron.

Even though the parameters that define the habitat for *D. geminata* are not yet fully understood, its temporal and spatial distribution suggest a range of potential factors

including light availability play an important role (James et al., 2014; Whitton et al., 2009).

In contrast to *D. geminata*, the Tasmanian *G. tarraleahae*/*T. flocculosa* has a preference for low-light. In Tarraleah No. 1 canal fouling prevails on the northern wall which is more shaded by the vegetation (Perkins et al., 2009). Though the general hydraulic preference for *D. geminata* blooms includes relatively low, stable flows (Kilroy 2004; Spaulding and Elwell 2007), a high degree of variation was found in *D. geminata* presence or absence relative to flow velocity (Kirkwood et al., 2007). In contrast, the Tasmanian *G. tarraleahae*/*T. flocculosa* distribution is limited to high velocity areas (water velocity in Tarraleah No. 1 canal has an average of 2.1 m s^{-1} , with maximum flow rate of $24 \text{ m}^3 \text{ s}^{-1}$).

In conclusion, due to its broad environmental tolerance and on the basis of a comparison of light, temperature, water flow and water chemistry conditions in New Zealand (Bray, 2014) and Tasmania, it is possible to conclude that, if introduced, *Didymosphenia* would be able to establish itself in Tasmanian Hydro Canals, where the overall conditions are similar to those encountered in New Zealand water courses, but may not necessarily cause high biomass blooms.

Chapter 7

General conclusions, management and mitigation of biofouling

Stalk- or pad-forming benthic and epiphytic/epipellic diatoms represent an important constituent of the biofouling community, and their presence on illuminated submerged natural and artificial surfaces causes significant technical and hydrodynamic problems for a number of industries (Townsin 2003; Schultz et al., 2011), both in freshwater and marine environments. Biofouling on ships' hulls results in increased roughness, increased frictional resistance and correspondingly higher fuel consumption. Additional costs include hull cleaning, paint removal and replacement and associated environmental compliance measures (Callow and Callow, 2002; Schultz et al., 2011). The saving to the shipping industry through the use of antifouling coatings is estimated to be ~ US\$22.64 billion per year. The presence of a biofilm on transfer surfaces of heat exchangers cooled by seawater reduces the heat transfer rate by 20 to 50% and incurs a global expenditure of over US\$15 billion per year to control the problem (<http://www.birmingham.ac.uk>). Similarly, the direct economic costs of biofouling control to the aquaculture industry (e.g. fouling on fish farm netting) are substantial, with conservative estimates of 5–10% of production costs attributed to biofouling (Lane and Willemsen 2004). Globally, this equates to costs of US\$1.5 to 3 billion per year (Fitridge et al., 2012).

The present thesis focused on the impact of fouling diatoms on the Tasmanian hydro-electricity industry, as well as concerns on how the potential future introduction of a New Zealand invasive diatom could aggravate this problem. In terms of loss of water flow for hydro-electricity generation, the greatest problems are caused by diatoms that form long stalks. A 310% increase in local skin friction coefficient was measured for a biofilm dominated by long filamentous algae streamers, and a 50% increase was measured for a biofilm dominated by a low-form

gelatinous diatom. (Andrewartha et al., 2008). Furthermore EPS diatom stalks persist well after the diatom cells themselves have died off, which means that methods that kill the diatoms are not necessarily full-proof in solving the fouling problem. This work thus focused on the environmental conditions that stimulate stalk formation of key diatom species of concern.

In hydro-electricity generating open-air canals operated by Hydro Tasmania the biofouling represents an estimated 1.8-17.6 tonnes dry weight in the 19.7 km long Tarraleah No. 1 (Perkins et al., 2009), which was the focus of this study. The stalk forming diatom *Gomphonema tarraleahae* has been identified as the main late-succession biofilm species in these canals, which together with the earlier stage *Tabellaria flocculosa* can cause up to 10% reduction in flow carrying capacity (Andrewartha et al., 2010; reviewed in **Chapter 1**). The presence of biofouling in Tarraleah No. 1 Canal causes increased drag, which in turn results in either a reduction in freeboard (distance between the water surface and the top of the canal walls) to maintain flow rate or a decrease in flow rate to maintain acceptable freeboard levels to avoid overtopping (Andrewartha et al., 2007; Barton et al., 2010; Perkins et al., 2010). Engineering studies have demonstrated that the effective roughness of the Tarraleah biofilm is much greater than its physical roughness, which has implications for the friction drag (Walker et al. 2013). The present work aimed to improve our understanding of the biological processes underpinning hydrocanal biofilm development and its associated implications for frictional drag.

The present work successfully explored the application of PAM fluorometry nutrient bioassays on diatom fouling communities. This method provides instantaneous assessment of physiological health of biofouling, nutrients and light adaptation status. Rapid Light Curves (RLC) characterised via PAM fluorometry also represents a non-intrusive tool for assessing steady-state photoacclimation status or photoprotective capacity (Serôdio et al., 2006).

Rapid Light Curves (RLC) characterised via PAM fluorometry confirmed that biofouling at Tarraleah No. 1 Canal preferred low light conditions (maximum 80 $\mu\text{mol photons m}^{-2} \text{s}^{-1}$) and hence grew more prolifically on the north wall of the canal which received less light. The Tarraleah nutrient bioassays showed a surprising decline of light curves as well as physiological health (F_v/F_m) in response

to high silica addition at both walls at all depths, whilst the supply of nitrogen and phosphorus instead triggered an increase in F_v/F_m , pointing to growth limitation of N and P-nutrients in the oligotrophic canal water (**Chapter 2**). Tarraleah waters generally were low in N and P nutrients (maximum 0.71 and 0.022 mg L⁻¹) but showed highly variable Si concentrations peaking in winter months (4-5 mg L⁻¹) and decreasing down to 1 mg L⁻¹ when heavy diatom fouling developed in spring and early summer. The Redfield ratio is the optimal atomic ratio of C:N:P found in phytoplankton cells and reflecting that of open ocean waters. The nitrogen, silica and phosphorus concentrations in Tarraleah No. 1 water significantly diverged from the Redfield-Brzezinski nutrient ratio proposed for diatoms, which also includes silica (C:Si:N:P=106:15:16:1) (Brzezinski, 1985). Averaged over the seasons the Si:N:P of Tarraleah waters was 461:30:1 pointing to both nitrogen and phosphorus limitation.

In spite of considerable efforts we failed to replicate Tarraleah fouling communities in an experimental flow tank in the laboratory. An experimental pipe test rig (**Chapter 3**) was therefore successfully constructed beside Tarraleah No. 1 Canal. This set-up allowed the monitoring of biofouling growth in four different experimental pipe sections, showing how with temperature and flow being equal that different substrate (metal, opaque PVC, frosted PVC and clear PVC) and light conditions (0 in the metal pipe and maximum of 6, 1937 and 2957 $\mu\text{mol photons m}^{-2} \text{ s}^{-1}$ in opaque PVC, frosted PVC and clear PVC pipes, respectively) induced the development of different biofouling communities with varying proportions of diatoms and bacterial slimes. It was remarkable that in the metal pipe the fouling was alive and growing, after up to a maximum of 82 days in absolute darkness, and with its photosynthetic apparatus operating effectively ($F_v/F_m > 0.40$) when light was provided. Smayda and Mitchell-Innes (1974) similarly previously found that 7 out of 9 diatom species retained their photosynthetic capacity in the dark for 90 days and that for some species dark survival was inversely related to temperature. Veuger and van Oevelen (2011) also reported survival of diatoms in dark, cold, sediments with their pigments being retained intact, also suggesting that diatoms maintain their photosynthetic capacity in the dark. Nutrient bioassays revealed that the biofouling in the metal pipe positively responded to nitrogen, which could be

explained by the fact that in various diatom species the maximum time of surviving dark/anoxic conditions is positively correlated with the maximum intracellular NO_3^- concentration (Kamp 2011). Silica instead again depressed the Rapid Light Curves in the opaque and clear PVC pipes confirming how the addition of this nutrient is, for poorly understood reasons, not well tolerated by these oligotrophic diatoms.

Comparative field experiments were conducted during spring on the freshwater species *G. tarraleahae* (from Tasmania), the related *G. cf. manubrium* (Lake Rotoiti, New Zealand) and *D. geminata* (Buller River, New Zealand), testing the effect of nutrients (phosphorus, nitrogen and silica) and light on growth and stalk-formation. In spite of considerable efforts we did not succeed in producing viable *G. tarraleahae* still cultures in the laboratory. Comparative laboratory experiments were therefore also performed on Tasmanian cultures of the marine stalk-forming species *Licmophora flabellata* (a common fouling species on fish farm netting), to test the additional role of temperature and turbulence (**Chapter 4**).

For *L. flabellata* the most significant parameter was light, which stimulated both growth rates (maximally 0.55 divisions/day) and stalk formation as well as stalk length at the highest intensity tested ($233 \mu\text{mol photons m}^{-2} \text{s}^{-1}$). An increase in turbulence (from 2.5 to 4.16 Hz; generated with an orbital shaker table) reduced stalk length but not growth rates, whilst variation in nutrients concentration and temperature did not affect *Licmophora* growth or stalk formation. These results suggest that *L. flabellata* is a high-light adapted estuarine fouling diatom and that stalk formation and branching for this species are more likely to happen in relatively calm nutrient-rich waters (**Chapter 4**). Further experiments with *Licmophora* grown under still higher light intensities are recommended to confirm this.

In New Zealand the pest diatom *Didymosphenia geminata* was first recorded in 2004 in the lower Waiau River (Kilroy, 2004; Kilroy et al., 2008) and is now considered the first non-toxic diatom to cause strong negative effects on freshwater aquatic environments due to its high biomass (Blanco and Ector, 2009). The nuisance value and negative impacts from extensive New Zealand *Didymosphenia geminata* diatom fouling, or ‘rock snot’ are of considerable concern to Hydropower operations, were this species ever to be accidentally introduced into Tasmania. As with *G. tarraleahae* (30-45 μm long and 10 μm wide, stalks up to 4mm long), the

New Zealand *Didymosphenia* biofouling problems derive from massive production of persistent extracellular stalks but these problems are worse because of the much larger cell size of the latter (60–140 μm long and 25–43 μm wide, stalks up to 250 μm long) (Krammer and Lange-Bertalot, 1986) (reviewed in **Chapter 5**).

Similarly, *G. tarraleahae*, *D. geminata* and *G. cf. manubrium* in New Zealand freshwaters exhibited a depressed RLC and F_v/F_m values in response to high silica addition, but a positive short term response to additional tests with iron. According to Martin-Jézéquel et al (2002), cellular energy for silicification and transport comes from aerobic respiration without any direct involvement of photosynthetic energy. Therefore, diatom silicon metabolism differs from that of other major limiting nutrients such as nitrogen and phosphorus, which are closely linked to photosynthetic metabolism. A possible explanation for the unexpected response to silica addition relates to the application of unrealistically high silica concentrations to these diatom species adapted to oligotrophic waters. This was also suggested by additional tests on the estuarine species *L. flabellata*, which being adapted to high nutrient concentration, was not inhibited by N, P and Si addition (**Chapter 6**). Further investigations are necessary to better comprehend our silica bioassay results. It remains to be resolved how these results compare with the more rapid (minutes) positive changes in fluorescence signals (Nutrient Induced Fluorescent Transients, NIFTs) by diatoms in response to silica limitation as observed by Lippemeier et al. (1999) and to which extent our 20 minutes bioassay experiments can predict long term growth and biomass responses.

In contrast to *G. tarraleahae* in Tasmania, *D. geminata* in New Zealand's Buller River also showed preferences for low nutrient concentration, with blooms occurring only in waters with low phosphorus content (Bothwell et al., 2012), while being tolerant towards a wide range of light intensities. Moreover, whilst the Tasmanian *G. tarraleahae* distribution was limited to high velocity areas of the canal (2.1 m s^{-1}), a high degree of variation was found in *D. geminata* presence or absence with regard to flow velocity (Kirkwood et al., 2007). On the basis of a comparison of light, temperature, water flow and water chemistry conditions in New Zealand (Bray, 2014) and Tasmania, it is possible to conclude that if

Didymosphenia were accidentally introduced into Tarraleah it would be able to establish itself but may not necessarily cause high biomass blooms.

Mitigation strategies at Tarraleah No. 1 Canal currently include the emptying of the canal approximately twice a year and removal of the biofouling by scrubbing the walls and the bottom of the canal with rotating brushes attached to tractors and bobcats. Although this temporarily improves the water flow, the long term effectiveness of this method is not clear. Alternative mitigation solutions such as removal of shore-line vegetation and the application of white painted panels have shown better promise to increase light-intensity to mitigate low-light adapted *G. tarraleahae*. However, the recurrent cost of painting the canal every few years makes this approach financially not viable. If a future *Didymosphenia* invasion into Tarraleah were to be detected at an early stage, the emergency application of the copper-based biocide GemexTM (undesirable from a drinking water perspective) or potentially even short-term N and P loading may need to be considered. Manipulating Si:N:P ratios, to generate suitable algal species composition in aquatic environments, remains a poorly understood and therefore high risk management approach however (Officer & Ryther 1980).

The biological research presented in this thesis highlights that, in contradiction to traditional engineering approaches which view biofouling as a “black box”, different stalk-forming fouling diatom species have distinctive ecological requirements which call for species-specific mitigation approaches. *Licmophora* is more sensitive to turbulence, *Gomphonema* is sensitive to high light, and *Didymosphenia* is sensitive to high phosphorus. Other biofouling diatom species also need to be studied in future.

A major challenge remains the prevention of biofouling attachment to the substrate, and to discourage the initial contact or “first kiss” (Wetherbee et al., 1998), without the use of toxic, polluting, metal-based compounds as constituents of antifouling paints, which pose serious environmental problems. This challenging task requires continued research.

References

- Andersen, R.A. (2005). Algal culturing techniques. New York: Elsevier. 596 pp.
- Andrewartha, J. (2010). The effect of freshwater biofilms on turbulent boundary layers and the implications for hydroelectric canals. (Ph. D. thesis, University of Tasmania, Hobart).
- Andrewartha, J., Perkins, K., Sargison, J., Osborn, J., Walker, G., Henderson, A., and Hallegraef, G. (2010). Drag force and surface roughness measurements on freshwater biofouled surfaces. *Biofouling* 26, 487-496.
- Andrewartha, J., Sargison, J., and Perkins, K. (2007). The effect of *Gomphonema* and filamentous algae streamers on hydroelectric canal capacity and turbulent boundary layer structure. In 16th Australasian Fluid Mechanics Conference (Gold Coast, Australia). p. 241-246.
- Andrewartha, J.M., Sargison, J. E. and Perkins, K. J. (2008). The influence of freshwater biofilms on drag in hydroelectric power schemes. *WSEAS Transactions on Fluid Mechanics* 3.3: 201-206.
- Barton, A.F., Sargison, J.E., Osborn, J.E., Perkins, K., and Hallegraef, G. (2010). Characterizing the roughness of freshwater biofilms using a photogrammetric methodology. *Biofouling* 26, 439-448.
- Beardall, J., Young, E., and Roberts, S. (2001). Approaches for determining phytoplankton nutrient limitation. *Aquatic Science* 63, 44-69.
- Becking, L.G.M.B. (1934). *Geobiologie, of Inleiding Tot de Milieukunde: Met Literatuurlijst en Index* (Van Stockum and Zoon, The Hague).
- Beer, S., Björk, M., Gademann, R., and Ralph, P. (2001). Measurements of photosynthetic rates in seagrasses. In: Short, F.T., Coles, R.G. (Eds.), *Global seagrass research methods*. Elsevier, Amsterdam, 183-198.
- Beer, S., Vilenkin, B., Weil, A., Veste, M., Susel, L., and Eshel, A. (1999). Measuring photosynthetic rates in seagrasses by pulse amplitude modulated (PAM) fluorometry. *Marine Ecology Progress Series* 174, 293-300.
- Berges, J.A., Charlebois, D.O., Mauzerall, D.C., and Falkowski, P.G. (1996). Differential effects of nitrogen limitation on photosynthetic efficiency of photosystems I and II in microalgae. *Plant Physiology* 110, 689-696.
- Biggs, B.J., Goring, D.G., and Nikora, V.I. (1998). Subsidy and stress responses of stream periphyton to gradients in water velocity as a function of community growth form. *Journal of Phycology* 34, 598-607.

Blanco, S., and Ector, L. (2009). Distribution, ecology and nuisance effects of the freshwater invasive diatom *Didymosphenia geminata* (Lyngbye) M. Schmidt: a literature review. *Nova Hedwigia* 88, 3-4.

Borchardt, M.A. (1996). Nutrients. In R. J. Stevenson, M. L. Bothwell, and R. L. Lowe [eds.], *Algal ecology freshwater benthic ecosystems*. Academic Press San Diego. pp. 183-227.

Bothwell, M.L., Sherbot, D., Roberge, A.C. and Daley, R.J. (1993). Influence of natural ultraviolet radiation on lotic periphytic diatom community growth, biomass accrual, and species composition: short-term versus long-term effects. *Journal of Phycology*, 29(1), 24-35.

Bothwell, M., Sherbot, D., Deniseger, J., Wright, H., Lynch, D., and Kelly, D. (2006). Blooms of *Didymosphenia geminata* in rivers on Vancouver Island 1990 to present: a sign of environmental change or a new invasive species. In American Fisheries Society Western Division Meeting, pp. 15-16.

Bothwell, M., and Spaulding, S. (2008). Synopsis of the 2007 International Workshop on *Didymosphenia geminata*. In Proceedings of the 2007 International Workshop on *Didymosphenia geminata*. Canadian Technical Report of Fisheries and Aquatic Sciences. Vol. 2795. 2008. pp. xiii-xxxi.

Bothwell, M.L., Lynch, D.R., Wright, H., and Deniseger, J. (2009). On the boots of fishermen: The history of Didymo blooms on Vancouver Island, British Columbia. *Fisheries* 34, 382-388.

Bothwell, M.L., Kilroy, C., Taylor, B.W., Ellison, E.T., James, D.A., Gillis, C.A., Blandon, K.D. and Silins, U. (2012). Iron is not responsible for *Didymosphenia geminata* bloom formation in phosphorus-poor rivers. *Canadian Journal of Fisheries and Aquatic Sciences*, 69(11), 1723-1727.

Bray, J.P. (2014) The invasion ecology of *Didymosphenia geminata*. (Ph. D. thesis, University of Canterbury, New Zealand).

Brzezinski M.A. (1985) The Si:C:N ratio of marine diatoms: interspecific variability and the effect of some environmental variables. *Journal of Phycology* 21, 347-357

Brown, C.A. (2008). Changes in the composition and growth of invertebrates in rocky mountain streams due to blooms of the nuisance diatom *Didymosphenia geminata*. Abstracts NABS 56th Ann. Meet., Salt lake City, UT.

Bureau of Meteorology (2008). Tasmanian climate averages. Tarraleah Village. http://www.bom.gov.au/climate/averages/tables/cw_095018.shtml

Byers, J.E., Reichard, S., Randall, J.M., Parker, I.M., Smith, C.S., Lonsdale, W., Atkinson, I., Seastedt, T., Williamson, M., and Chornesky, E. (2002). Directing research to reduce the impacts of nonindigenous species. *Conservation Biology* 16, 630-640.

- Callow, M.E. (1993). A review of fouling in freshwaters. *Biofouling* 7, 313-327.
- Callow, M.E., and Callow, J.A. (2002). Marine biofouling: a sticky problem. *Biologist* 49, 1-5.
- Campbell, M.L. (2008). Organism impact assessment: risk analysis for post-incursion management. *ICES Journal of Marine Science: Journal du Conseil* 65, 795-804.
- Catford, J.A., Jansson, R., and Nilsson, C. (2009). Reducing redundancy in invasion ecology by integrating hypotheses into a single theoretical framework. *Diversity and Distributions* 15, 22-40.
- Characklis, W., and Cooksey, K. (1983). Biofilms and microbial fouling. *Adv. Appl. Microbiol* 29, 93-138.
- Clearwater, S.J., Jellyman, P.G., Biggs, B.J., Hickey, C.W., Blair, N., and Clayton, J.S. (2011). Pulse-dose application of chelated copper to a river for *Didymosphenia geminata* control: Effects on macroinvertebrates and fish. *Environmental Toxicology and Chemistry* 30, 181-195.
- Colautti, R.I., and MacIsaac, H.J. (2004). A neutral terminology to define 'invasive' species. *Diversity and Distributions* 10, 135-141.
- Coutts, A.D., and Taylor, M.D. (2004). A preliminary investigation of biosecurity risks associated with biofouling on merchant vessels in New Zealand. *New Zealand Journal of Marine and Freshwater Research* 38, 215-229.
- Cullis, J.D., Gillis, C.A., Bothwell, M.L., Kilroy, C., Packman, A. and Hassan, M. (2012). A conceptual model for the blooming behavior and persistence of the benthic mat-forming diatom *Didymosphenia geminata* in oligotrophic streams. *Journal of Geophysical Research: Biogeosciences*, 117 (G2) G00N03, doi:10.1029/2011JG001891.
- Daniel, G.F., Chamberlain, A.H.L., and Jones, E.B.G. (1987). Cytochemical and electron microscopical observations on the adhesive materials of marine fouling diatoms. *British Phycological Journal* 22, 101-118.
- Dodds, W.K. (1990). Hydrodynamic constraints on evolution of chemically mediated interactions between aquatic organisms in unidirectional flows. *Journal of Chemical Ecology* 16, 1417-1430.
- Ellwood, N., and Whitton, B. (2007). Importance of organic phosphate hydrolyzed in stalks of the lotic diatom *Didymosphenia geminata* and the possible impact of atmospheric and climatic changes. *Hydrobiologia* 592, 121-133.
- Elwell, L.C., Gillis, C.-A., Kunza, L.A., and Modley, M.D. (2014). Management challenges of *Didymosphenia geminata*. *Diatom Research* 29, 303-305.
- Falasco, E., and Bona, F. (2013). Recent findings regarding non-native or poorly known diatom taxa in north-western Italian rivers. *Journal of Limnology* 72, 35-51.

Falkowski, P., and Kiefer, D.A. (1985). Chlorophyll a fluorescence in phytoplankton: relationship to photosynthesis and biomass. *Journal of Plankton Research* 7, 715-731.

Falkowski, P.G., and Raven, J.A. (2013). *Aquatic photosynthesis* (Princeton University Press). 512 pp.

Finlay, B.J., Monaghan, E.B., and Maberly, S.C. (2002). Hypothesis: the rate and scale of dispersal of freshwater diatom species is a function of their global abundance. *Protist* 153, 261-273.

Fitridge, I., Dempster, T., Guenther, J. and de Nys, R. (2012). The impact and control of biofouling in marine aquaculture: a review. *Biofouling*, 28(7), 649-669.

Flöder, S., and Kilroy, C. (2009). *Didymosphenia geminata* (Protista, Bacillariophyceae) invasion, resistance of native periphyton communities, and implications for dispersal and management. *Biodiversity and Conservation* 18, 3809-3824.

Geider, R.J., Roche, J., Greene, R.M., and Olaizola, M. (1993). Response of the photosynthetic apparatus of *Phaeodactylum tricornutum* (Bacillariophyceae) to nitrate, phosphate, or iron starvation1. *Journal of Phycology* 29, 755-766.

Goldman, J.C. (1986). On phytoplankton growth rates and particulate C: N: P ratios at low light. *Limnology and Oceanography* 31, 1358-1363.

Gretz, M. (2008). The stalks of didymo. In *Proceedings of the 2007 International Workshop on Didymosphenia geminata*. Canadian Technical Report on Fisheries and Aquatic Sciences, 21 pp.

Guadayol, Ò., Peters, F., Stiansen, J.E., Marrasé, C. and Lohrmann, A. (2009). Evaluation of oscillating grids and orbital shakers as means to generate isotropic and homogeneous small-scale turbulence in laboratory enclosures commonly used in plankton studies. *Limnology and Oceanography: Methods*, 7(4), 287-303.

Hannan, P.J., Swinnerton, J.W., Lamontagne, R.A. and Patouillet, C. (1980). Effects of UV-B on algal growth rate and trace gas production. *Aquatic Toxicology, ASTM STP*, 707, 177-190.

Hecky, R., and Kilham, P. (1988). Nutrient limitation of phytoplankton in freshwater and marine environments: a review of recent evidence on the effects of enrichment. *Limnology and Oceanography* 33, 796-822.

Henley, W.J. (1993). Measurement and interpretation of photosynthetic light-response curves in algae in the context of photoinhibition and diel changes. *Journal of Phycology* 29, 729-739.

Hoagland, K.D., Roemer, S.C., and Rosowski, J.R. (1982). Colonization and community structure of two periphyton assemblages, with emphasis on the diatoms (Bacillariophyceae). *American Journal of Botany* 69:188-213.

- Hoagland, K.D., Rosowski, J.R., Gretz, M.R., and Roemer, S.C. (1993). Diatom extracellular polymeric substances: function, fine structure, chemistry, and physiology. *Journal of Phycology* 29, 537-566.
- Holland, D., Roberts, S., and Beardall, J. (2004). Assessment of the nutrient status of phytoplankton: a comparison between conventional bioassays and nutrient-induced fluorescence transients (NIFTs). *Ecological Indicators* 4, 149-159.
- Honeywill, C. (1998). A study of British *Licmophora* species and a discussion of its morphological features. *Diatom Research* 13, 221-271.
- Hudson, M. (2013). Biofouling in Hydro Tasmania Pipelines (Honours thesis, University of Tasmania, Hobart). 112 pp.
- Hustedt, F., and Pascher, A. (1930). Die Süßwasser-Flora Mitteleuropas: Heft 10: Bacillariophyta (Diatomeae) (Verlag Von Gustav Fischer).
- Hutchinson, G.E. (1967). A Treatise on Limnology. Vol. 2: Introduction to lake biology and the limnoplankton. J. New York, John Wiley and Sons. 185 pp.
- Hydro Tasmania (2006). Annual Report. 185 pp.
- Itakura, S., Imai, I. and Itoh, K. (1997). "Seed bank" of coastal planktonic diatoms in bottom sediments of Hiroshima Bay, Seto Inland Sea, Japan. *Marine biology*, 128(3), 497-508.
- James, D.A., Mosel, K., and Chipps, S.R. (2014). The influence of light, stream gradient, and iron on *Didymosphenia geminata* bloom development in the Black Hills, South Dakota. *Hydrobiologia* 721, 117-127.
- Jellyman, P., Clearwater, S., Clayton, J., Kilroy, C., Blair, N., Hickey, C., and Biggs, B. (2011). Controlling the invasive diatom *Didymosphenia geminata*: an ecotoxicity assessment of four potential biocides. *Archives of Environmental Contamination and Toxicology* 61, 115-127.
- Johnson, L.M., Hoagland, K.D., and Gretz, M.R. (1995). Effects of bromide and iodide on stalk secretion in the biofouling diatom *Achnanthes longipes* (Bacillariophyceae). *Journal of Phycology* 31, 401-412.
- Jokiel, P.L. and York, R.H. (1984). Importance of ultraviolet radiation in photoinhibition of microalgal growth¹. *Limnology and Oceanography* 29(1), 192-198.
- Jonsson, G., Jonsson, I., Bjornsson, M., and Einarsson, S. (2000). Using regionalization in mapping the distribution of the diatom species *Didymosphenia geminata* (Lyngb.) M. Smith in Icelandic rivers. *Proceedings-International Association of Theoretical and Applied Limnology* 27, 340-343.
- Kamp, A., de Beer, D., Nitsch, J.L., Lavik, G. and Stief, P. (2011). Diatoms respire nitrate to survive dark and anoxic conditions. *Proceedings of the National Academy of Sciences*, 108(14), 5649-5654.

Kautsky, H., Appel, W., and Amann, H. (1960). Chlorophyll fluoreszenz und Kohlensäure assimilation XIII. Die Fluoreszenzkurve und die Photochemie der Pflanze. *Biochem 2*, 277-292.

Kawecka, B., and Sanecki, J. (2003). *Didymosphenia geminata* in running waters of southern Poland—symptoms of change in water quality? *Hydrobiologia 495*, 193-201.

Keller, M.D., Selvin, R.C., Claus, W., and Guillard, R.R. (1987). Media for the culture of oceanic ultraphytoplankton. *Journal of Phycology 23*, 633-638.

Kilroy, C. (2004). A new alien diatom, *Didymosphenia geminata* (Lyngbye) Schmidt: its biology, distribution, effects and potential risks for New Zealand fresh waters. NIWA Client Report CHC2004-128. For Environment Southland.

Kilroy, C., and Bothwell, M. (2011). Environmental control of stalk length in the bloom-forming, freshwater benthic diatom *Didymosphenia geminata* (Bacillariophyceae). *Journal of Phycology 47*, 981-989.

Kilroy, C., Larned, S., and Biggs, B. (2009). The non-indigenous diatom *Didymosphenia geminata* alters benthic communities in New Zealand rivers. *Freshwater Biology 54*, 1990-2002.

Kilroy, C., Snelder, T., and Sykes, J. (2005). Likely environments in which the nonindigenous freshwater diatom, *Didymosphenia geminata*, can survive. New Zealand. National Institute of Water and Atmospheric Research Ltd, Christchurch.

Kilroy, C., Snelder, T.H., Floerl, O., Vieglais, C.C., and Dey, K.L. (2008). A rapid technique for assessing the suitability of areas for invasive species applied to New Zealand's rivers. *Diversity and Distributions 14*, 262-272.

Kilroy, C., and Unwin, M. (2011). The arrival and spread of the bloom-forming freshwater diatom *Didymosphenia geminata* in New Zealand. *Aquatic Invasions 6*, 249-262.

Kirkwood, A.E., Shea, T., Jackson, L.J., and McCauley, E. (2007). *Didymosphenia geminata* in two Alberta headwater rivers: an emerging invasive species that challenges conventional views on algal bloom development. *Canadian Journal of Fisheries and Aquatic Sciences 64*, 1703-1709.

Krammer, K. and Lange-Bertalot, H. (1986). Bacillariophyceae. I. Teil. Naviculaceae. In *Süsswasserflora von Mitteleuropa*. Band 2/1. pp. 876

Kuhajek, J. M. and Wood, S. A. (2014). Novel techniques for the short-term culture and laboratory study of *Didymosphenia geminata*. *Diatom Research, 29*(3), 293-301.

Lagerstedt, M.A. (2007). *Didymosphenia geminata*; an example of a biosecurity leak in New Zealand. Thesis in partial fulfilment of requirements for M.Sc. in Environmental Sciences, University of Canterbury, New Zealand: 94 pp.

Lane A. and Willemsen, P. (2004) Collaborative effort looks into biofouling. Fish Farming International, September 2004, 34-35

Larned, S., Biggs, B., Blair, N., Burns, C., Jarvie, B., Jellyman, D., Kilroy, C., Leathwick, J., Lister, K., and Nagels, J. (2006). Ecology of *Didymosphenia geminata* in New Zealand: habitat and ecosystem effects—Phase 2. NIWA Client Report CHC2006-086, NIWA Project MAF06507.

Larned, S.T., and Santos, S.R. (2000). Light-and nutrient-limited periphyton in low order streams of Oahu, Hawaii. *Hydrobiologia* 432, 101-111.

Lavery, J., Kurek, J., Rühland, K., Gillis, C., Pisaric, M., and Smol, J. (2014). Exploring the environmental context of recent *Didymosphenia geminata* proliferation in Gaspésie, Quebec, using paleolimnology. *Canadian Journal of Fisheries and Aquatic Sciences* 71, 616-626.

Levasseur, M., Thompson, P.A., and Harrison, P.J. (1993). Physiological acclimation of marine phytoplankton to different nitrogen sources. *Journal of Phycology* 29, 587-595.

Lewis, R.J., Johnson, L.M., and Hoagland, K.D. (2002). Effects of cell density, temperature and light intensity on growth and stalk production in the biofouling diatom *Achnanthes longipes* (Bacillariophyceae). *Journal of Phycology* 38, 1125-1131.

Lippemeier, S., Hartig, P., and Colijn, F. (1999). Direct impact of silicate on the photosynthetic performance of the diatom *Thalassiosira weissflogii* assessed by on- and off-line PAM fluorescence measurements. *Journal of Plankton Research* 21(2), 269-283.

Lippemeier, S., Hintze, R., Vanselow, K., Hartig, P., and Colijn, F. (2001). In-line recording of PAM fluorescence of phytoplankton cultures as a new tool for studying effects of fluctuating nutrient supply on photosynthesis. *European Journal of Phycology* 36, 89-100.

Lock, M.A., and John, P.H. (1979). Effect of flow patterns on uptake of phosphorus by river periphyton. *Limnology and Oceanography* 24(2), 376-383.

Lockwood, J.L., Cassey, P., and Blackburn, T. (2005). The role of propagule pressure in explaining species invasions. *Trends in Ecology and Evolution* 20, 223-228.

Lodge, D.M., Williams, S., MacIsaac, H.J., Hayes, K.R., Leung, B., Reichard, S., Mack, R.N., Moyle, P.B., Smith, M., and Andow, D.A. (2006). Biological invasions: recommendations for US policy and management. *Ecological Applications* 16, 2035-2054.

Mack, R.N., Ruiz, G., and Carlton, J. (2003). Global plant dispersal, naturalization, and invasion: pathways, modes, and circumstances. *Invasive species: vectors and management strategies*, 3-30.

- Mack, R.N., Simberloff, D., Mark Lonsdale, W., Evans, H., Clout, M., and Bazzaz, F.A. (2000). Biotic invasions: causes, epidemiology, global consequences, and control. *Ecological Applications* 10, 689-710.
- Marshall, H.L., Geider, R.J., and Flynn, K.J. (2000). A mechanistic model of photoinhibition. *New Phytologist* 145, 347-359.
- Martin-Jézéquel, V., Hildebrand, M., and Brzezinski, M. A. (2000). Silicon metabolism in diatoms: implications for growth. *Journal of Phycology* 36.5: 821-840.
- Maxwell, K., and Johnson, G.N. (2000). Chlorophyll fluorescence—a practical guide. *Journal of Experimental Botany* 51, 659-668.
- Medlin, L.K., Fryxell, G.A., and Cox, E.R. (1985). Successional sequences of microbial colonization on three species of Rhodophycean macroalgae. *Annals of Botany* 56, 399-413.
- Meseguer Yebra, D., Kiil, S., Weinell, C.E., and Dam-Johansen, K. (2006). Presence and effects of marine microbial biofilms on biocide-based antifouling paints. *Biofouling* 22, 33-41.
- Miller, M.P., McKnight, D.M., Cullis, J.D., Greene, A., Vietti, K., and Liptzin, D. (2009). Factors controlling streambed coverage of *Didymosphenia geminata* in two regulated streams in the Colorado Front Range. *Hydrobiologia* 630, 207-218.
- Mitbavkar, S., and Anil, A.C. (2007). Species interactions within a fouling diatom community: roles of nutrients, initial inoculum and competitive strategies. *Biofouling* 23, 99-112.
- Molino, P.J., and Wetherbee, R. (2008). The biology of biofouling diatoms and their role in the development of microbial slimes. *Biofouling* 24, 365-379.
- Müller, P., Li, X.-P., and Niyogi, K.K. (2001). Non-photochemical quenching. A response to excess light energy. *Plant Physiology* 125, 1558-1566.
- Myers, J.H., Simberloff, D., Kuris, A.M., and Carey, J.R. (2000). Eradication revisited: dealing with exotic species. *Trends in Ecology and Evolution* 15, 316-320.
- Newsom, L. (1978). Eradication of plant pests—con. *Bulletin of the ESA* 24, 35-40.
- Nowell, A., and Jumars, P. (1984). Flow environments of aquatic benthos. *Annual Review of Ecology and Systematics*, 303-328.
- Officer, C.B. and J.H. Ryther (1980). The possible importance of silicon in marine eutrophication. *Marine Ecology Progress Series* 3.1, 83-91.

- Parkhill, J.P., Maillet, G., and Cullen, J.J. (2001). Fluorescence-based maximal quantum yield for psii as a diagnostic of nutrient stress. *Journal of Phycology* 37, 517-529.
- Patil, J.S., and Anil, A.C. (2005). Quantification of diatoms in biofilms: standardisation of methods. *Biofouling* 21, 181-188.
- Patrick, R., and Reimer, C. (1975). The diatoms of the United States, exclusive of Alaska and Hawaii Vol. 2 Part 1. Monographs of the Academy of Natural Sciences of Philadelphia 13. 213 pp.
- Percival, E. (1979). The polysaccharides of green, red and brown seaweeds: their basic structure, biosynthesis and function. *British Phycological Journal* 14, 103-117.
- Perkins, K.J., Sargison, J., and Hallegraeff, G. (2009). Diatom fouling problems in a Tasmanian hydro canal, including the description of *Gomphonema tarraleahae* sp. nov. *Diatom Research* 24, 377-391.
- Perkins, K.J. (2010). Taxonomy, ecophysiology and mitigation of fouling diatoms in a hydro electric canal at Tarraleah (Tasmania). (Ph. D. thesis, University of Tasmania, Hobart). 163 pp.
- Perkins, K.J., Andrewartha, J.M., McMin, A., Cook, S.S., and Hallegraeff, G.M. (2010). Succession and physiological health of freshwater microalgal fouling in a Tasmanian hydropower canal. *Biofouling* 26, 637-644.
- Petrou, K., Doblin, M., Smith, R., Ralph, P., Shelly, K., and Beardall, J. (2008). State transitions and nonphotochemical quenching during a nutrient-induced fluorescence transient in phosphorus-starved *Dunaliella tertiolecta*. *Journal of Phycology* 44, 1204-1211.
- Pfeifer, R., and McDiffett, W. (1975). Some factors affecting primary productivity of stream riffle communities. *Archiv Fur Hydrobiologie* 1975. 75, 306-317.
- Picologlou, B.F., Characklis, W.G., and Zilver, N. (1980). Biofilm growth and hydraulic performance. *Journal of the Hydraulics Division* 106, 733-746.
- Pimentel, D., Lach, L., Zuniga, R., and Morrison, D. (2000). Environmental and economic costs of nonindigenous species in the United States. *BioScience* 50, 53-65.
- Pimentel, D., Zuniga, R., and Morrison, D. (2005). Update on the environmental and economic costs associated with alien-invasive species in the United States. *Ecological Economics* 52, 273-288.
- Pyšek, P., and Richardson, D.M. (2006). The biogeography of naturalization in alien plants. *Journal of Biogeography* 33, 2040-2050.

Quick, W.P., and Neuhaus, H.E. (1997). The regulation and control of photosynthetic carbon assimilation, in: C.H. Foyer, P.W. Quick (Eds.), *A Molecular Approach to Primary Metabolism in Plants*, Taylor and Francis, 41-62.

Ralph, P.J., and Gademann, R. (2005). Rapid light curves: a powerful tool to assess photosynthetic activity. *Aquatic Botany* 82, 222-237.

Redfield, A.C. (1958). The biological control of chemical factors in the environment. *American Scientist* 46, 205-221.

Reimann, B.E.F., Lewin, J.C. and Volcani, B.E. (1965). Studies on the biochemistry and fine structure of silica shell formation in diatoms I. The structure of the cell wall of *Cylindrotheca fusiformis* Reimann and Lewin. *The Journal of Cell Biology*, 24(1), 39-55.

Reiter, M.A. (1986). Interactions between the hydrodynamics of flowing water and the development of a benthic algal community. *Journal of Freshwater Ecology* 3, 511-517.

Richardson, D.M., Pyšek, P., Rejmánek, M., Barbour, M.G., Panetta, F.D., and West, C.J. (2000). Naturalization and invasion of alien plants: concepts and definitions. *Diversity and Distributions* 6, 93-107.

Root, S., and O'Reilly, C.M. (2012). Didymo control: increasing the effectiveness of decontamination strategies and reducing spread. *Fisheries* 37, 440-448.

Rost, A.L., Fritsen, C.H., and Davis, C.J. (2011). Distribution of freshwater diatom *Didymosphenia geminata* in streams in the Sierra Nevada, USA, in relation to water chemistry and bedrock geology. *Hydrobiologia* 665, 157-167.

Rousseau, V., Leynaert, A., Daoud, N., and Lancelot, C. (2002). Diatom succession, silicification and silicic acid availability in Belgian coastal waters (Southern North Sea). *Marine Ecology Progress Series* 236, 61-73.

Sabater, S., Navarro, E., and Guasch, H. (2002). Effects of copper on algal communities at different current velocities. *Journal of Applied Phycology* 14, 391-398.

Sakshaug, E., Bricaud, A., Dandonneau, Y., Falkowski, P.G., Kiefer, D.A., Legendre, L., Morel, A., Parslow, J., and Takahashi, M. (1997). Parameters of photosynthesis: definitions, theory and interpretation of results. *Journal of Plankton Research* 19, 1637-1670.

Salta, M., Wharton, J.A., Blache, Y., Stokes, K.R., and Briand, J.F. (2013). Marine biofilms on artificial surfaces: structure and dynamics. *Environmental Microbiology* 15, 2879-2893.

Schmidt, M. (1899). *Atlas der Diatomaceenkunde*. Heft 13. 472 pls. 1877.

- Schreiber, U. (2004). Pulse-amplitude-modulation (PAM) fluorometry and saturation pulse method: an overview. In Chlorophyll a Fluorescence, ed. GC Papageorgiou, Govindjee, (Springer), pp. 279-319.
- Schreiber, U., Schliwa, U., and Bilger, W. (1986). Continuous recording of photochemical and non-photochemical chlorophyll fluorescence quenching with a new type of modulation fluorometer. *Photosynthesis Research* 10, 51-62.
- Schultz, M., Bendick, J., Holm, E., and Hertel, W. (2011). Economic impact of biofouling on a naval surface ship. *Biofouling* 27, 87-98.
- Schweiger, E.W., Ashton, I.W., Muhlfeld, C.C., Jones, L.A., and Bahls, L.L. (2011). The distribution and abundance of a nuisance native alga, *Didymosphenia geminata*, in streams of Glacier National Park: Climate drivers and management implications. *Park Science* 28, 88-91.
- Serôdio, J., Vieira, S., Cruz, S. and Coelho, H. (2006). Rapid light-response curves of chlorophyll fluorescence in microalgae: relationship to steady-state light curves and non-photochemical quenching in benthic diatom-dominated assemblages. *Photosynth Res* 90:29-43.
- Shelly, K., Higgins, T., Beardall, J., Wood, B., McNaughton, D., and Heraud, P. (2007). Characterising nutrient-induced fluorescence transients (NIFTs) in nitrogen-stressed *Chlorella emersonii* (Chlorophyta). *Phycologia* 46, 503-512.
- Silvester, N., and Sleigh, M. (1985). The forces on microorganisms at surfaces in flowing water. *Freshwater Biology* 15, 433-448.
- Simberloff, D. (1986). Introduced insects: a biogeographic and systematic perspective. In *Ecology of biological invasions of North America and Hawaii* (Springer), pp. 3-26.
- Simberloff, D. (2003a). Eradication—preventing invasions at the outset. *Weed Science* 51, 247-253.
- Simberloff, D. (2003b). How much information on population biology is needed to manage introduced species? *Conservation Biology* 17, 83-92.
- Simberloff, D. (2009). We can eliminate invasions or live with them. Successful management projects. *Biological Invasions* 11, 149-157.
- Smayda, T.J. and Mitchell-Innes, B. (1974). Dark survival of autotrophic, planktonic marine diatoms. *Marine Biology*, 25(3), 195-202.
- Smayda TJ (1990). Novel and nuisance phytoplankton blooms in the sea: Evidence for a global epidemic. In: Graneli E, Sundström B, Edler L, Anderson DM (eds) *Toxic marine phytoplankton*. Elsevier Science Publishers, Amsterdam, pp 20–40
- Spaulding, S. and Elwell, L. (2007). Increase in nuisance blooms and geographic expansion of the freshwater diatom *Didymosphenia geminata*: recommendations

for response. USEPA Region 8. United States Geological Survey White Paper web publication, January, 33 pp.

Spaulding, S.A., Hermann, K., Steuven, G. and Erickson, J.W. (2005). A nuisance diatom species: *Didymosphenia geminata* in western streams. US EPA.

Spaulding, S.A., Kilroy, C., and Edlund, M. (2010). Diatoms as non-native species. The diatoms: applications for the environmental and earth sciences. 2nd ed. Edited by JP Smol and E. Stoermer. Cambridge University Press, Cambridge, UK, 560-569.

Stevenson, R.J. (1983). Effects of current and conditions simulating autogenically changing microhabitats on benthic algal immigration. *Ecology* 64, 1514-1524.

Stevenson, R.J., and Glover, R. (1993). Effects of algal density and current on ion transport through periphyton communities. *Limnology and Oceanography* 38, 1276-1281.

Stevenson, R.J., and Pan, Y. (1999). Assessing environmental conditions in rivers and streams with diatoms. The diatoms: applications for the environmental and earth sciences (ed. by E.F. Stoermer and J.P. Smol) 469, 12-40.

Stohlgren, T.J., and Schnase, J.L. (2006). Risk analysis for biological hazards: what we need to know about invasive species. *Risk Analysis* 26, 163-173.

Sundareshwar, P.V., Upadhayay, S., Abessa, M., Honomichl, S., Berdanier, B., Spaulding, S.A., Sandvik, C. and Trennepohl, A. (2011). *Didymosphenia geminata*: Algal blooms in oligotrophic streams and rivers. *Geophysical Research Letters*, 38(10). L10405. doi: 10.1029/2010GL046599.

Sweat, L.H., and Johnson, K.B. (2013). The effects of fine-scale substratum roughness on diatom community structure in estuarine biofilms. *Biofouling* 29, 879-890.

Taylor, G., Evans, L., Callow, M., and Christie, A. (1976). The biology of slime films. 2 parts. *Shipping World and Shipbuilder* 169, 857-859

Thompson, S.E., Taylor, A.R., Brownlee, C., Callow, M.E., and Callow, J.A. (2008). The role of nitric oxide in diatom adhesion in relation to substratum properties. *Journal of Phycology* 44, 967-976.

Thomson, B.E., Worrest, R.C. and Van Dyke, H. (1980). The growth response of an estuarine diatom (*Melosira nummuloides* [Dillw.] Ag.) to UV-B (290–320 nm) radiation. *Estuaries*, 3(1), 69-72.

Townsin, R.L. (2003). The ship hull fouling penalty. *Biofouling*, 19(S1), 9-15.

Vanormelingen, P., Verleyen, E., and Vyverman, W. (2008). The diversity and distribution of diatoms: from cosmopolitanism to narrow endemism. *Biodiversity and Conservation* 17, 393-405.

Veuger, B. and van Oevelen, D. (2011). Long-term pigment dynamics and diatom survival in dark sediment. *Limnology and Oceanography*, 56(3), 1065-1074.

Vyverman, W., Sabbe, K., Mann, D., Kilroy, C., Vyverman, R., Vanhoutte, K., and Hodgson, D. (1998). *Eunophora* gen. nov.(Bacillariophyta) from Tasmania and New Zealand: description and comparison with *Eunotia* and amphoroid diatoms. *European Journal of Phycology* 33, 95-111.

Walker, J.M., Sargison, J.E. and Henderson, A.D. (2013). Turbulent boundary-layer structure of flows over freshwater biofilms. *Experiments in Fluids*, 54(12), 1-17.

Wetherbee, R., Lind, J.L., Burke, J., and Quatrano, R.S. (1998). The First Kiss: Establishment and control of initial adhesion by raphid diatoms. *Journal of Phycology* 34, 9-15.

White, A., and Critchley, C. (1999). Rapid light curves: A new fluorescence method to assess the state of the photosynthetic apparatus. *Photosynthesis Research* 59, 63-72.

Whitford, L., and Schumacher, G. (1961). Effect of current on mineral uptake and respiration by a fresh-water alga. *Limnology and Oceanography* 6, 423-425.

Whitton, B., Ellwood, N., and Kawecka, B. (2009). Biology of the freshwater diatom *Didymosphenia*: a review. *Hydrobiologia* 630, 1-37.

Williamson, M. (1993). Invaders, weeds and the risk from genetically manipulated organisms. *Experientia* 49, 219-224.

Williamson, M. (1996). *Biological invasions*, Vol 15 (Springer). pp.244.

Wood, M., and Oliver, R. (1995). Fluorescence Transients in Response to Nutrient Enrichment of Nitrogen- and Phosphorus-limited *Microcystis aeruginosa* Cultures and Natural Phytoplankton Populations: a Measure of Nutrient Limitation. *Functional Plant Biology* 22, 331-340.

Woods, D.C., Fletcher, R.L. and Jones, E.B.G. (1986). Diatom fouling of in-service shipping with particular reference to the influence of hydrodynamic forces. In *Proceedings of the ninth international diatom symposium*. Bristol: Biopress (pp. 49-59).

Wykoff, D.D., Davies, J.P., Melis, A., and Grossman, A.R. (1998). The regulation of photosynthetic electron transport during nutrient deprivation in *Chlamydomonas reinhardtii*. *Plant Physiology* 117, 129-139.

Zargiel, K.A. and Swain, G.W. (2014). Static vs dynamic settlement and adhesion of diatoms to ship hull coatings. *Biofouling*, 30(1), 115-129.

Zavaleta, E.S., Hobbs, R.J., and Mooney, H.A. (2001). Viewing invasive species removal in a whole-ecosystem context. *Trends in Ecology and Evolution* 16, 454-459.

